# Alkyl Transfer to Metal Thiolates and Models for the Repair of DNA Alkylation Damage

by

Jonathan J. Wilker

B. S. Chemistry
University of Massachusetts at Amherst, 1991

Submitted to the Department of Chemistry

in Partial Fulfillment of the Requirements for the Degree of

Doctor of Philosophy in Chemistry

at the
Massachusetts Institute of Technology
February 1997



Signature of Author _____
Department of Chemistry
September 17, 1996

Certified by _____
Stephen J. Lippard
Professor of Chemistry
Thesis Supervisor

Accepted by _____
Dietmar Seyferth
Chairman
Departmental Committee on Graduate Students

Stephen J. Lippard
Professor of Chemistry

Dietmar Seyferth
Professor of Chemistry

James R. Williamson
Professor of Chemistry

## Table of Contents

# Alkyl Transfer to Metal Thiolates and Models for the Repair of DNA Alkylation Damage

by

Jonathan J. Wilker

Submitted to the Department of Chemistry
on September 18, 1996 in Partial Fulfillment of the
Requirements for the Degree of Doctor of Philosophy in Chemistry

## ABSTRACT

We describe the alkylation reactions of various metal thiolate complexes. The compounds $[(CH_3)_4N]_2[M(SC_6H_5)_4]$ (M = Zn(II), Co(II), Cd(II), Hg(II)), $[(CH_3)_4N][Zn(SC_6H_5)_3(MeIm)]$, (MeIm = 1-methylimidazole) $[Zn(SC_6H_5)_2(MeIm)_2]$, $[(C_4H_9)_4N][Hg(SC_6H_5)_3]$, $(CH_3)_4N(PF_6)$, $[(C_4H_9)_4N]_2[Fe_4S_4(SC_6H_5)_4]$, $[(C_4H_9)_4N]_2$-$[Fe_4S_4(SC_2H_5)_4]$, $[(C_2H_5)_4N]_3[Fe_4S_4(SC_2H_5)_4]$, and $[(C_2H_5)_4N]_2[Fe(SC_2H_5)_4]$ were all reacted with the methylating agent $(CH_3O)_3PO$. In all cases, methyl transfer was observed, however the nature of products varied amongst the complexes examined. Solution equilibria studies elucidated ion pairing of and ligand dissociation from the parent complex $[(CH_3)_4N]_2[Zn(SC_6H_5)_4]$ in dimethyl sulfoxide (DMSO) solution. A dissociated thiolate was determined to be the nucleophile active in methyl transfer. Kinetic studies revealed differences in the nucleophilicity and ligand dissociation properties of the compounds studied. Syntheses and single crystal X-ray structures of the new compounds $[(CH_3)_4N][Zn(SC_6H_5)_3(MeIm)]$, $[Zn(SC_6H_5)_2$-$(MeIm)_2]$, and $[Co(SC_6H_5)_2(MeIm)_2]$ are reported. Our results are discussed in the context of protein repair of deoxyribonucleic acid (DNA) alkylation damage. We propose a mechanism of alkylphosphotriester repair by the *Escherichia coli* Ada protein.

Thesis Supervisor: Stephen J. Lippard
Title: Professor of Chemistry

## List of Tables

## List of Figures

## List of Schemes

## List of Equations

## List of Appendices

## Acknowledgments

During the past five years, I have come into the debt of many. Some, for their help with the chemistry that follows. Others, for their perspectives, attitudes, goodhearted nature, sense of fun, and sanity. At the risk of exceeding the length of the thesis itself, please indulge my gratitude.

Not a single page here would exist without the guidance of Steve Lippard, my research advisor. His approach to chemistry is exemplary. Meticulous and careful, insightful and significant. Somehow, he has managed to assemble the greatest possible group of people to work with and learn from. In pushing me farther than I had cared for at times, Steve has turned me into the best chemist I am capable of being. If I could thank him for only one thing, it would be the scientist he has made of me. I hope sincerely that his approach to chemistry has worn off somewhat and that I can carry a little of his ability with me outside the lab.

Andreja Bakač is wonderful. After Steve, she has been the single largest asset to my chemistry. Without her guidance, I would still be back a few pages into Chapter One, scratching my head, and wondering "what the heck is going on with these silly thiolates?" Her guidance was perfect. Never giving me the answers, but letting me know that an answer is, indeed, there to be found. In this manner, Andreja got me to the solutions of my kinetic woes and taught me a little, tiny piece of kinetics in the process. Her expertise in chemistry is eclipsed only by her warmth as a person. Anyone who knows her will agree.

The group down in the departmental spectroscopy lab is incredibly helpful- Jim Simms, Scott Gardner, Debbie Gardner, and Jeanne Owens. They'll do anything possible to facilitate an experiment. And they're all terrific people. None of the NMR data that follows would exist without them.

I'm delighted to have had the opportunity to work with Karen Wetterhahn in the past year. She initiated the mercury chemistry, did much of it herself, and got me to think about toxic metals. In the process, we had fun with the chemistry and happened upon some interesting results.

Six years ago, Richard Holm did two wonderful things for me. First, he took this clueless undergraduate off the street and let me into his lab. Second, he introduced me to the wonderful field of bioinorganic chemistry. I can't imagine that my time in his lab benefited him in any way, but it sure was important to me. Mike Maroney, my undergraduate advisor at UMass, followed through on my introduction to this subdivision of chemistry. He nurtured my interest and encouraged me to continue my studies. He has been continually willing to help with advice and letters. Always with a smile and a joke (although not always a good one!). These two scientists are responsible for enabling me to embark upon this thesis.

Members of the Lippard lab, past and present, are responsible for making my stay here enjoyable. Never hesitating to stop their own work, listen to problems, and take time to lend expertise to the situation at hand. I've always appreciated the working environment you guys have created. Allow me to single out a handful for special mention.

In pursuit of the perfect onion ring, my good friend Rajesh Manchanda was always willing to seek adventure. Rajesh is rather sensitive about his ethnic origins, being raised in Delhi, India, and all. A well meaning salutation of "Good morning Mr. Towelhead," will, invariably, be meet with a rapid and biting response of "That's DOCTOR Towelhead to you!!" Along with the taxpayers of Saugus, I am grateful for your willingness to leave the lab for a bit and get some local culture.

Never again can I look at a ski lift without thinking of Susanna Herold. Maybe she pushed me off because she was being shown up on the slopes. Or it was one too many bad stories about Europe. I like to think it was all to save that poor little boy heading for the cliff. Whenever I wanted a hardy laugh, I just headed to your bench and was never disappointed. I can't even imagine how dull things would have been without you around. And I must express my profound appreciation for all the time you spent listening to my problems with thiolates. For all the nights in which we *felt* we knew what the molecules were doing, but couldn't quite prove it, let this thesis be Volume 1, Number 1 of your *Journal of Chemical Feelings*. There will always be an ice cold root beer waiting for you in my 'fridge. "Did I thank you? I will."

Bless the souls of Dave Coufal and Andy Gelasco for their demonstrated proficiency in all computer matters. Dave, by now you must cringe every time you see me. "What's wrong with the computers this time, Wilker?" But if you weren't so gosh darned fun to bug, there wouldn't have been half the troubles that there were! And Andy, I must admit to being impressed with how far you've come with a UMass degree!

Whenever things got just *too* ridiculous, Tricia Takahara was there with a good roll of the eyes. And she introduced me to the Osborne Family of Little Rock through Deb the Celeb. Maria Bautista is so cool, I say we make her an honorary American. Christy Chow is another great person with perspectives that helped me through. I'm glad we've kept in touch. And Sofi Elmroth is *everybody's* favorite Swede. She even gave me a Swedish Viking Helmet! You can read all about it in her journal *Helmetica Chimica Acta*.

A labmate, apartmentmate, and friend, Linda Doerrer has been around from the beginning to share all the ups and downs of the graduate school emotional roller coaster. It's wonderful to see you finish up and move on. I hope the year in England doesn't quelch the Anglophile in you. Watch out for the Christmas cakes and Marmite (even if they tell you it's English peanut butter).

Another resident of the "Love Shack" apartment was Larry Rozsnyai. There aren't numbers large enough to count the nights we stayed up wondering, deciding, planning, and fretting over our futures. Don't ever stop questioning things- that's what defines your personality. But I'm hoping that you someday find whatever it is that will make you happy. (And if I had to take a guess, I'd say it's a woman!) Hopefully, there will be more days in which we're mountain biking out in the woods somewhere, discussing corporate mergers and the like. Perhaps, we'll next meet over a fine cigar. Best of luck in your new career!

I know of no one more self-satisfied than Boris Golubovic. Mind you, I see no problem with that. There is no better story of how a friendship began. From the hurricane to Villiam, the expert mover. You've got a nice car there, Boris. Even the

color. Enjoy all your expensive toys and always buy the best. You'll never regret it. Wei to go!

Robert Grotzfeld is certainly the coolest German I've ever met. He's got an admirable enthusiasm for life. And he can appreciate Americana to its fullest. He just bought himself a huuuuge Lincoln Town Car and simply loves it. Robert and I flew down to Washington. D. C. together to run in the Marine Corps Marathon. It was a wonderful time and we even beat Oprah.

My friendship with Ellen Rhinard is exceptionally meaningful. She is among the warmest, most amiable, and humorous of all my peers. Along with our pal Scott Blackwell, we set out upon our first, real, American road trips. Together, we meandered through the south, stopping at random places like Chunky, Mississippi and Junction City, Arkansas. We watched alligator wrestling in the Everglades and blasted country music through the radio of our driveaway car in the streets of Nashville. We ate our way through the finest Texas and Florida have to offer. Ellen helped pull a prank on my friends Geoff and Rick that, alone, made the five years at MIT worthwhile. I truly hope that your boat finds its rudder. You deserve only the very best. Along with the happy citizens of Little Rock, I bid you P-E-A-C-E.

And speaking of road trip buddies, Geoff Zassenhaus is among the best. "He's a good man, but he's not quite right in the head." It was out in the Badlands with Geoff that I learned just how religious a hike can be. He also taught me how many times I can have a run-in with the law. "You boys a little far from home?" Together, we got to see the most amusing and American sights known. From the Kellogg's Headquarters in Michigan to the Spam Museum in Minnesota to Carhenge in Nebraska and, of course, the shrine of shrines, Graceland. We ate at the best places- in South Dakota at the Wrangler Cafe for pancakes and Whimp's for the greatest steak dinner ever . And the most superb Pizza Hut in all of Wyoming. We always stayed in the finest establishments. From Grandma's in Custer, South Dakota to Chez Opel in the various, hospitable parts of Italy. There are many road trips to take in the future and I hope you never lose your wanderlust. I'll see you back at Agate Fossil Beds National Monument when the rattlers are a bitin'.

Rick Seto, Mike Beeltje, and Willie Delker are three more friends from UMass who have been around these past five years. I've considered myself lucky to have good friends in the area and you guys are why. Rick has made sure we all kept our ties to the Pioneer Valley strong. He's got the place to stay when we want to meet for late night coffee at Jake's in Northhampton. Mike never hesitates to provide a self deprecating story for our amusement. And Willie, well, he was the first of the group to go and get married, so we always have something to kid him about.

Finally, a special thank you to my family. Mom and Dad have always encouraged me to pursue my aspirations. All the while keeping the pursuit in mind over the goal. Mom babied me with food and Dad has been taking great care of my Cadillac. Everyone has enjoyed having Papa back in Boston so we can see him more often. And it'll be great to have my sister Julie back home soon. I'm glad I decided to stay close by these past five years. This thesis is dedicated to my loving family.

To Mom, Dad, my sister Julie, and Papa

Alchemy, however, is a chaste prostitute, who has many lovers but disappoints all and grants her favors to none. She transforms the haughty into fools, the rich into paupers, the philosophers into dolts, and the deceived into loquacious deceivers...

From *Annalium Hirsaugensium Tomi II*
by Johannes Trithemius, 1690.

Translated by Umberto Eco in *Foucault's Pendulum*

*Chapter One*

# Alkyl Transfer to Metal Thiolates: Kinetics, Active Species Identification, and Relevance to the DNA Methylphosphotriester Repair Center of *Escherichia coli* Ada

## Abstract

The Ada protein of *Escherichia coli* employs a $[Zn(S\text{-}cys)_4]^{2-}$ site to repair deoxyribonucleic acid alkylphosphotriester lesions. The alkyl group is transferred to a cysteine thiolate in a stoichiometric reaction. We describe a functional model for this chemistry in which a thiolate of $[(CH_3)_4N]_2[Zn(SC_6H_5)_4]$ accepts a methyl group from $(CH_3O)_3PO$. The thiolate $(CH_3)_4N(SC_6H_5)$ is also active in methyl transfer, but the thiol $C_6H_5SH$ fails to react. These observations suggest that zinc binding of the cysteine responsible for alkyl transfer in Ada prevents protonation by accessible solvent, maintaining the residue in the active thiolate state. Conductivity measurements and kinetic studies demonstrate that $[(CH_3)_4N]_2[Zn(SC_6H_5)_4]$ forms ion pairs in dimethyl sulfoxide (DMSO) solution, which exhibit negligible demethylation activity relative to that of the solvated $[Zn(SC_6H_5)_4]^{2-}$ dianion. The ion pairing equilibrium constant was determined to be $K_{IP} = 13 \pm 4\ M^{-1}$, from which the concentrations of the active $[Zn(SC_6H_5)_4]^{2-}$ and the relatively inert $\{[(CH_3)_4N][Zn(SC_6H_5)_4]\}^-$ species could be estimated. The reaction of $[Zn(SC_6H_5)_4]^{2-}$ with $(CH_3O)_3PO$ is overall second-order, first-order with respect to each reagent. A second-order rate constant for this reaction, $k_{Zn}$, was determined to be $(1.6 \pm 0.3) \times 10^{-2}\ M^{-1}s^{-1}$. Ligand dissociation occurs in both the tetrathiolate species $[Zn(SC_6H_5)_4]^{2-}$ and the ion pair $\{[(CH_3)_4N][Zn(SC_6H_5)_4]\}^-$, as determined by $^1H$ NMR spectroscopy. From $^1H$ NMR spectral studies, an equilibrium constant for ligand dissociation from $\{[(CH_3)_4N][Zn(SC_6H_5)_4]\}^-$, $K_{DissocIP}$, was determined to be $(1.0 \pm 0.9) \times 10^{-2}$ M. This value was taken as a lower limit for the equilibrium constant for thiolate dissociation from the $[Zn(SC_6H_5)_4]^{2-}$ dianion, $K_{Dissoc}$. From kinetic data and this lower limit for ligand loss, all reactivity of $[(CH_3)_4N]_2[Zn(SC_6H_5)_4]$ toward

$(CH_3O)_3PO$ could be attributed to dissociated thiolate. Metal complexes representing alternative zinc protein sites were examined for methyl transfer ability. Pseudo-first-order rate constants provided the following trend: $[(CH_3)_4N]_2[Zn(SC_6H_5)_4]$ > $[(CH_3)_4N][Zn(SC_6H_5)_3(MeIm)]$ > $[Zn(SC_6H_5)_2(MeIm)_2]$. These data suggest that $[Zn(S\text{-cys})_4]^{2-}$ is the optimal protein zinc center for alkylphosphotriester repair. The reactivity of cobalt(II) and cadmium(II) tetrathiolate analogs was also investigated. A mechanism for in vivo alkylphosphotriester repair by the Ada protein involving a transiently dissociated cysteine thiolate is proposed.

**Introduction**

Proteins capable of repairing DNA alkylation damage occur in most organisms.[1-3] One of the best studied examples is the Ada protein of *Escherichia coli*. Ada is responsible for repair of $O^6$-alkylguanine, $O^4$-alkylthymine, and the $S_p$ diastereomer of alkylphosphotriesters.[4-6] The lesions are repaired by stoichiometric and irreversible transfer of the offending alkyl group to cysteine residues of the protein.[4,6-12] Separate active sites are present for mending the two alkylation damage types.[4,10,11] Base alkylation is repaired in the C-terminal portion of Ada by Cys321,[7,11,12] which is embedded in the sequence Asn-$X_6$-Pro-Cys-His-Arg-Val-$X_9$-Tyr-$X_{13/14}$-Glu, conserved by all known $O^6$-alkylguanine transferases.[13] Phosphate damage is repaired by alkyl transfer to Cys69,[10,11] one of four cysteine residues bound to a zinc ion in the N-terminus of Ada.[8,14-16]

The use of a $[Zn(S\text{-cys})_4]^{2-}$ site to repair alkylphosphotriesters raises several questions for the inorganic chemist. Why is Cys69, the residue responsible for repair, coordinated to zinc? Why does the ligand environment of this zinc ion comprise four cysteine residues? When the cysteine thiolate accepts an alkyl group from an alkylphosphotriester, is it coordinated to zinc or transiently dissociated? How does the nucleophilicity of a metal thiolate compare to that of the analogous thiolate alone? Why was zinc selected over other metal ions?

Previously, we used $[(CH_3)_4N]_2[Zn(SC_6H_5)_4]$ to mimic the $[Zn(S\text{-cys})_4]^{2-}$ site of Ada and $(CH_3O)_3PO$ to represent a DNA methylphosphotriester lesion in a functional model system.[17] Methyl transfer from $(CH_3O)_3PO$ to a thiolate of $[(CH_3)_4N]_2[Zn(SC_6H_5)_4]$ occurred in deuterated dimethyl sulfoxide (DMSO-*d6*) solution, but zinc was not required for this reaction. Methyl transfer from $(CH_3O)_3PO$ to benzenethiolate, $(CH_3)_4N(SC_6H_5)$, readily took place. The anal-

ogous thiol, $C_6H_5SH$, however, was unreactive toward $(CH_3O)_3PO$. We concluded that zinc coordination of Cys69 maintains this residue as a thiolate active in alkylphosphotriester repair, preventing protonation and inactivation by accessible water.

In the present report, we further analyze the reaction between $[(CH_3)_4N]_2[Zn(SC_6H_5)_4]$ and $(CH_3O)_3PO$ in DMSO. Included in this analysis are the order dependencies of each reagent to provide an overall rate equation, characterization of ion pairing and ligand dissociation, and analysis of whether or not the thiolate accepting a methyl group from $(CH_3O)_3PO$ is bound to zinc. The methyl transfer properties of cobalt(II) and cadmium(II) analogs are also explored, and the general nucleophilic character of free versus metal-bound thiolates is discussed.

## Experimental

**General.** All procedures were carried out under an argon or nitrogen atmosphere using standard Schlenk and glove box techniques. Solvents were dried, degassed, and distilled according to standard procedures.[18,19] NMR spectra were recorded at 25 ± 1 °C on Varian Unity 300 and VXR-500 instruments. All $^{31}P\{^1H\}$ NMR spectra were recorded on samples with phosphorus concentrations of 211 mM. For solubility reasons, all NMR spectra were taken in DMSO-*d6*. The parent complex $[(CH_3)_4N]_2[Zn(SC_6H_5)_4]$ was synthesized according to a literature procedure.[20] The compounds $[(CH_3)_4N][Zn(SC_6H_5)_3(MeIm)]$ and $[Zn(SC_6H_5)_2(MeIm)_2]$ were prepared as reported previously.[17]

**Kinetics.** All kinetic runs were performed under pseudo-first-order conditions with the concentration of thiolate or metal thiolate in excess over $(CH_3O)_3PO$ to prevent more than one equivalent of methyl transfer. Reaction

kinetics were monitored by $^1$H NMR spectroscopy in DMSO-*d6* at 24.5 (± 0.6) °C. Typical $^1$H NMR parameters for kinetic studies included 4 scans per spectrum, 40 second relaxation delay between scans, and 60 spectra per experiment. The total time of data collection was 6 h. Solution volumes were standardized by using calibrated 1 mL volumetric flasks. Concentrations of reactants and products were determined by referencing peak integrals to the methyl resonances of $(CH_3)_4N^+$ counterions, the concentration of which was determined from starting material quantities and known solution volumes. Rate constants were determined by curve fitting $(CH_3O)_3PO$ concentration-versus-time plots with a standard, integrated expression for first-order decay.[21] Pseudo-first-order rate constants (Table 1.1) were determined in triplicate, and the reported values are averages of the three kinetic runs with errors reflecting one standard deviation.

**Conductivity.** Conductivity measurements were recorded on a Fisher Scientific Model 09-326 conductivity meter equipped with a platinum electrode. The instrument response was calibrated with NIST conductivity calibration standards of KCl purchased from Fisher Scientific. All solution temperatures were 24 ± 1 °C.

**$(CH_3)_4N(SC_6H_5)$.** Benzenethiol (13.3 g, 121 mmol) was added to an ethanol (50 mL) solution of $(CH_3)_4N(OH)\cdot 5H_2O$ (21.8 g, 120 mmol). The solvent was removed under vacuum to yield a colorless solid that was recrystallized from boiling acetonitrile. $^1$H NMR (DMSO-*d6*): δ 3.08 (s, 12 H, $(CH_3)N^+$), 6.40 (t, 1 H, *p*-H), 6.64 (t, 2 H, *m*-H), 7.00 (d, 2 H, *o*-H). Anal. Calcd for $C_{10}H_{17}NS$: C, 65.52; H, 9.35; N, 7.64. Found: C, 65.83; H, 9.66; N, 7.91.

**$[(CH_3)_4N]_2[Co(SC_6H_5)_4]$.** This compound was prepared by modification of a literature procedure.[22] A methanol (40 mL) solution of $Co(NO_3)_2\cdot 6H_2O$ (8.74 g, 30.0 mmol) was added to a methanol (80 mL) solution of $C_6H_5SH$ (22.9

g, 208 mmol), $(C_2H_5)_3N$ (21.0 g, 208 mmol), and $(CH_3)_4NCl$ (7.50 g, 68.3 mmol) over 45 min with stirring. Addition of isopropanol (45 mL) and overnight storage at -20 °C provided green crystals (9.08 g, 14.1 mmol, 47%) that were collected by filtration, washed with isopropanol, and dried in vacuo. Anal. Calcd for $C_{32}H_{44}N_2S_4Co$: C, 59.69; H, 6.89; N, 4.35. Found: C, 59.21; H, 6.88; N, 4.28.

**$[(CH_3)_4N]_2[Cd(SC_6H_5)_4]$.** A literature synthesis was modified to obtain this complex.[20] Benzenethiol (8.91 g, 80.9 mmol), $(C_4H_9)_3N$ (12.5 g, 124 mmol), and $(CH_3)_4NCl$ (5.51 g, 50.3 mmol) were combined in methanol (175 mL). To this solution was added $Cd(NO_3)_2{\cdot}4H_2O$ (2.58 g, 8.36 mmol) in methanol (25 mL) over 2 h. Normal butanol (125 mL) was added over 10 min and the reaction solution was stored at -20 °C overnight. The resulting colorless crystals were collected, washed with *n*-$C_4H_9OH$, and dried in vacuo. These crystals were recrystallized from $CH_3CN$ (50 mL), collected by filtration, washed with *n*-$C_4H_9OH$, and dried in vacuo. $^1H$ NMR (DMSO-*d6*): δ 3.05 (s, 24 H, $(CH_3)N^+$), 6.62 (t, 4 H, *p*-H), 6.75 (t, 8 H, *m*-H), 7.36 (d, 8 H, *o*-H). Anal. Calcd for $C_{32}H_{44}N_2S_4Cd$: C, 55.11; H, 6.36; N, 4.02. Found: C, 55.02; H, 6.33; N, 4.02.

## Results

**Reaction of $[(CH_3)_4N]_2[Zn(SC_6H_5)_4]$ with $(CH_3O)_3PO$.** As shown by time dependent $^1H$ NMR spectroscopy in Figure 1.1, a 1:1 mixture of $[(CH_3)_4N]_2[Zn(SC_6H_5)_4]$ and $(CH_3O)_3PO$ in DMSO-*d6* reacts quantitatively to form $CH_3SC_6H_5$, $(CH_3O)_2PO_2^-$, and $\{Zn(SC_6H_5)_3\}^-$. The $CH_3SC_6H_5$ product is not coordinated to zinc because its $^1H$ NMR resonances are identical to those of an authentic sample. The zinc-containing reaction product retains three bound thiolates, which are equivalent by $^1H$ NMR spectroscopy. The $^{31}P\{^1H\}$ NMR peak of $(CH_3O)_2PO_2^-$ is broad ($\Delta\nu_{1/2}$ = 60 Hz) relative to that of a gen-

uine sample of $(NH_4)[(CH_3O)_2PO_2]$ ($\Delta\nu_{1/2}$ = 5.1 Hz). Owing to the high freezing point of DMSO-*d6* (18 °C), we were unable to cool the NMR sample significantly. Heating the reaction solution, however, sharpens $^{31}P\{^1H\}$ NMR lines of the $(CH_3O)_2PO_2^-$ product. From these results, we conclude that $(CH_3O)_2PO_2^-$ is in dynamic equilibrium between zinc-bound and free states. Scheme 1.1 depicts the reaction between $[(CH_3)_4N]_2[Zn(SC_6H_5)_4]$ and $(CH_3O)_3PO$. Attempts to crystallize the zinc-containing reaction product from DMSO solutions for single crystal X-ray structural analysis afforded only crystals of $[(CH_3)_4N]_2[Zn(SC_6H_5)_4]$.

A kinetic analysis was undertaken to understand better methyl transfer from $(CH_3O)_3PO$ to $[(CH_3)_4N]_2[Zn(SC_6H_5)_4]$. As shown in Figure 1.2, the reaction is first-order in $(CH_3O)_3PO$. By maintaining the $(CH_3O)_3PO$ concentration at a constant value of 8.5 mM and varying $[(CH_3)_4N]_2[Zn(SC_6H_5)_4]$ from 30.0 to 181, mM we obtained data for a plot of pseudo-first-order rate constant ($k_{obs}$) versus $[(CH_3)_4N]_2[Zn(SC_6H_5)_4]$ concentration (Figure 1.3). The leveling off at high concentrations of $[(CH_3)_4N]_2[Zn(SC_6H_5)_4]$ suggested the formation of $\{[(CH_3)_4N][Zn(SC_6H_5)_4]\}^-$ ion pairs.

**Ion Pairing.** The conductivity of $[(CH_3)_4N]_2[Zn(SC_6H_5)_4]$ in DMSO solution further indicated the presence of ion pairing, as revealed by curvature in the plot with increasing $[(CH_3)_4N]_2[Zn(SC_6H_5)_4]$ concentration (Figure 1.4). In order to evaluate the effect of ion pairing on the reaction of $[(CH_3)_4N]_2[Zn(SC_6H_5)_4]$ with $(CH_3O)_3PO$, we performed kinetic studies in the presence of added $(CH_3)_4N(PF_6)$ to increase the concentration of the ion paired species $\{[(CH_3)_4N][Zn(SC_6H_5)_4]\}^-$. The $k_{obs}$ values were diminished relative to those obtained in analogous runs without added $(CH_3)_4N(PF_6)$ (data not shown).

A model was formulated to describe the effect of ion pairing on the methyl transfer reaction. This model separates the reactivity of $[Zn(SC_6H_5)_4]^{2-}$ from that of the ion paired species $\{[(CH_3)_4N][Zn(SC_6H_5)_4]\}^-$. As shown in Scheme 1.2, the model proposes that $[Zn(SC_6H_5)_4]^{2-}$ is competent to react with $(CH_3O)_3PO$ but the less charged $\{[(CH_3)_4N][Zn(SC_6H_5)_4]\}^-$ is not. This assumption is consistent with the observation that the reaction of $[Zn(SC_6H_5)_3(MeIm)]^-$ with $(CH_3O)_3PO$ has a pseudo-first-order rate constant an order of magnitude lower than that of $[Zn(SC_6H_5)_4]^{2-}$ (Table 1.1).

We designate the concentration of $[Zn(SC_6H_5)_4]^{2-}$, solvated but not ion paired, as $[\{Zn(SC_6H_5)_4\}^{2-}]_{free}$; the concentration of $(CH_3)_4N^+$ not involved in ion pairing as $[(CH_3)_4N^+]_{free}$; and the concentration of ion paired zinc species as $[\{[(CH_3)_4N][Zn(SC_6H_5)_4]\}^-]$. The equilibrium constant for ion pairing, $K_{IP}$, is defined in eq 1.1 and the total zinc in eq 1.2. The observed pseudo-first-order

$$K_{IP} = \frac{[\{(CH_3)_4][Zn(SC_6H_5)_4]\}^-]}{[\{Zn(SC_6H_5)_4{}^{2-}\}]_{free}\,[(CH_3)_4N^+]_{free}} \qquad (1.1)$$

$$[Zn^{2+}]_{tot} = [\{Zn(SC_6H_5)_4\}^{2-}]_{free} + [\{[(CH_3)_4N][Zn(SC_6H_5)_4]\}^-] \qquad (1.2)$$

rate constant for the reaction of $[(CH_3)_4N]_2[Zn(SC_6H_5)_4]$ with $(CH_3O)_3PO$, $k_{obs}$, is the product of the true second-order rate constant, $k_{Zn}$, and $[\{Zn(SC_6H_5)_4\}^{2-}]_{free}$ (eq 1.3). Eqs 1.1-1.3 can be rearranged to provide an

$$k_{obs} = k_{Zn}\,[\{Zn(SC_6H_5)_4\}^{2-}]_{free} \qquad (1.3)$$

expression for $[(CH_3)_4N^+]_{free}$ in terms of $k_{Zn}$, $k_{obs}$, $K_{IP}$, and $[Zn^{2+}]_{tot}$ (eq 1.4,

$$[(CH_3)_4N^+]_{free} = \frac{k_{Zn}\,[Zn^{2+}]_{tot} - k_{obs}}{K_{IP}\,k_{obs}} \qquad (1.4)$$

derived in Appendix A1.1). From eq 1.4, it is clear that a plot of $[Zn^{2+}]_{tot}/k_{obs}$ versus $[(CH_3)_4N^+]_{free}$ yields a slope of $K_{IP}/k_{Zn}$ and an ordinate intercept of $1/k_{Zn}$. This plot thus affords both $K_{IP}$ and $k_{Zn}$ if the $(CH_3)_4N^+{}_{free}$ concentrations are known.

The $(CH_3)_4N^+{}_{free}$ concentrations were obtained by the following iterative procedure. For each $[(CH_3)_4N]_2[Zn(SC_6H_5)_4]$ concentration at which a kinetic run was performed (Figure 1.3), an initial guess of $[(CH_3)_4N^+]_{free}$ was made. Plotting $[Zn^{2+}]_{tot}/k_{obs}$ versus $[(CH_3)_4N^+]_{free}$ provided a rough estimate of the ion pairing equilibrium constant, $K_{IP}$, and the second-order rate constant, $k_{Zn}$, from eq 1.4. By using eqs 1.1 and 1.2, substitution and rearrangement afforded an expression for $[(CH_3)_4N^+]_{free}$ in terms only of $K_{IP}$ and $[Zn^{2+}]_{tot}$ (eq 1.5, derived in Appendix A1.2). The initial $K_{IP}$ value was

$$[(CH_3)_4N^+]_{free} = \frac{K_{IP}\,[Zn^{2+}]_{tot} - 1 \pm \left((K_{IP}\,[Zn^{2+}]_{tot})^2 + 6K_{IP}\,[Zn^{2+}]_{tot} + 1\right)^{1/2}}{2\,K_{IP}} \qquad (1.5)$$

used in eq 1.5 to estimate the $(CH_3)_4N^+{}_{free}$ concentrations. Replotting $[Zn^{2+}]_{tot}/k_{obs}$ versus $[(CH_3)_4N^+]_{free}$ yielded superior $K_{IP}$ and $k_{Zn}$ values. This process was repeated until the $[(CH_3)_4N^+]_{free}$, $K_{IP}$, and $k_{Zn}$ values converged. The final iteration of such a $[Zn^{2+}]_{tot}/k_{obs}$ versus $[(CH_3)_4N^+]_{free}$ plot is shown in Figure 1.5. From the ordinate intercept, we obtained a second-order rate constant for the reaction of $[Zn(SC_6H_5)_4]^{2-}$ and $(CH_3O)_3PO$ of $(1.6 \pm 0.3) \times 10^{-2}$

$M^{-1}s^{-1}$ (Table 1.2). This plot also afforded an ion pairing equilibrium constant, $K_{IP}$, of $13 \pm 4\ M^{-1}$ (Table 1.2).

With this value of $K_{IP}$, the exact concentration of $[\{Zn(SC_6H_5)_4\}^{2-}]_{free}$ available for reaction with $(CH_3O)_3PO$ is known for any starting $[(CH_3)_4N]_2[Zn(SC_6H_5)_4]$ concentration. A plot of $k_{obs}$ versus $[\{Zn(SC_6H_5)_4\}^{2-}]_{free}$ concentration provided the reaction order dependence on $[\{Zn(SC_6H_5)_4\}^{2-}]_{free}$. As shown in Figure 1.6, this plot gave a straight line with an intercept at the origin. From the plot, we conclude that the reaction of $[Zn(SC_6H_5)_4]^{2-}$ and $(CH_3O)_3PO$ is first-order with respect to $[\{Zn(SC_6H_5)_4\}^{2-}]_{free}$ concentration. With the order dependencies of both reagents known, we arrived at the final rate equation for the reaction of $[(CH_3)_4N]_2[Zn(SC_6H_5)_4]$ and $(CH_3O)_3PO$, eq 1.6.

$$-\frac{d[\{Zn(SC_6H_5)_4\}^{2-}]}{dt} = k_{Zn}\,[\{Zn(SC_6H_5)_4\}^{2-}]\,[(CH_3O)_3PO] \qquad (1.6)$$

**Ligand Dissociation.** We next address the question of whether the active species is a zinc-bound or free thiolate. Eq 1.7 describes situations in

$$k_{obs} = k_{Zn}\,[\{Zn(SC_6H_5)_4\}^{2-}]_{free} + k_{PhS}\,[C_6H_5S^-] \qquad (1.7)$$

which the observed reactivity of $[(CH_3)_4N]_2[Zn(SC_6H_5)_4]$, parameterized by $k_{obs}$, can be ascribed exclusively to zinc-bound thiolate, completely dissociated thiolate, or a combination of the two. In this equation, the second-order rate constant for reaction of dissociated benzenethiolate is $k_{PhS}$. To discern the relative contributions of $[Zn(SC_6H_5)_4{}^{2-}]_{free}$ and $C_6H_5S^-$ to the $[(CH_3)_4N]_2[Zn(SC_6H_5)_4]$ reactivity, the concentrations of each species are required.

Figure 1.7 displays the aromatic region of the $^1H$ NMR spectra of $(CH_3)_4N(SC_6H_5)$, $[(CH_3)_4N]_2[Zn(SC_6H_5)_4]$, $[(CH_3)_4N][Zn(SC_6H_5)_3(MeIm)]$, and $[Zn(SC_6H_5)_2(MeIm)_2]$ in DMSO-*d6*. For $(CH_3)_4N(SC_6H_5)$, the peaks are sharp with well resolved spin-spin coupling. For $[(CH_3)_4N]_2[Zn(SC_6H_5)_4]$, however, they are broad and display almost no splitting. The spectra of $[(CH_3)_4N][Zn(SC_6H_5)_3(MeIm)]$ and $[Zn(SC_6H_5)_2(MeIm)_2]$ are sharper and have better resolved spin-spin coupling. Ligand dissociation accounts for the line broadening trend of $[Zn(SC_6H_5)_4]^{2-}$ > $[Zn(SC_6H_5)_3(MeIm)]^-$ > $[Zn(SC_6H_5)_2(MeIm)_2]$. The $[Zn(SC_6H_5)_4]^{2-}$ dianion is expected to dissociate a thiolate ligand more readily than $[Zn(SC_6H_5)_3(MeIm)]^-$. Neutral $[Zn(SC_6H_5)_2(MeIm)_2]$ is even less likely to dissociate such a ligand. The results in Figure 1.7 indicate that the rate of ligand dissociation, as measured by line widths, increases with increasing thiolate content of the complexes. Since the exchange is fast on the $^1H$ NMR time scale, we cannot determine from these data alone the extent of ligand dissociation by integrating peaks associated with the zinc-bound and dissociated benzenethiolate. On the other hand, the rapid exchange permits us to discount ligand dissociation as a rate-determining step in the reaction of $[(CH_3)_4N]_2[Zn(SC_6H_5)_4]$ with $(CH_3O)_3PO$, owing to the low rate constants of methyl transfer (Table 1.1).

Scheme 1.3 depicts the consequences of ligand dissociation on the reaction of non-ion paired $[Zn(SC_6H_5)_4]^{2-}$ with $(CH_3O)_3PO$. Free benzenethiolate will react with $(CH_3O)_3PO$ as indicated (Table 1.1). Although the identity of the zinc species following thiolate dissociation is unknown, solvent binding to the empty coordination site is likely. The resulting zinc species will have one less negative charge compared to $[Zn(SC_6H_5)_4]^{2-}$. We assume reactivity of the solvated species $[Zn(SC_6H_5)_3(DMSO)]^-$ to be negligible relative to

$[Zn(SC_6H_5)_4]^{2-}$ and $C_6H_5S^-$. The extent of ligand dissociation is defined by an equilibrium constant, $K_{Dissoc}$, given in eq 1.8.

$$K_{Dissoc} = \frac{[\{Zn(SC_6H_5)_3(DMSO)\}^-]\,[C_6H_5S^-]}{[\{Zn(SC_6H_5)_4\}^{2-}]_{free}} \qquad (1.8)$$

**Combined Effects of Ion Pairing and Ligand Dissociation.** In order to define completely the reactivity of $[(CH_3)_4N]_2[Zn(SC_6H_5)_4]$ in DMSO, knowledge of both ion pairing and ligand dissociation processes is required. The extent of $[Zn(SC_6H_5)_3(DMSO)]^-$ ion pairing will be significantly less than that of $[Zn(SC_6H_5)_4]^{2-}$ owing to the reduced charge. In addition, the ion paired product $\{[(CH_3)_4N][Zn(SC_6H_5)_4]\}^-$ can dissociate a thiolate ligand. Scheme 1.4 depicts these possibilities. With $[(CH_3)_4N^+]_{free}$ representing the concentration of tetramethylammonium ion not involved in ion pairing, the equilibrium constant for ligand dissociation from the ion paired complex $\{[(CH_3)_4N][Zn(SC_6H_5)_4]\}^-$, $K_{DissocIP}$, is given by eq 1.9. Dissociation of the

$$K_{DissocIP} = \frac{[\{Zn(SC_6H_5)_3(DMSO)\}^-]\,[C_6H_5S^-]\,[(CH_3)_4N^+]_{free}}{[\{[(CH_3)_4N][Zn(SC_6H_5)_4]\}^-]} \qquad (1.9)$$

anionic benzenethiolate ligand will occur more readily from $[Zn(SC_6H_5)_4]^{2-}$ than $\{[(CH_3)_4N][Zn(SC_6H_5)_4]\}^-$ because of its greater negative charge. The equilibrium constant for dissociation from $[Zn(SC_6H_5)_4]^{2-}$, $K_{Dissoc}$, will therefore be greater than from $\{[(CH_3)_4N][Zn(SC_6H_5)_4]\}^-$, $K_{DissocIP}$ (eq 1.10).

$$K_{Dissoc} > K_{DissocIP} \qquad (1.10)$$

As depicted in Scheme 1.4, addition of $(CH_3)_4N^+$ to a solution of $[Zn(SC_6H_5)_4]^{2-}$ will shift the ion pairing equilibrium toward $\{[(CH_3)_4N]$-$[Zn(SC_6H_5)_4]\}^-$. Addition of $C_6H_5S^-$ to a DMSO solution containing the ligand dissociated complex $[Zn(SC_6H_5)_3(DMSO)]^-$ will convert this complex into the two forms of zinc tetrathiolate, $[Zn(SC_6H_5)_4]^{2-}$ and $\{[(CH_3)_4N][Zn(SC_6H_5)_4]\}^-$. In order to drive experimentally these solution equilibria toward the ion paired tetrathiolate, $\{[(CH_3)_4N][Zn(SC_6H_5)_4]\}^-$, both $(CH_3)_4N^+$ and $C_6H_5S^-$, in the form of $(CH_3)_4N(SC_6H_5)$, were added to DMSO-*d6* solutions of $[(CH_3)_4N]_2[Zn(SC_6H_5)_4]$ at varying ratios. While keeping the concentration of $[(CH_3)_4N]_2[Zn(SC_6H_5)_4]$ constant at 50.0 mM, we introduced varied quantities of $(CH_3)_4N(SC_6H_5)$, affording solutions with $(CH_3)_4N(SC_6H_5)$ to $[(CH_3)_4N]_2[Zn(SC_6H_5)_4]$ ratios of 1:1, 5:1, 7.5:1, and 10:1. The $^1H$ NMR spectra of these solutions are shown in Figure 1.8.

Peak broadening persists in $(CH_3)_4N(SC_6H_5)$ and $[(CH_3)_4N]_2$-$[Zn(SC_6H_5)_4]$ mixtures with ratios of 1:1, 5:1, 7.5:1, and 10:1. The spectra of these mixtures, however, exhibit two sets of benzenethiolate resonances. For example, the 5:1 solution displays one set of phenyl proton resonances at 6.41 (para), 6.66 (meta), and 7.01 (ortho) ppm and another at 6.61 (para), 6.74 (meta), and 7.44 (ortho) ppm (Figure 1.8C). The separation into two discrete resonance sets, in addition to a slightly enhanced degree of peak splitting, is most pronounced at the higher ratios (Figure 1.8C, D). When $(CH_3)_4N(PF_6)$ was added to a solution of $[(CH_3)_4N]_2[Zn(SC_6H_5)_4]$ to increase the amount of ion paired zinc tetrathiolate, the benzenethiolate $^1H$ NMR resonances become somewhat sharper than in a solution of $[(CH_3)_4N]_2[Zn(SC_6H_5)_4]$ alone (data not shown). This sharpening is due to increased amounts of ion paired complex and less ligand dissociation from this ion paired complex than the $[Zn(SC_6H_5)_4]^{2-}$ dianion (eq 1.10). We therefore assign the two sets of benzene-

thiolate resonances in $[(CH_3)_4N]_2[Zn(SC_6H_5)_4]$ solutions with added $(CH_3)_4N(SC_6H_5)$ to $\{[(CH_3)_4N][Zn(SC_6H_5)_4]\}^-$ and $C_6H_5S^-$. The upfield set of peaks have similar shifts to those of $(CH_3)_4N(SC_6H_5)$ and are so assigned.

From the concentrations of $\{[(CH_3)_4N][Zn(SC_6H_5)_4]\}^-$ and $C_6H_5S^-$ obtained from integrating the $^1H$ NMR peaks, a value for the ligand dissociation equilibrium constant from the ion paired complex, $K_{DissocIP}$ (eq 1.9), was computed. The $[\{Zn(SC_6H_5)_3(DMSO)\}^-]$ and $[(CH_3)_4N^+]_{free}$ concentrations were obtained in the following manner. The desired $[(CH_3)_4N^+]_{free}$ value is given by eq 1.11, in which both $[(CH_3)_4N^+]_{total}$ and $[\{[(CH_3)_4N][Zn(SC_6H_5)_4]\}^-]$ are

$$[(CH_3)_4N^+]_{free} = [(CH_3)_4N^+]_{total} - [\{[(CH_3)_4N][Zn(SC_6H_5)_4]\}^-] \quad (1.11)$$

known quantities. Under the conditions of added $(CH_3)_4N(SC_6H_5)$, the $[\{Zn(SC_6H_5)_3(DMSO)\}^-]$ concentration is determined from eq 1.12, in which

$$[\{Zn(SC_6H_5)_3(DMSO)\}^-] = [Zn^{2+}]_{total} - [\{[(CH_3)_4N][Zn(SC_6H_5)_4]\}^-] \quad (1.12)$$

$[Zn^{2+}]_{total}$ and $[\{[(CH_3)_4N][Zn(SC_6H_5)_4]\}^-]$ are known. Note that this expression does not include non-ion-paired zinc tetrathiolate, $[\{Zn(SC_6H_5)_4\}^{2-}]_{free}$, since the appearance of separate $^1H$ NMR resonances for $\{[(CH_3)_4N][Zn(SC_6H_5)_4]\}^-$ and $C_6H_5S^-$ in solutions of $[(CH_3)_4N]_2[Zn(SC_6H_5)_4]$ with added $(CH_3)_4N(SC_6H_5)$ indicates that most of the zinc tetrathiolate is ion paired. If such is not the case, the concentration of $\{[(CH_3)_4N][Zn(SC_6H_5)_4]\}^-$ may be overestimated, resulting in an underestimate of the $K_{DissocIP}$ value (eq 1.9). In any event, we now have all the concentrations required to compute $K_{DissocIP}$ by eq 1.9 and, consequently, can set a *lower limit* for the desired equilibrium constant for ligand loss from $[Zn(SC_6H_5)_4^{2-}]_{free}$, $K_{Dissoc}$ (eq 1.10).

Substitution of eqs 1.11 and 1.12 into eq 1.9 provides an expression for $K_{DissocIP}$ in terms of known quantities (eq 1.13). Measured concentrations of

$$K_{DissocIP} = \frac{\left([Zn^{2+}]_{total} - [(N^+ZnS_4)^-]\right)[C_6H_5S^-]\left([(CH_3)_4N^+]_{total} - [(N^+ZnS_4)^-]\right)}{[(N^+ZnS_4)^-]}$$

$$\text{where } [(N^+ZnS_4)^-] = [\{[(CH_3)_4N][Zn(SC_6H_5)_4]\}^-] \quad (1.13)$$

$\{[(CH_3)_4N][Zn(SC_6H_5)_4]\}^-$ and $[C_6H_5S^-]$ from the solutions with $(CH_3)_4N(SC_6H_5)$ to $[(CH_3)_4N]_2[Zn(SC_6H_5)_4]$ ratios of 5:1, 7.5:1, and 10:1 were used in eq 1.13 to obtain three independent values of $K_{DissocIP}$. An average of these results, reflecting one standard deviation, provides a $K_{DissocIP}$ value of $(1.0 \pm 0.9) \times 10^{-2}$ M (Table 1.2).

**Reactivity of $[(CH_3)_4N]_2[Zn(SC_6H_5)_4]$ Due to Dissociated $C_6H_5S^-$.** With this $K_{DissocIP}$ value, we have a lower limit for dissociation from the non-ion paired zinc tetrathiolate species $[Zn(SC_6H_5)_4^{2-}]_{free}$. Thus, $K_{Dissoc} \geq (1.0 \pm 0.9) \times 10^{-2}$ M (Table 1.2). Pseudo-first-order kinetic studies of the reaction of $[(CH_3)_4N]_2[Zn(SC_6H_5)_4]$ with $(CH_3O)_3PO$ at 5.0 mM and 1.0 mM afford a rate constant of $(8.2 \pm 0.6) \times 10^{-5}$ $s^{-1}$ (Table 1.1). We now consider how much of this reactivity might be due to dissociated benzenethiolate. From the lower limit of $K_{Dissoc}$ we can obtain a lower limit of benzenethiolate dissociated from zinc. As shown in eq 1.14 and Scheme 1.3, the concentrations of

$$[C_6H_5S^-]_{Zn} = [\{Zn(SC_6H_5)_3(DMSO)\}^-] \quad (1.14)$$

dissociated benzenethiolate and $[Zn(SC_6H_5)_3(DMSO)]^-$ are equal. This equality and the expression for the concentration of starting zinc complex, $[Zn^{2+}]_{start}$

(eq 1.15), can be substituted into eq 1.8, which defines $K_{Dissoc}$. Rearrangement

$$[Zn^{2+}]_{start} = [\{Zn(SC_6H_5)_4\}^{2-}]_{free} + [\{Zn(SC_6H_5)_3(DMSO)\}^-] \quad (1.15)$$

affords eq 1.16, derived in Appendix A1.3. Note that $[Zn^{2+}]_{start}$ is $[Zn^{2+}]_{total}$

$$[C_6H_5S^-] = \frac{-K_{Dissoc} \pm \left(K_{Dissoc}^2 + 4\,K_{Dissoc}\,[Zn_{start}]\right)^{1/2}}{2} \quad (1.16)$$

exclusive of the ion paired tetrathiolate, $\{[(CH_3)_4N][Zn(SC_6H_5)_4]\}^-$. The low, 5.0 mM concentration of $[(CH_3)_4N]_2[Zn(SC_6H_5)_4]$ used in this analysis was chosen to minimize ion pairing such that only $[Zn(SC_6H_5)_4^{2-}]_{free}$ and $[Zn(SC_6H_5)_3(DMSO)]^-$ concentrations were significant. By using the lower limit for $K_{Dissoc}$ and a $Zn^{2+}{}_{start}$ concentration of 5.0 mM from the kinetic runs of interest, a minimum $[C_6H_5S^-]_{Zn}$ concentration of 3.7 ± 0.4 mM was obtained. Relative to the starting $[(CH_3)_4N]_2[Zn(SC_6H_5)_4]$ concentration of 5.0 mM, this lower limit is significant and warrants further examination.

Kinetic studies of the reaction between 5.0 mM $(CH_3)_4N(SC_6H_5)$ and 1.0 mM $(CH_3O)_3PO$ provided a pseudo-first-order rate constant of (1.1 ± 0.3) x $10^{-4}$ $s^{-1}$ (Table 1.1). Since the reaction of $[(CH_3)_4N]_2[Zn(SC_6H_5)_4]$ with $(CH_3O)_3PO$ is second-order (eq 1.6), it is reasonable to assume that the reaction between $(CH_3)_4N(SC_6H_5)$ and $(CH_3O)_3PO$ is also second-order and follows the rate law shown in eq 1.17. With this assumption, the pseudo-first-order rate constant

$$-\frac{d[C_6H_5S^-]}{dt} = k_{PhS}\,[C_6H_5S^-]\,[(CH_3O)_3PO] \quad (1.17)$$

for benzenethiolate, $k_{obs}$, depends upon the second-order rate constant ($k_{PhS}$) and concentration of benzenethiolate ($[C_6H_5S^-]$), as indicated in eq 1.18. From

$$k_{obs} = k_{PhS}\,[C_6H_5S^-] \qquad (1.18)$$

the pseudo-first-order rate constant of (1.1 ± 0.3) x $10^{-4}$ $s^{-1}$ (Table 1.1) and eq 1.18, the second-order rate constant for benzenethiolate reacting with $(CH_3O)_3PO$, $k_{PhS}$, is (2.2 ± 0.6) x $10^{-2}$ $M^{-1}s^{-1}$ (Table 1.2). From this value, the 3.7 ± 0.4 mM lower limit of benzenethiolate concentration derived from $[(CH_3)_4N]_2[Zn(SC_6H_5)_4]$, and eqs 1.7 and 1.18, we compute a calculated $k_{obs}$ value, $k_{calc}$, of (8 ± 4) x $10^{-5}$ $s^{-1}$ (Table 1.2). This calculated value compares quite favorably with the measured pseudo-first-order rate constant of (8.2 ± 0.6) x $10^{-5}$ $s^{-1}$ for the reaction of 5.0 mM $[(CH_3)_4N]_2[Zn(SC_6H_5)_4]$ and 1.0 mM $(CH_3O)_3PO$ (Table 1.1). *We therefore conclude that dissociated thiolate is accountable for all the measured reactivity of* $[(CH_3)_4N]_2[Zn(SC_6H_5)_4]$. Scheme 1.5 summarizes the solution behavior of $[(CH_3)_4N]_2[Zn(SC_6H_5)_4]$ with respect to ion pairing, ligand dissociation, and reactivity with $(CH_3O)_3PO$.

**Metal Ion Variation.** In order to address the question of why zinc may have evolved for repair of alkylphosphotriesters by Ada, we explored the reactivity of cobalt(II) and cadmium(II) tetrathiolate complexes. Both $[(CH_3)_4N]_2[Co(SC_6H_5)_4]$ and $[(CH_3)_4N]_2[Cd(SC_6H_5)_4]$ react with $(CH_3O)_3PO$. Products from reaction with the cobalt complex are similar to those obtained in a stoichiometric reaction of $[(CH_3)_4N]_2[Zn(SC_6H_5)_4]$ with $(CH_3O)_3PO$. The thioether $CH_3SC_6H_5$ is not coordinated to the cobalt center, as indicated by $^1H$ NMR resonances which were identical to those of a genuine sample. The phosphate $(CH_3O)_2PO_2^-$ appears to be in an equilibrium between metal-bound and free states, as demonstrated by a broad ($\Delta\nu_{1/2}$ = 238 Hz) $^{31}P\{^1H\}$ NMR

resonance similar to that observed in the zinc reaction. As indicated in Table 1.1, $[(CH_3)_4N]_2[Co(SC_6H_5)_4]$ exhibits a pseudo-first-order rate constant significantly less than that of $[(CH_3)_4N]_2[Zn(SC_6H_5)_4]$.

Products for a 1:1 reaction between $[(CH_3)_4N]_2[Cd(SC_6H_5)_4]$ and $(CH_3O)_3PO$ are slightly different than for the zinc and cobalt complexes. Again, the methylated product $CH_3SC_6H_5$ is not coordinated to the $\{Cd(SC_6H_5)_3\}^-$ product moiety according to $^1H$ NMR spectroscopy. A sharp ($\Delta\nu_{1/2}$ = 3.6 Hz) $^{31}P\{^1H\}$ NMR product peak, however, differs from the broad resonances observed following the zinc and cobalt reactions. This sharp peak establishes that $(CH_3O)_2PO_2^-$ is not in an equilibrium between cadmium-bound and dissociated states. Currently, we cannot determine whether $(CH_3O)_2PO_2^-$ is coordinated to cadmium or free. The $^{113}Cd$ NMR spectrum of a 510 mM $[(CH_3)_4N]_2[Cd(SC_6H_5)_4]$ solution in DMSO-*d6* exhibits a peak at 569 ppm, in good agreement with literature values for similar complexes.[23,24] A $^{113}Cd$ NMR spectrum following a stoichiometric reaction between 510 mM $[(CH_3)_4N]_2[Cd(SC_6H_5)_4]$ and 510 mM $(CH_3O)_3PO$, however, displays no signal. This lack of signal in a $^{113}Cd$ NMR spectrum has precedence and is often attributed to exchange broadening.[24-26] The cadmium form of the methylphosphotriester repair active 10 kDa N-terminal fragment of Ada (Cd-N-Ada10) also displays no $^{113}Cd$ NMR resonance after alkylphosphotriester repair.[8] As is the case with the cobalt tetrathiolate complex, reaction of $[(CH_3)_4N]_2[Cd(SC_6H_5)_4]$ and $(CH_3O)_3PO$ proceeds with a pseudo-first-order rate constant less than that of $[(CH_3)_4N]_2[Zn(SC_6H_5)_4]$ (Table 1.1).

## Discussion

**Mechanism of Demethylation of Trimethylphosphate by Zinc Model Complexes; Comparison to Ada.** The present results illustrate methyl

transfer from a phosphotriester to a zinc thiolate model in a reaction that mimics Ada repair of DNA methylphosphotriesters. Repair of methylphosphotriesters in Ada, therefore, is probably an intrinsic property of the $[Zn(S\text{-cys})_4]^{2-}$ moiety, unlike Ada repair of alkylated base lesions such as $O^6$-methylguanine and $O^4$-methylthymine, which requires a structurally complex system of amino acid residues hydrogen bonded to the substrate.[13] Products of the reaction between $[(CH_3)_4N]_2[Zn(SC_6H_5)_4]$ and $(CH_3O)_3PO$ are not completely analogous to those found in the protein system, however. The methylated thiolate $CH_3SC_6H_5$ does not remain coordinated, whereas methylated Cys69 is apparently metal-bound in both the zinc and cadmium forms of Ada.[8,9] The phosphate product $(CH_3O)_2PO_2^-$ is partially coordinated in the model, whereas the protein presumably releases the repaired substrate to permit genome binding for transcriptional regulation.[27-31]

The reaction between $[(CH_3)_4N]_2[Zn(SC_6H_5)_4]$ and $(CH_3O)_3PO$ is second-order, first-order with respect to each reagent, with a rate constant of $(1.6 \pm 0.3) \times 10^{-2}$ $M^{-1}s^{-1}$ at 24.5 ($\pm$ 0.6) °C (Table 1.2). By comparison, Ada repair of a methylphosphotriester lesion occurs in aqueous buffer at 4 °C with a second-order rate constant of $2.8 \times 10^2$ $M^{-1}s^{-1}$.[32] It is not surprising that the protein effects methyl transfer with a rate constant higher than that of a model complex. Proteins evolve to provide optimal substrate binding, orientation, and transition state stabilization.[33,34] In addition, there are many differences between the protein and our synthetic analogs. In this study, we employed aromatic thiolates, which are less basic than the aliphatic cysteine residues of Ada.[35] Solvent differences ($H_2O$ versus DMSO) and the energetics of $(CH_3O)_3PO$ rather than a DNA methylphosphotriester are additional factors which contribute to kinetic differences between the protein and model chemistry.

NMR investigations of the active 10 kDa N-terminal Ada protein

fragment containing the $[Zn(S\text{-}cys)_4]^{2-}$ center (N-Ada10) revealed that the residue responsible for alkylphosphotriester repair (Cys69) is bound to zinc.[14,15] The cadmium-substituted form of this protein fragment, however, exhibited no $^1H$-$^{113}Cd$ scalar coupling involving the β-protons of Cys69.[8,14] By contrast, such scalar coupling was observed for the three other cysteine ligands of zinc (Cys38, Cys 42, and Cys72). Reactions of N-Ada10 with the methylating agent $CH_3I$ demonstrated that, not only is Cys69 more nucleophilic than the other cysteine ligands, but Cys69 is the most nucleophilic site in the protein fragment.[36] Our model studies indicate that metal-bound thiolates must have rate constants for methyl transfer less than that of free thiolate (Table 1.1). Combining these results with those for the protein fragment, we propose a repair mechanism for Ada involving the Cys69 residue in equilibrium between coordinated and free states. The zinc-bound state prevents protonation while the transiently dissociated state presents a thiolate nucleophile to the alkylphosphotriester lesion for alkyl transfer. This mechanism is consistent with a proposal in which the Cys69 thiolate is in equilibrium between a zinc-bound state and one hydrogen bonded to the proximal (~3.2 Å) backbone amide N-H of Gln73.[36] In such a case, the thiolate "in flight" between the zinc and the amide hydrogen may serve as the repair active nucleophile.

Recently, a zinc-dependent alkyl transfer reaction was discovered in *E. coli* cobalamin-independent methionine synthase, which catalyzes methionine formation from methyltetrahydrofolate and homocysteine.[37] Methylation of the homocysteine sulfur appears to require transient thiolate binding of this substrate to zinc in the enzyme. The present results strongly support the proposal[37] that the probable role of zinc in this system is to create or preserve a thiolate nucleophile for methylation.

**Other Zinc Thiolate Complexes.** The reactivity of complexes representing $[Zn(S\text{-cys})_4]^{2-}$, $[Zn(S\text{-cys})_3(N\text{-his})]^-$, and $[Zn(S\text{-cys})_2(N\text{-his})_2]$ protein sites has also been explored. All three compounds, $[(CH_3)_4N]_2[Zn(SC_6H_5)_4]$, $[(CH_3)_4N][Zn(SC_6H_5)_3(MeIm)]$, and $[Zn(SC_6H_5)_2(MeIm)_2]$, react with $(CH_3O)_3PO$ to yield products analogous to those found in the parent $[(CH_3)_4N]_2[Zn(SC_6H_5)_4]$ system. Pseudo-first-order rate constants of these reactions follow the trend $[(CH_3)_4N]_2[Zn(SC_6H_5)_4] > [(CH_3)_4N][Zn(SC_6H_5)_3(MeIm)] > [Zn(SC_6H_5)_2(MeIm)_2]$ (Table 1.1). The low rate constant for reaction of $[Zn(SC_6H_5)_2(MeIm)_2]$ indicates that $[Zn(S\text{-cys})_2(N\text{-his})_2]$ sites possess a very low level of nucleophilicity. This lack of reactivity is consistent with the use of the $[Zn(S\text{-cys})_2(N\text{-his})_2]$ center for structural purposes and may account in part for the prominence of this motif in nature.[38-41]

Sharp and well resolved $^1H$ NMR peaks (Figure 1.7) and low conductivity readings (Figure 1.4) for the neutral complex $[Zn(SC_6H_5)_2(MeIm)_2]$ indicate little benzenethiolate dissociation. If, as suggested, all reactivity of $[(CH_3)_4N]_2[Zn(SC_6H_5)_4]$ is due to a dissociated thiolate, the lesser degree of ligand dissociation from $[(CH_3)_4N][Zn(SC_6H_5)_3(MeIm)]$ should yield a lower level of reactivity toward trimethylphosphate. Such is indeed the case, as indicated by the low $k_{obs}$ value in reaction with $(CH_3O)_3PO$ (Table 1.1). If the dianionic $[Zn(S\text{-cys})_4]^{2-}$ protein center can dissociate a ligand readily, as suggested for Ada, a $[Zn(S\text{-cys})_3(N\text{-his})]^-$ site would be less likely to do so. Thiolate loss from the $[Zn(S\text{-cys})_2(N\text{-his})_2]$ would be even more unlikely. Our results suggest that, if the three cysteines of Ada other than Cys69 were to be mutated to histidine residues, rate constants for alkylphosphotriester repair would diminish as the number of histidine ligands increased.

**Comparison to Cobalt and Cadmium Analogs.** The selection of zinc by Ada as the metal ion of choice for alkylphosphotriester repair site could have occurred for a variety of reasons.[33,38] Redox active ions such as cobalt(II) and iron(II) would be poor choices owing to the possibility of redox damage to the DNA substrate or protein. The present results show that metal ions other than zinc may be less adept at methylphosphotriester repair. In particular, the cobalt(II) and cadmium(II) complexes $[(CH_3)_4N]_2[Co(SC_6H_5)_4]$ and $[(CH_3)_4N]_2$-$[Cd(SC_6H_5)_4]$ react with $(CH_3O)_3PO$ with rate constants lower than that of the zinc analog $[(CH_3)_4N]_2[Zn(SC_6H_5)_4]$ (Table 1.1). Thus, not only is zinc redox inactive, it may also provide a higher rate constant for alkylphosphotriester repair than other metal ions. The cadmium form of N-Ada10 repairs a methylphosphotriester lesion with a second-order rate constant one quarter the value of the zinc form.[32] A similar trend is observed with model chemistry, methyl transfer to $[(CH_3)_4N]_2[Cd(SC_6H_5)_4]$ occurring with a pseudo-first-order rate constant almost one third that of the zinc complex $[(CH_3)_4N]_2[Zn(SC_6H_5)_4]$ (Table 1.1). We interpret these differences in reactivity to varying degrees of ligand dissociation. Cadmium exhibits a higher affinity for sulfur donors than zinc, as evidenced by literature binding constants for thiourea.[42,43] An analogous heightened ability of cadmium to bind the benzenethiolate ligand will result in less dissociated ligand and, hence, decreased reactivity. Cobalt(II) ions also display higher thiourea binding constants than zinc.[42,43] This finding correlates well with our data, in which the rate constant of methyl transfer for the cobalt complex $[(CH_3)_4N]_2[Co(SC_6H_5)_4]$ is less than that found for the analogous zinc complex.

The sulfur-based reactions of metal thiolate complexes have been studied extensively.[44-50] Comprehensive reactant and product characterizations were completed in such studies, but the exact identities of reactive

species have remained elusive. To the best of our knowledge, the present investigation is the first in which the reactivity of a simple thiolate is compared to that of its metal complexes. Although ligand dissociation makes direct comparisons between metal-bound and free thiolate difficult, our kinetic results reveal the general trend that metal complexes have decreased reactivity, and hence less nucleophilicity, than the metal-free counterpart. The proposed phenomenon of metal-enhanced nucleophilicity is not observed in our work.[15,49] Coordination to a metal ion withdraws electron density from the sulfur and reduces thiolate nucleophilicity.

**Conclusions**

A functional model for Ada repair of alkylphosphotriester DNA damage has been developed in which methyl transfer occurs from $(CH_3O)_3PO$ to $[(CH_3)_4N]_2[Zn(SC_6H_5)_4]$. The simple thiolate $(CH_3)_4N(SC_6H_5)$ is also capable of methyl transfer, whereas the thiol $C_6H_5SH$ is inactive. From these observations, we infer that zinc binding of Cys69, the Ada residue responsible for alkylphosphotriester repair, prevents protonation and maintains this residue in the repair-active thiolate state. Conductivity, kinetic, and $^1H$ NMR experiments show that the complex $[(CH_3)_4N]_2[Zn(SC_6H_5)_4]$ forms ion pairs in DMSO solution with an equilibrium constant for ion pairing, $K_{IP}$, of $13 \pm 4$ $M^{-1}$ (Table 1.2). The reaction between solvated $[Zn(SC_6H_5)_4]^{2-}$ and $(CH_3O)_3PO$ is a second-order process, first-order with respect to each reagent and exhibits a second-order rate constant, $k_{Zn}$, of $(1.6 \pm 0.3) \times 10^{-2}$ $M^{-1}s^{-1}$ (Table 1.2). The zinc tetrathiolates $[Zn(SC_6H_5)_4]^{2-}$ and $\{[(CH_3)_4N][Zn(SC_6H_5)_4]\}^-$ undergo appreciable degrees of ligand dissociation. Addition of $(CH_3)_4N(SC_6H_5)$ to solutions of $[(CH_3)_4N]_2[Zn(SC_6H_5)_4]$ both increased the formation of ion pairs with the zinc tetrathiolate dianion and drove the dissociation equilibria

toward the bound states increasing the concentration of $\{[(CH_3)_4N][Zn(SC_6H_5)_4]\}^-$. Examination of these solutions by $^1H$ NMR spectroscopy yielded an equilibrium constant for dissociation from $\{[(CH_3)_4N][Zn(SC_6H_5)_4]\}^-$, $K_{DissocIP}$, of $(1.0 \pm 0.9) \times 10^{-2}$ M. This equilibrium constant is the lower limit for the equilibrium constant for ligand loss from $[Zn(SC_6H_5)_4]^{2-}$, $K_{Dissoc}$. By using this lower limit, the reactivity of $[(CH_3)_4N]_2[Zn(SC_6H_5)_4]$ was ascribed completely to dissociated benzenethiolate.

Metal complexes representing alternative protein sites were examined for reactivity with $(CH_3O)_3PO$. Pseudo-first-order rate constants provided the following trend: $[(CH_3)_4N]_2[Zn(SC_6H_5)_4] > [(CH_3)_4N][Zn(SC_6H_5)_3(MeIm)] > [Zn(SC_6H_5)_2(MeIm)_2]$. These data suggest that $[Zn(S\text{-cys})_4]^{2-}$ is the optimal zinc center for alkylphosphotriester repair and that $[Zn(S\text{-cys})_2(N\text{-his})_2]$ sites lack an appreciable degree of nucleophilicity. Cobalt and cadmium tetrathiolate complexes also react with $(CH_3O)_3PO$, but with rate constants less than that of the zinc analog. These differences in reactivity of the metal thiolate complexes are attributed to varied degrees of thiolate dissociation.

Based upon our results and published studies on the protein, we propose a mechanism for alkylphosphotriester repair in Ada where a transiently dissociated Cys69 ligand is the nucleophile responsible for accepting an alkyl moiety from the DNA alkylphosphotriester lesion. The zinc-bound state prevents protonation and deactivation of the cysteine thiolate nucleophile. Finally, our kinetic data indicate that metal thiolate moieties display generally decreased nucleophilicity relative to that of free thiolates.

**Acknowledgments**

This research was supported by grant CA34992 from the National Cancer Institute. We are grateful to A. Bakač and S. Herold for many valuable discussions. We thank R. Matthews for kindly providing a preprint of reference 37. J. J. W. is predoctoral trainee under N.C.I. training grant CA09112.

**References**

(1) Friedberg, E. C.; Walker, G. C.; Siede, W. *DNA Repair and Mutagenesis*; ASM Press: Washington D. C., 1995.

(2) Friedberg, E. C. *BioEssays* **1994**, *16*, 645-649.

(3) Lindahl, T. *Nature* **1993**, *362*, 709-715.

(4) McCarthy, T. V.; Lindahl, T. *Nucl. Acid Res.* **1985**, *13*, 2683.

(5) Teo, I.; Sedgwick, B.; Demple, B.; Li, B.; Lindahl, T. *EMBO J.* **1984**, *3*, 2151-2157.

(6) Demple, B.; Jacobsson, A.; Olsson, M.; Robins, P.; Lindahl, T. *J. Biol. Chem.* **1982**, *257*, 13776-13780.

(7) Moore, M. H.; Gulbis, J. M.; Dodson, E. J.; Demple, B.; Moody, P. C. E. *EMBO J.* **1994**, *13*, 1495-1501.

(8) Myers, L. C.; Cushing, T. D.; Wagner, G.; Verdine, G. L. *Chem. and Biol.* **1994**, *1*, 91-97.

(9) Ohkubo, T.; Sakashita, H.; Sakuma, T.; Kainosho, M.; Sekiguchi, M.; Morikawa, K. *J. Am. Chem. Soc.* **1994**, *116*, 6035-6036.

(10) Sedgwick, B.; Robins, P.; Totty, N.; Lindahl, T. *J. Biol. Chem.* **1988**, *263*, 4430-4433.

(11) Takano, K.; Nakabeppu, Y.; Sekiguchi, M. *J. Mol. Biol.* **1988**, *201*, 261-271.

(12) Demple, B.; Sedgwick, B.; Robins, P.; Totty, N.; Waterfield, M. D.; Lindahl, T. *Proc. Natl. Acad. Sci. U. S. A.* **1985**, *82*, 2688-2692.

(13) Wibley, J. E. A.; McKie, J. H.; Embrey, K.; Marks, D. S.; Douglas, K. T.; Moore, M. H.; Moody, P. C. E. *Anti-Cancer Drug Design* **1995**, *10*, 75-95.

(14) Myers, L. C.; Terranova, M. P.; Ferentz, A. E.; Wagner, G.; Verdine, G. L. *Science* **1993**, *261*, 1164-1167.

(15) Myers, L. C.; Verdine, G. L.; Wagner, G. *Biochemistry* **1993**, *32*, 14089-14094.

(16) Myers, L. C.; Terranova, M. P.; Nash, H. M.; Markis, M. A.; Verdine, G. L. *Biochemistry* **1992**, *31*, 4541-4547.

(17) Wilker, J. J.; Lippard, S. J. *J. Am. Chem. Soc.* **1995**, *117*, 8682-8683.

(18) Perrin, D. D.; Armarego, W. L. F. *Purification of Laboratory Chemicals*; Third ed.; Butterworth-Heinemann Ltd.: Boston, 1988.

(19) Gordon, A. J.; Ford, R. A. *The Chemist's Companion. A Handbook of Practical Data, Techniques, and References*; John Wiley and Sons: New York, 1972.

(20) Dance, I. G.; Choy, A.; Scudder, M. L. *J. Am. Chem. Soc.* **1984**, *106*, 6285-6295.

(21) Wilkins, R. G. *Kinetics and Mechanism of Reactions of Transition Metal Complexes*; 2nd ed.; VCH Publishers Inc.: New York, 1991.

(22) Dance, I. G. *J. Am. Chem. Soc.* **1979**, *101*, 6264-6273.

(23) Coleman, J. E. In *Methods in Enzymology*; Riordan, J. F. and Vallee, B. L., Ed.; Academic Press: Boston, 1993; Vol. 227, pp 16-43.

(24) Summers, M. F. *Coord. Chem. Rev.* **1988**, *86*, 43-134.

(25) Keller, A. D.; Drakenberg, T.; Briggs, R. W.; Armitage, I. M. *Inorg. Chem.* **1985**, *24*, 1170-1174.

(26) Armitage, I. M.; Otvos, J. D. In *Biological Magnetic Resonance*; Berliner, L. J. and Reuben, J., Ed.; Plenum Press: New York, 1984; Vol. 4, pp 79-144.

(27) Saget, B. M.; Walker, G. C. *Proc. Natl. Acad. Sci. U. S. A.* **1994**, *91*, 9730-9734.

(28) Shevell, D. E.; Friedman, B. M.; Walker, G. C. *Mutat. Res.* **1990**, *233*, 53-72.

(29) Nakabeppu, Y.; Sekiguchi, M. *Proc. Natl. Acad. Sci. U. S. A.* **1986**, *83*, 6297-6301.

(30) Teo, I.; Sedgwick, B.; Kilpatrick, M. W.; McCarthy, T. V.; Lindahl, T. *Cell* **1986**, *45*, 315-324.

(31) Volkert, M. R.; Nguyen, D. C. *Proc. Natl. Acad. Sci. U. S. A.* **1984**, *81*, 4110-4114.

(32) Myers, L. C.; Jackow, F.; Verdine, G. L. *J. Biol. Chem.* **1995**, *270*, 6664-70.

(33) Lippard, S. J.; Berg, J. M. *Principles of Bioinorganic Chemistry*; University Science Books: Mill Valley, CA, 1994.

(34) Fersht, A. *Enzyme Structure and Mechanism*; Second ed.; W. H. Freeman and Co.: New York, 1985.

(35) Crampton, M. R. In *The Chemistry of the Thiol Group*; Patai, S., Ed.; John Wiley and Sons: New York, 1974, pp 379-415.

(36) Myers, L. C.; Wagner, G.; Verdine, G. L. *J. Am. Chem. Soc.* **1995**, *117*, 10749-10750.

(37) Gonzalez, J. C.; Peariso, K.; Penner-Hahn, J. E.; Matthews, R. G. *Biochemistry*, In press.

(38) Berg, J. M.; Shi, Y. *Science* **1996**, *271*, 1081-1085.

(39) Klug, A.; Schwabe, J. W. R. *FASEB J.* **1995**, *9*, 597-604.

(40) Rhodes, D.; Klug, A. *Sci. Am.* **1993**, *268*, 56-65.

(41) Vallee, B. L.; Auld, D. S. *Acc. Chem. Res.* **1993**, *26*, 543-551.

(42) Martell, A. E.; Smith, R. M. *Critical Stability Constants*; Plenum Press: New York, 1982; Vol. 5: First Supplement.

(43) Martell, A. E.; Smith, R. M. *Critical Stability Constants*; Plenum Press: New York, 1977; Vol. 3.

(44) Buonomo, R. M.; Font, I.; Maguire, M. J.; Reibenspies, J. H.; Tuntulani, T.; Darensbourg, M. Y. *J. Am. Chem. Soc.* **1995**, *117*, 963-973.

(45) Ram, M. S.; Riordan, C. G.; Ostrander, R.; Rheingold, A. L. *Inorg. Chem.* **1995**, *34*, 5884-5892.

(46) Wilker, J. J.; Gelasco, A.; Pressler, M. A.; Day, R. O.; Maroney, M. J. *J. Am. Chem. Soc.* **1991**, *113*, 6342-6343.

(47) Mills, D. K.; Reibenspies, J. H.; Darensbourg, M. Y. *Inorg. Chem.* **1990**, *29*, 4364-4366.

(48) Lindoy, L. F.; Busch, D. H. *Inorg. Chem.* **1974**, *13*, 2494-2498.

(49) Blinn, E. L.; Busch, D. H. *J. Am. Chem. Soc.* **1968**, *90*, 4280-4285.

(50) Busch, D. H.; Jr., J. A. B.; Jicha, D. C.; Thompson, M. J.; Morris, M. L. In *Reactions of Coordinated Ligands and Homogeneous Catalysis*; Busch, D. H., Ed.; American Chemical Society: Washington D. C., 1963; Vol. 37, pp 125-142.

**Table 1.1.** Pseudo-First-Order Rate Constants for Reactions of Benzenethiolate and its Metal Complexes with $(CH_3O)_3PO$.[a]

| compound | $k$ ($s^{-1}$) |
|---|---|
| $[(CH_3)_4N]_2[Zn(SC_6H_5)_4]$ | $(8.2 \pm 0.6) \times 10^{-5}$ |
| $[(CH_3)_4N][Zn(SC_6H_5)_3(MeIm)]$ | $(6 \pm 1) \times 10^{-6}$ |
| $[Zn(SC_6H_5)_2(MeIm)_2]$ | $\leq 5 \times 10^{-8}$ |
| $(CH_3)_4N(SC_6H_5)$ | $(1.1 \pm 0.3) \times 10^{-4}$ |
| $[(CH_3)_4N]_2[Co(SC_6H_5)_4]$ | $(4 \pm 1) \times 10^{-5}$ |
| $[(CH_3)_4N]_2[Cd(SC_6H_5)_4]$ | $(3 \pm 1) \times 10^{-5}$ |

[a] Reactions were carried out with 5.0 mM thiolate or metal complex and 1.0 mM $(CH_3O)_3PO$ in DMSO-*d6*. With the exception of $[Zn(SC_6H_5)_2(MeIm)_2]$, all rate constants shown are an average of three kinetic runs. Error estimates reflect one standard deviation.

**Table 1.2.** Summary of Equilibrium and Rate Constants Discussed in the Text.

| constant | value |
|---|---|
| $k_{Zn}$ | $(1.6 \pm 0.3) \times 10^{-2}\ M^{-1}s^{-1}$ |
| $K_{IP}$ | $13 \pm 4\ M^{-1}$ |
| $K_{DissocIP}$ | $(1.0 \pm 0.9) \times 10^{-2}\ M$ |
| $K_{Dissoc}$ | $> (1.0 \pm 0.9) \times 10^{-2}\ M$ |
| $k_{PhS}$ | $(2.2 \pm 0.6) \times 10^{-2}\ M^{-1}s^{-1}$ |
| $k_{calc}$ | $(8 \pm 4) \times 10^{-5}\ s^{-1}$ |

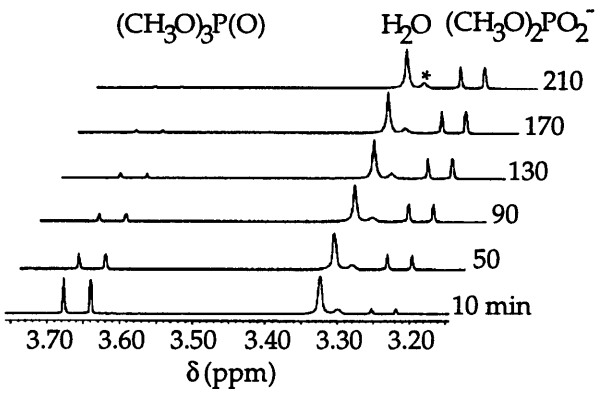


**Figure 1.1.** Aliphatic region $^{1}H$ NMR spectral changes used to follow the stoichiometric reaction of $[(CH_3)_4N]_2[Zn(SC_6H_5)_4]$ and $(CH_3O)_3PO$ in DMSO-*d6*. The reaction was run under pseudo-first-order conditions with excess $[(CH_3)_4N]_2[Zn(SC_6H_5)_4]$. The asterisk indicates a signal arising from $^{13}C$-$^{1}H$ coupling of the $(CH_3)_4N^+$ counterion.

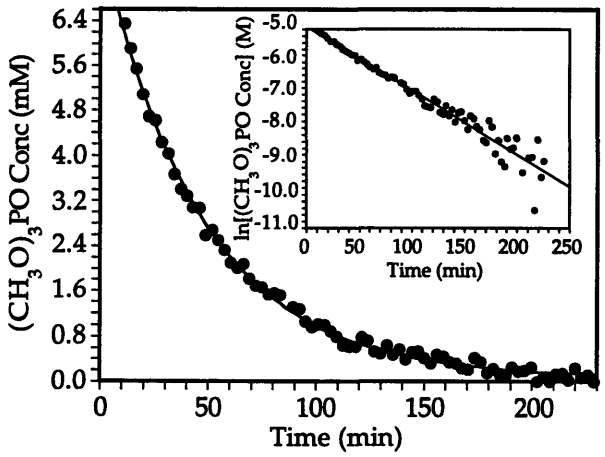


**Figure 1.2.** $(CH_3O)_3PO$ concentration versus time plot for a typical kinetic run of the reaction between $[(CH_3)_4N]_2[Zn(SC_6H_5)_4]$ and $(CH_3O)_3PO$. Pseudo-first-order conditions with $[(CH_3)_4N]_2[Zn(SC_6H_5)_4]$ in excess were employed. The data are fit to a first-order decay. The inset displays the natural log of $(CH_3O)_3PO$ concentration plotted against time. These data are fit to a line.

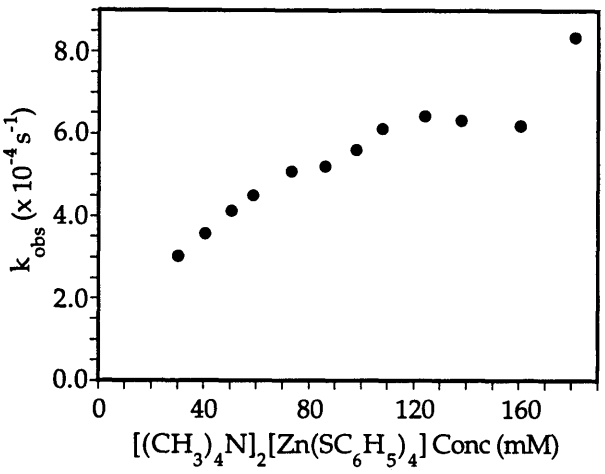


**Figure 1.3.** A $k_{obs}$ versus $[(CH_3)_4N]_2[Zn(SC_6H_5)_4]$ concentration plot. The $(CH_3O)_3PO$ concentration remained constant at 8.5 mM and $[(CH_3)_4N]_2[Zn(SC_6H_5)_4]$ concentration was varied over the range indicated.

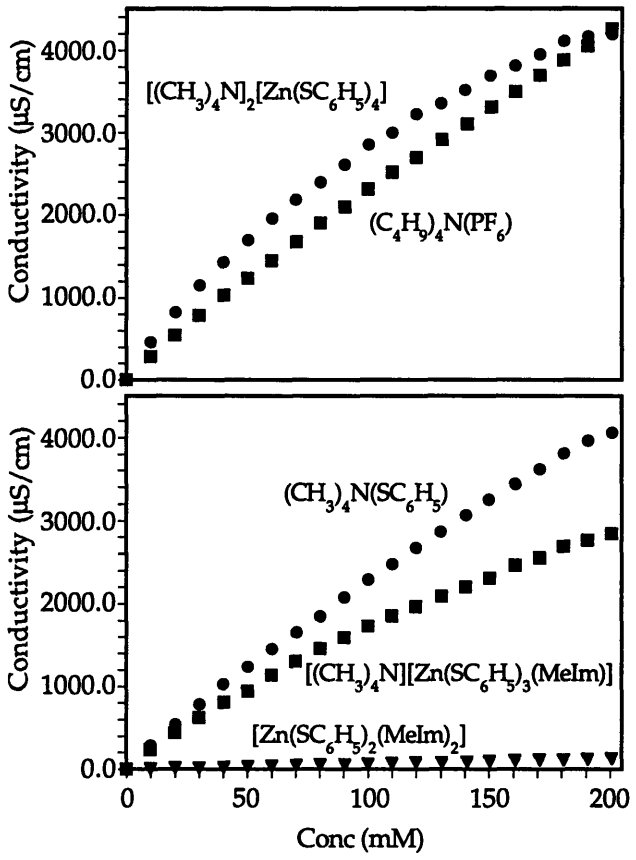


**Figure 1.4.** Conductivity versus concentration plots of $[(CH_3)_4N]_2[Zn(SC_6H_5)_4]$ (top), $(C_4H_9)_4N(PF_6)$ (top), $[(CH_3)_4N][Zn(SC_6H_5)_3(MeIm)]$ (bottom), $[Zn(SC_6H_5)_2(MeIm)_2]$ (bottom), and $(CH_3)_4N(SC_6H_5)$ (bottom) in DMSO.

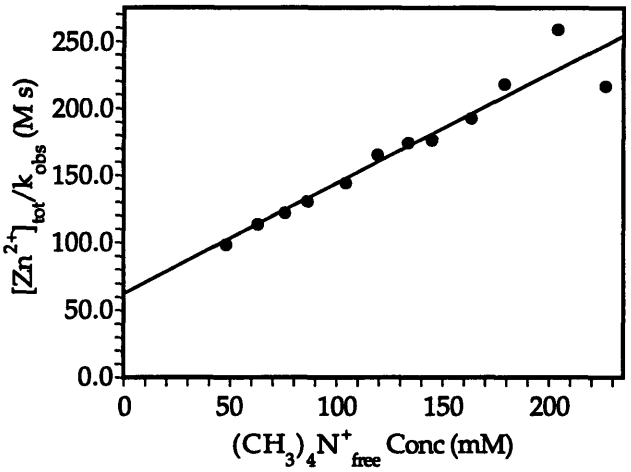


**Figure 1.5.** Final iteration of the $[Zn^{2+}]_{tot}/k_{obs}$ versus $[(CH_3)_4N^+_{free}]$ plots with a linear curve fit. The inverse ordinate intercept affords a second-order rate constant, $k_{Zn}$, of $(1.6 \pm 0.3) \times 10^{-2}$ $M^{-1}s^{-1}$. The slope of $K_{IP}/k_{Zn}$ yields an ion pairing equilibrium constant, $K_{IP}$, of $13 \pm 4$ $M^{-1}$.

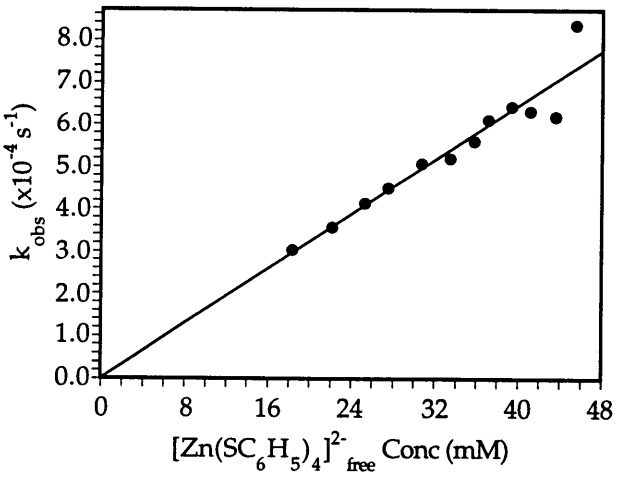


**Figure 1.6.** A $k_{obs}$ versus $[\{Zn(SC_6H_5)_4\}^{2-}]_{free}$ concentration plot with a linear curve fit indicating a first-order dependence of the reaction between $[(CH_3)_4N]_2[Zn(SC_6H_5)_4]$ and $(CH_3O)_3PO$ on $[\{Zn(SC_6H_5)_4\}^{2-}]_{free}$ concentration.

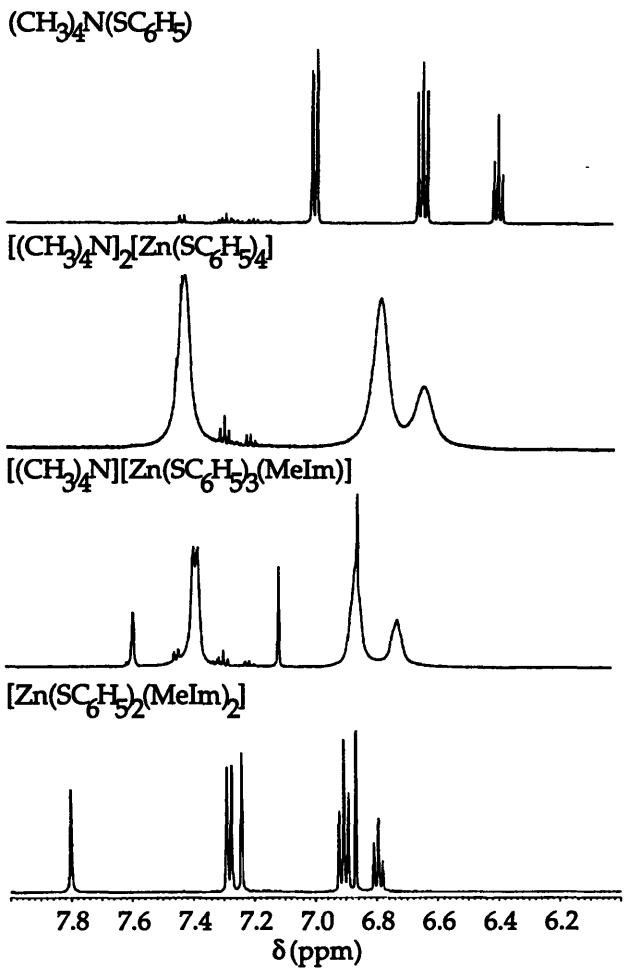


**Figure 1.7.** Aromatic region $^1H$ NMR spectra of $(CH_3)_4N(SC_6H_5)$, $[(CH_3)_4N]_2[Zn(SC_6H_5)_4]$, $[(CH_3)_4N][Zn(SC_6H_5)_3(MeIm)]$, and $[Zn(SC_6H_5)_2(MeIm)_2]$ in DMSO-*d6*.

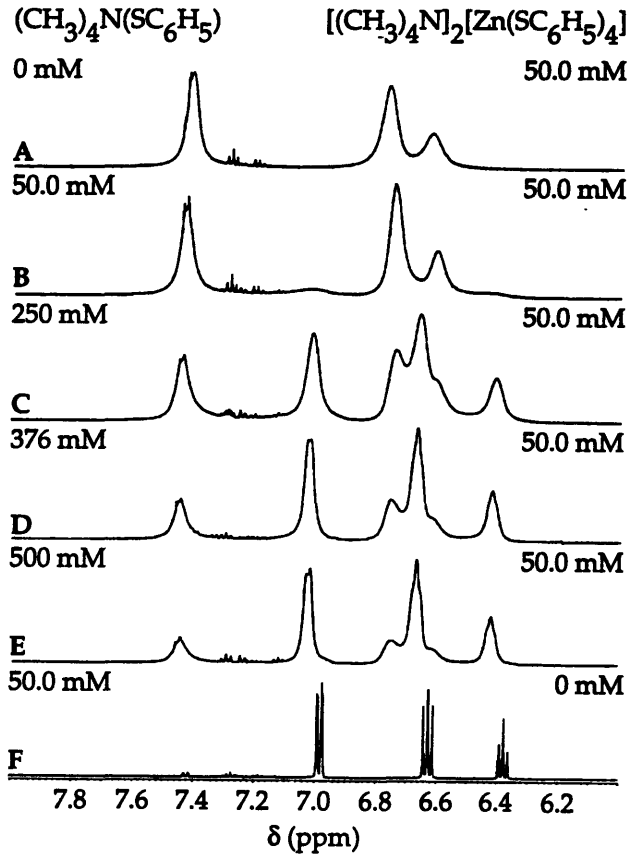


**Figure 1.8.** $^1$H NMR spectra of 50.0 mM $[(CH_3)_4N]_2[Zn(SC_6H_5)_4]$ (A), 50.0 mM $(CH_3)_4N(SC_6H_5)$ and 50.0 mM $[(CH_3)_4N]_2[Zn(SC_6H_5)_4]$ (1:1 ratio) (B), 250 mM $(CH_3)_4N(SC_6H_5)$ and 50.0 mM $[(CH_3)_4N]_2[Zn(SC_6H_5)_4]$ (5:1 ratio) (C), 376 mM $(CH_3)_4N(SC_6H_5)$ and 50.0 mM $[(CH_3)_4N]_2[Zn(SC_6H_5)_4]$ (7.5:1 ratio) (D), 500 mM $(CH_3)_4N(SC_6H_5)$ and 50.0 mM $[(CH_3)_4N]_2[Zn(SC_6H_5)_4]$ (10:1 ratio) (E), and 50.0 mM $(CH_3)_4N(SC_6H_5)$ (F) in DMSO-*d6*.

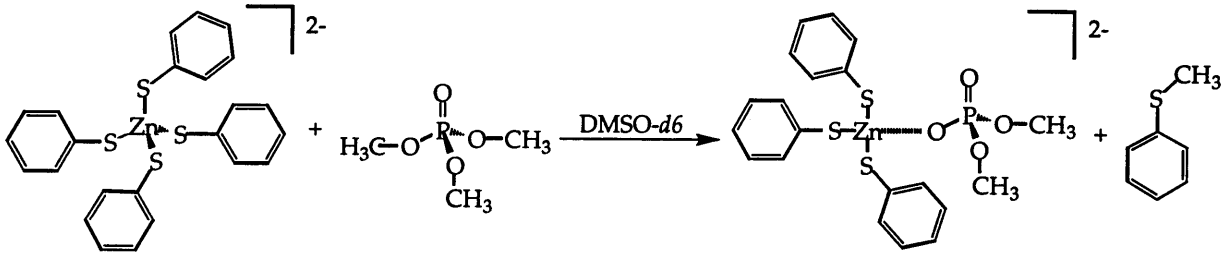


**Scheme 1.1**

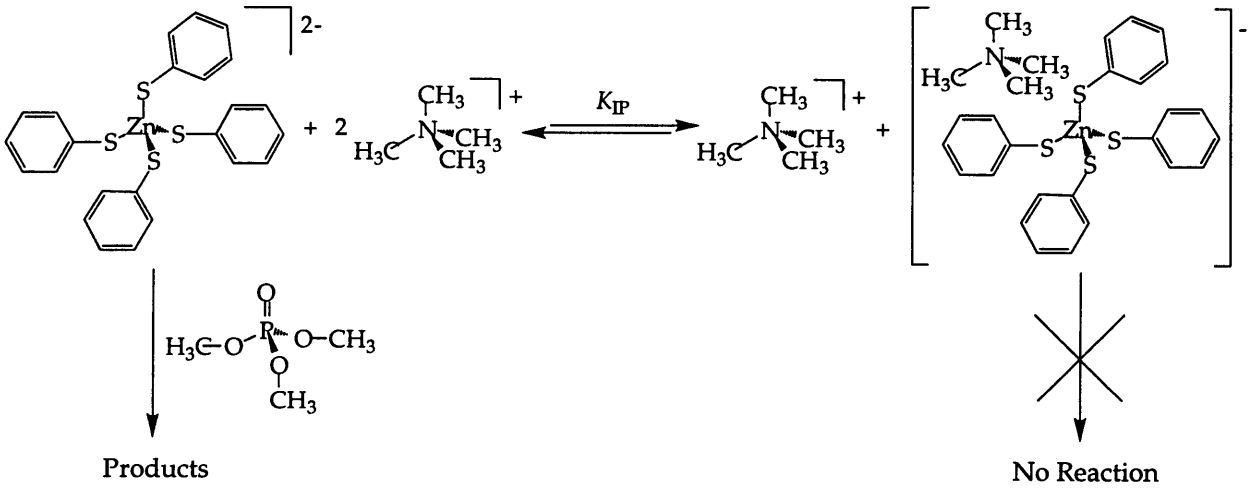


**Scheme 1.2**

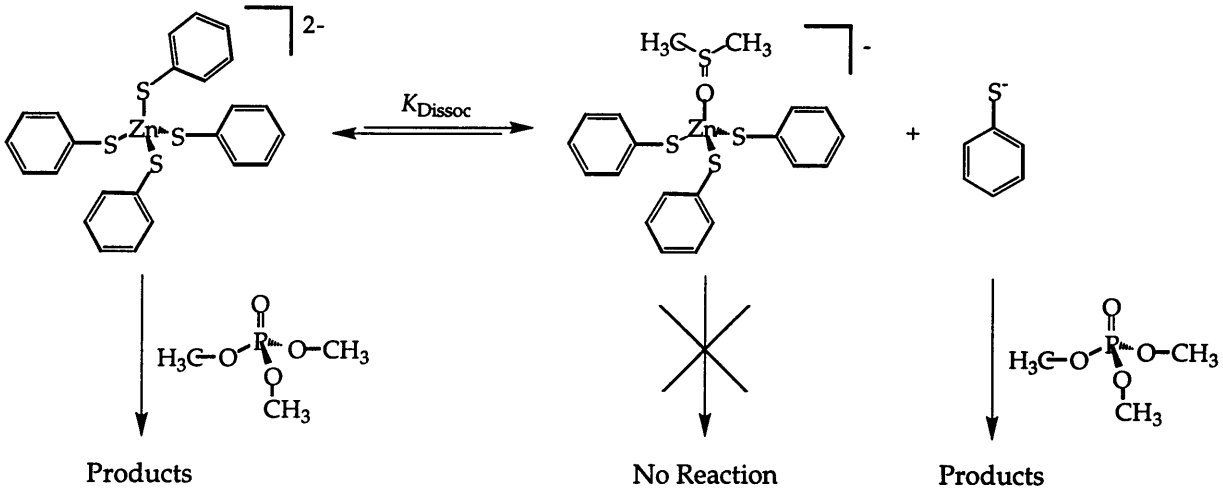


**Scheme 1.3**

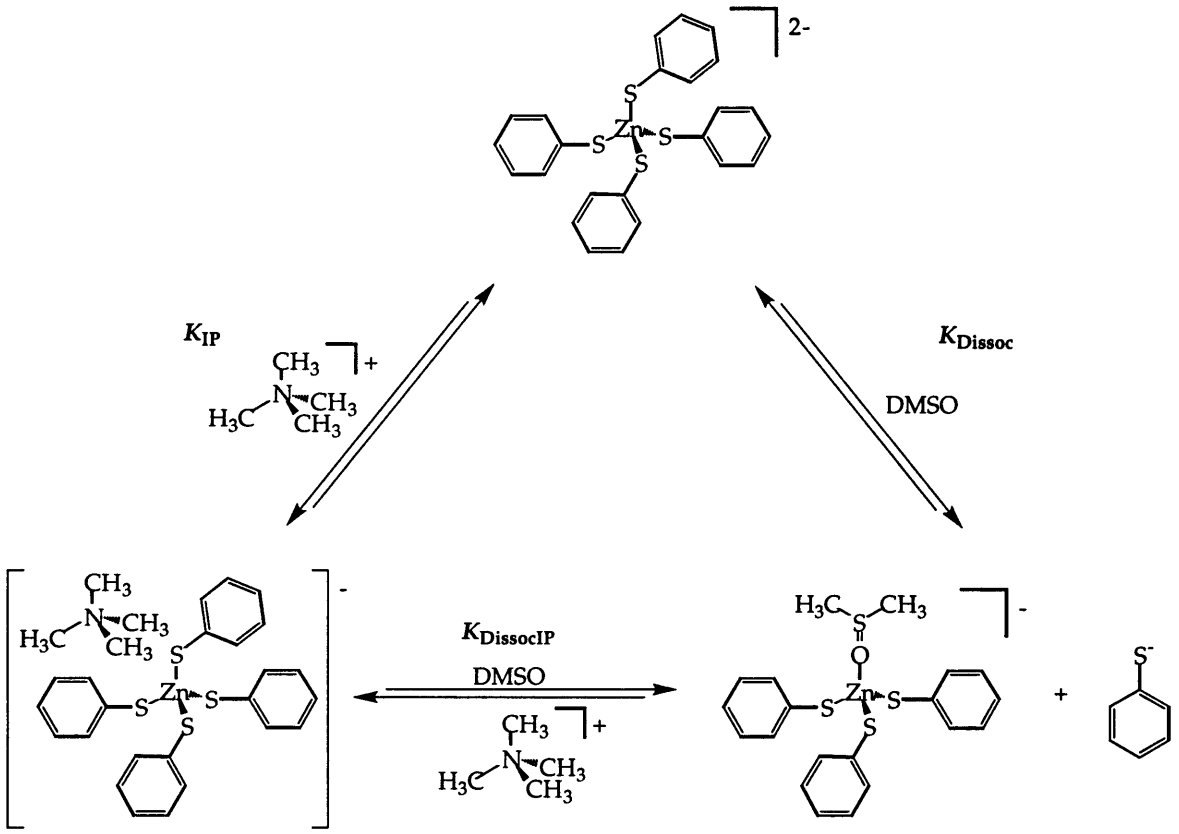


**Scheme 1.4**

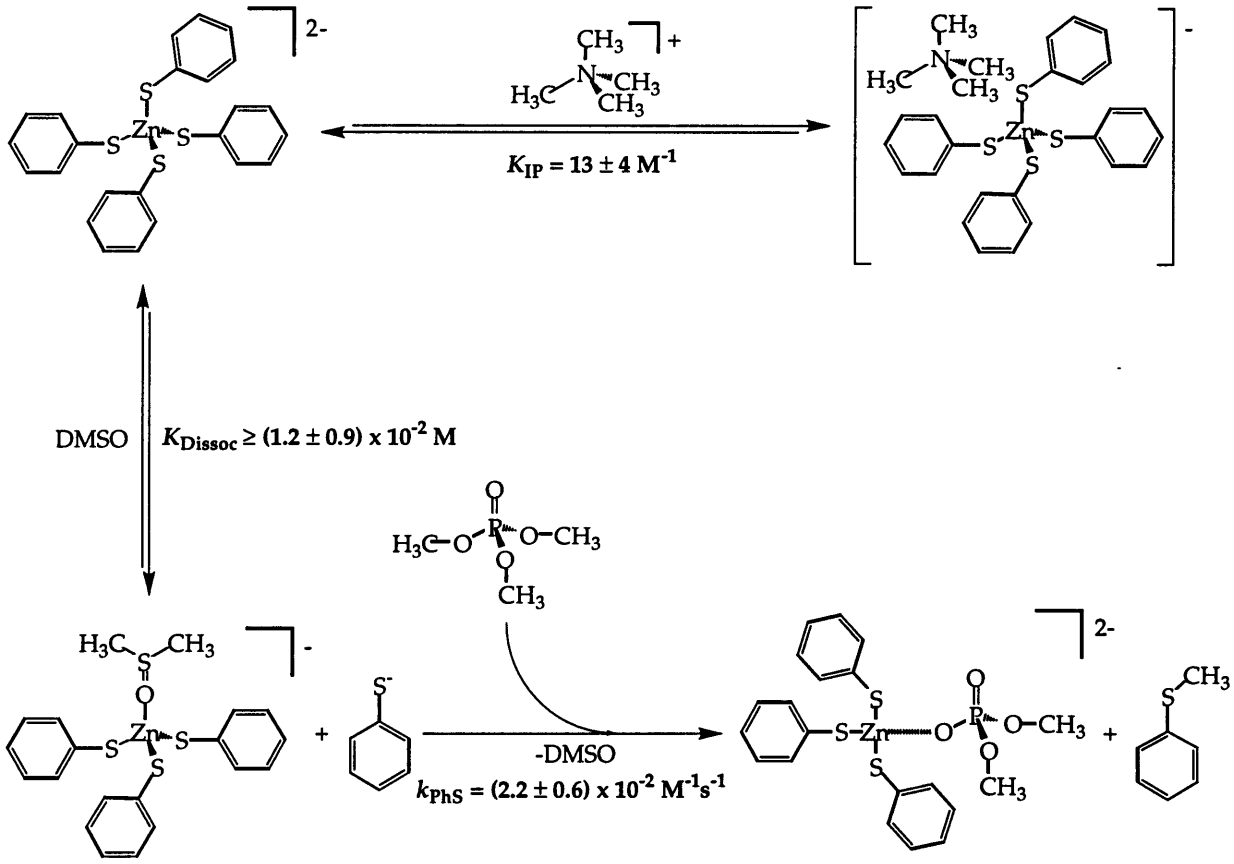
2-
+
$K_{IP} = 13 \pm 4\ M^{-1}$
-
DMSO
$K_{Dissoc} \geq (1.2 \pm 0.9) \times 10^{-2}$ M
-
+
-DMSO
$k_{PhS} = (2.2 \pm 0.6) \times 10^{-2}\ M^{-1}s^{-1}$
2-
+

**Scheme 1.5**

# Appendices

for

Chapter One

Alkyl Transfer to Metal Thiolates:
Kinetics, Active Species Identification, and Relevance to the DNA
Methylphosphotriester Repair Center of *Escherichia coli* Ada

**Appendix A1.1** Derivation of eq 1.4,

$$[(CH_3)_4N^+]_{free} = \frac{k_{Zn}\,[Zn^{2+}]_{tot} - k_{obs}}{K_{IP}\,k_{obs}}$$

**Appendix A1.2** Derivation of eq 1.5,

$$[(CH_3)_4N^+]_{free} = \frac{K_{IP}\,[Zn^{2+}]_{tot} - 1 \pm \left((K_{IP}\,[Zn^{2+}]_{tot})^2 + 6K_{IP}\,[Zn^{2+}]_{tot} + 1\right)^{1/2}}{2\,K_{IP}}$$

**Appendix A1.3** Derivation of eq 1.16,

$$[C_6H_5S^-] = \frac{-K_{Dissoc} \pm \left(K_{Dissoc}{}^2 + 4\,K_{Dissoc}\,[Zn_{start}]\right)^{1/2}}{2}$$

**Appendix A1.1** Derivation of eq 1.4.

$$[(CH_3)_4N^+]_{free} = \frac{k_{Zn}\,[Zn^{2+}]_{tot} - k_{obs}}{K_{IP}\,k_{obs}}$$

$$k_{obs} = k_{Zn}\,[\{Zn(SC_6H_5)_4\}^{2-}]_{free} \tag{A1.1.1}$$

$$k_{obs} = k_{Zn}\,[\{Zn(SC_6H_5)_4\}^{2-}]_{free}\,\frac{[Zn^{2+}]_{tot}}{[Zn^{2+}]_{tot}} \tag{A1.1.2}$$

$$[Zn^{2+}]_{tot} = [\{Zn(SC_6H_5)_4\}^{2-}]_{free} + [\{[(CH_3)_4N][Zn(SC_6H_5)_4]\}^-] \tag{A1.1.3}$$

$$k_{obs} = \frac{k\,[\{Zn(SC_6H_5)_4\}^{2-}]_{free}\,[Zn^{2+}]_{tot}}{[\{Zn(SC_6H_5)_4\}^{2-}]_{free} + [\{[(CH_3)_4N][Zn(SC_6H_5)_4]\}^-]} \tag{A1.1.4}$$

$$K_{IP} = \frac{[\{(CH_3)_4][Zn(SC_6H_5)_4]\}^-]}{[\{Zn(SC_6H_5)_4\}^{2-}]_{free}\,[(CH_3)_4N^+]_{free}} \tag{A1.1.5}$$

$$[\{[(CH_3)_4N][Zn(SC_6H_5)_4]\}^-] = K_{IP}\,[\{Zn(SC_6H_5)_4\}^{2-}]_{free}\,[(CH_3)_4N^+]_{free} \tag{A1.1.6}$$

$$k_{obs} = \frac{k_{Zn}\,[\{Zn(SC_6H_5)_4\}^{2-}]_{free}\,[Zn^{2+}]_{tot}}{[\{Zn(SC_6H_5)_4\}^{2-}]_{free} + K_{IP}\,[\{Zn(SC_6H_5)_4\}^{2-}]_{free}\,[(CH_3)_4N^+]_{free}} \tag{A1.1.7}$$

$$k_{obs} = \frac{k_{Zn}\,[Zn^{2+}]_{tot}}{1 + K_{IP}\,[(CH_3)_4N^+]_{free}} \tag{A1.1.8}$$

$$[(CH_3)_4N^+]_{free} = \frac{k_{Zn}\,[Zn^{2+}]_{tot} - k_{obs}}{K_{IP}\,k_{obs}} \tag{A1.1.9}$$

**Appendix A1.2** Derivation of eq 1.5.

$$[(CH_3)_4N^+]_{free} = \frac{K_{IP}\,[Zn^{2+}]_{tot} - 1 \pm \left((K_{IP}\,[Zn^{2+}]_{tot})^2 + 6K_{IP}\,[Zn^{2+}]_{tot} + 1\right)^{1/2}}{2\,K_{IP}}$$

$$K_{IP} = \frac{[\{(CH_3)_4][Zn(SC_6H_5)_4]\}^-]}{[\{Zn(SC_6H_5)_4\}^{2-}]_{free}\,[(CH_3)_4N^+]_{free}} \qquad \text{(A1.2.1)}$$

$$[Zn^{2+}]_{tot} = [\{Zn(SC_6H_5)_4\}^{2-}]_{free} + [\{[(CH_3)_4N][Zn(SC_6H_5)_4]\}^-] \qquad \text{(A1.2.2)}$$

$$[\{Zn(SC_6H_5)_4\}^{2-}]_{free} = [Zn^{2+}]_{tot} - [\{[(CH_3)_4N][Zn(SC_6H_5)_4]\}^-] \qquad \text{(A1.2.3)}$$

$$K_{IP} = \frac{[\{(CH_3)_4][Zn(SC_6H_5)_4]\}^-]}{\left\{[Zn^{2+}]_{tot} - [\{(CH_3)_4][Zn(SC_6H_5)_4]\}^-]\right\}\,[(CH_3)_4N^+]_{free}} \qquad \text{(A1.2.4)}$$

$$[(CH_3)_4N^+]_{free} = \frac{[\{(CH_3)_4][Zn(SC_6H_5)_4]\}^-]}{K_{IP}\,[Zn^{2+}]_{tot} - K_{IP}\left\{[\{(CH_3)_4][Zn(SC_6H_5)_4]\}^-]\right\}} \qquad \text{(A1.2.5)}$$

$$[(CH_3)_4N^+]_{total} = [(CH_3)_4N^+]_{free} + [\{[(CH_3)_4N][Zn(SC_6H_5)_4]\}^-] \qquad \text{(A1.2.6)}$$

$$[(CH_3)_4N^+]_{free} = [(CH_3)_4N^+]_{total} - [\{[(CH_3)_4N][Zn(SC_6H_5)_4]\}^-] \qquad \text{(A1.2.7)}$$

$$[(CH_3)_4N^+]_{total} = 2\,[Zn^{2+}]_{tot} \qquad \text{(A1.2.8)}$$

$$[(CH_3)_4N^+]_{free} = 2\,[Zn^{2+}]_{tot} - [\{[(CH_3)_4N][Zn(SC_6H_5)_4]\}^-] \qquad \text{(A1.2.9)}$$

$$[\{[(CH_3)_4N][Zn(SC_6H_5)_4]\}^-] = 2\,[Zn^{2+}]_{tot} - [(CH_3)_4N^+]_{free} \qquad \text{(A1.2.10)}$$

$$[(CH_3)_4N^+]_{free} = \frac{2\,[Zn^{2+}]_{tot} - [(CH_3)_4N^+]_{free}}{K_{IP}\,[Zn^{2+}]_{tot} - K_{IP}\left\{2\,[Zn^{2+}]_{tot} - [(CH_3)_4N^+]_{free}\right\}}$$

(A1.2.11)

$$[(CH_3)_4N^+]_{free} = [N^+]_{free} \qquad \text{(A1.2.12)}$$

$$2[Zn^{2+}]_{tot} - [N^+]_{free} = [N^+]_{free}\left\{K_{IP}[Zn^{2+}]_{tot} - K_{IP}\left(2[Zn^{2+}]_{tot} - [N^+]_{free}\right)\right\}$$

(A1.2.13)

$$2\,[Zn^{2+}]_{tot} - [N^+]_{free} =$$

$$K_{IP}\,[Zn^{2+}]_{tot}\,[N^+]_{free} - 2\,K_{IP}\,[Zn^{2+}]_{tot}\,[N^+]_{free} + K_{IP}\,([N^+]_{free})^2 \qquad \text{(A1.2.14)}$$

$$K_{IP}([N^+]_{free})^2 + [N^+]_{free}\left(K_{IP}[Zn^{2+}]_{tot} - 2K_{IP}[Zn^{2+}]_{tot} + 1\right) - 2[Zn^{2+}]_{tot} = 0$$

(A1.2.15)

$$K_{IP}\,([N^+]_{free})^2 - (K_{IP}\,[Zn^{2+}]_{tot} - 1)\,[N^+]_{free} - 2\,[Zn^{2+}]_{tot} = 0 \qquad \text{(A1.2.16)}$$

$$[N^+]_{free} = \frac{K_{IP}\,[Zn^{2+}]_{tot} - 1 \pm \left((-K_{IP}\,[Zn^{2+}]_{tot} + 1)^2 + 4\,K_{IP}\,(2\,[Zn^{2+}]_{tot})\right)^{1/2}}{2\,K_{IP}}$$

(A1.2.17)

$$[N^+]_{free} = \frac{K_{IP}\,[Zn^{2+}]_{tot} - 1 \pm \left((K_{IP}\,[Zn^{2+}]_{tot})^2 + 6\,K_{IP}\,[Zn^{2+}]_{tot} + 1\right)^{1/2}}{2\,K_{IP}}$$

(A1.2.18)

**Appendix A1.3** Derivation of eq 1.19.

$$[C_6H_5S^-] = \frac{-K_{Dissoc} \pm \left(K_{Dissoc}{}^2 + 4\,K_{Dissoc}\,[Zn_{start}]\right)^{1/2}}{2}$$

$$K_{Dissoc} = \frac{[\{Zn(SC_6H_5)_3(DMSO)\}^-]\,[C_6H_5S^-]}{[\{Zn(SC_6H_5)_4\}^{2-}]} \qquad \text{(A1.3.1)}$$

$$[C_6H_5S^-] = [\{Zn(SC_6H_5)_3(DMSO)\}^-] \qquad \text{(A1.3.2)}$$

$$K_{Dissoc} = \frac{[C_6H_5S^-]^2}{[\{Zn(SC_6H_5)_4\}^{2-}]} \qquad \text{(A1.3.3)}$$

$$[Zn^{2+}]_{start} = [\{Zn(SC_6H_5)_4\}^{2-}] + [\{Zn(SC_6H_5)_3(DMSO)\}^-] \qquad \text{(A1.3.4)}$$

$$[\{Zn(SC_6H_5)_4\}^{2-}] = [Zn^{2+}]_{start} - [C_6H_5S^-] \qquad \text{(A1.3.5)}$$

$$K_{Dissoc} = \frac{[C_6H_5S^-]^2}{[Zn^{2+}]_{start} - [C_6H_5S^-]} \qquad \text{(A1.3.6)}$$

$$[C_6H_5S^-]^2 = K_{Dissoc}\,[Zn^{2+}]_{start} - K_{Dissoc}\,[C_6H_5S^-] \qquad \text{(A1.3.7)}$$

$$[C_6H_5S^-]^2 + K_{Dissoc}\,[C_6H_5S^-] - K_{Dissoc}\,[Zn^{2+}]_{start} = 0 \qquad \text{(A1.3.8)}$$

$$[C_6H_5S^-] = \frac{-K_{Dissoc} \pm \left(K_{Dissoc}{}^2 + 4\,K_{Dissoc}\,[Zn^{2+}]_{start}\right)^{1/2}}{2} \qquad \text{(A1.3.9)}$$

*Chapter Two*

# Synthesis and X-ray Crystallographic Study of Models for Zinc Protein Sites

**Abstract**

In this chapter, we provide the syntheses and single crystal X-ray structures of three new thiolate complexes. The compound $[(CH_3)_4N][Zn(SC_6H_5)_3(MeIm)]$ (MeIm = 1-methylimidazole) was prepared to mimic a protein $[Zn(S\text{-cys})_3(N\text{-histidine})]^-$ site. Synthesis of $[Zn(SC_6H_5)_2(MeIm)_2]$ was accomplished to obtain a suitable model for the zinc finger protein moiety $[Zn(S\text{-cys})_2(N\text{-his})_2]$. The cobalt species $[Co(SC_6H_5)_2(MeIm)_2]$ was prepared and shown to be isomorphous and isostructural with the zinc analog. Structural comparisons are made with zinc thiolate compounds reported previously.

**Introduction**

In Chapter 1, we described a functional model for repair of DNA alkylation damage by the $[Zn(S\text{-cysteine})_4]^{2-}$ site of *Escherichia coli* Ada. The tetrakis(benzenethiolato)zinc(II) complex $[Zn(SC_6H_5)_4]^{2-}$ was used to mimic the zinc center in Ada and $(CH_3O)_3PO$ represented a DNA alkylphosphotriester lesion. Facile methyl transfer in DMSO solution afforded $[(CH_3)_4N]_2\{Zn(SC_6H_5)_3\text{-}[(CH_3O)_2PO_2]\}$ and $CH_3SC_6H_5$ reaction products. We chose $[(CH_3)_4N]_2[Zn(SC_6H_5)_4]$[1] owing to its simplicity. To date, there are no known examples of isolated tetrakis(*alkyl*thiolato)zinc(II) complexes.

Given the alkyl transfer activity of the $[Zn(S\text{-cys})_4]^{2-}$ center in Ada, we wondered whether alternative zinc thiolate protein sites such as $[Zn(S\text{-cys})_3(N\text{-histidine})]^-$ and $[Zn(S\text{-cys})_2(N\text{-his})_2]$ would be similarly capable of alkylphosphotriester repair. In order to explore this possibility in models, we needed complexes analogous to $[(CH_3)_4N]_2[Zn(SC_6H_5)_4]$ which mimicked $[Zn(S\text{-cys})_3(N\text{-his})]^-$ and $[Zn(S\text{-cys})_2(N\text{-his})_2]$ centers.

The most relevant available complexes were $[(C_3H_7)_4N]\{Zn[S\text{-}2,3,5,6\text{-}(CH_3)_4\text{-}C_6H]_3(MeIm)\}$[2] (MeIm is 1-methylimidazole), $\{Zn[S\text{-}2,3,5,6\text{-}(CH_3)_4\text{-}C_6H]_2(MeIm)_2\}$,[3] and $[Zn\{S\text{-}2,4,6\text{-}[C(CH_3)_3]\text{-}C_6H_2\}_2(MeIm)_2]$[4], depicted in Figure 2.1. These compounds had the correct number of thiolates and MeIm to represent the metal-binding side chain of histidine. The tetrathiolate analogues were lacking, however. To explore the relative reactivity of complexes in a series $[Zn(SR)_{4-x}(Im)_x]^{(2-x)-}$, we required that all members have the same thiolate ligand. Potential steric effects arising from the bulky alkyl groups of the ligands $^-$S-2,3,5,6-$(CH_3)_4$-$C_6H$ and $^-$S-2,4,6-$[C(CH_3)_3]$-$C_6H_2$ are likely to alter the nucleophilicity in these known zinc compounds relative to the thiolates of $[(CH_3)_4N]_2[Zn(SC_6H_5)_4]$. Thus, we attempted to explore the alkyl transfer properties in the $[Zn(SR)_{4-x}(Im)_x]^{(2-x)-}$ series by synthesis of $[(CH_3)_4N][Zn(SC_6H_5)_3\text{-}$

(MeIm)] and $[Zn(SC_6H_5)_2(MeIm)_2]$. The cobalt complex $[Co(SC_6H_5)_2(MeIm)_2]$ was prepared as well.

**Experimental**

**General.** All procedures were carried out under argon or nitrogen atmosphere using standard Schlenk and glove box techniques. NMR spectra were recorded at 25 ± 1 °C on a Varian Unity 300 instrument.

**$[(CH_3)_4N][Zn(SC_6H_5)_3(MeIm)]$.** Anhydrous $ZnCl_2$ (27.5 mmol) was dissolved in a methanol (55 mL) solution of $C_6H_5SH$ (83.1 mmol) and Li metal (83.1 mmol). After stirring for 3 h, MeIm (27.9 mmol) was added and stirring was continued for 2.5 h. Crystalline $(CH_3)_4NCl$ (27.8 mmol) was dissolved in the reaction solution and *n*-$C_4H_9OH$ (50 mL) was added over a 25 min period. The solution was kept at -20 °C overnight. Crystals (23.9 mmol, 87%) were collected by filtration, washed with *n*-$C_4H_9OH$ and dried in vacuo. $^1H$ NMR (DMSO-$d_6$): δ 3.06 (s, 12 H, $(CH_3)_4N^+$), 3.61 (s, 3 H, $-CH_3$), 6.71 (t, 3 H, *p*-H), 6.84 (s, 1 H, imid H-5), 6.85 (t, 6 H, *m*-H), 7.11 (s, 1 H, imid H-4), 7.37 (d, 6 H, *o*-H), 7.60 (s, 1 H, imid H-2). Anal. Calcd for $C_{26}H_{33}N_3S_3Zn$: C, 56.87; H, 6.06; N, 7.65. Found: C, 56.74; H, 6.03; N, 7.58.

**$[Zn(SC_6H_5)_2(MeIm)_2]$.** The compound $[Zn(SC_6H_5)_2(MeIm)_2]$ was prepared by modification of a literature procedure for $\{Zn[S\text{-}2,3,5,6\text{-}(CH_3)_4\text{-}C_6H]_2(MeIm)_2\}$.[3] Anhydrous $ZnCl_2$ (13.6 mmol) was added to an ethanol (250 mL) solution of $C_6H_5SH$ (27.7 mmol) and Li metal (31.1 mmol). After 2 h stirring, MeIm (37.6 mmol) was added and stirring was continued for 15 min. Ethanol was removed in vacuo to yield a white, dry solid. Addition of toluene (250 mL) and refluxing for 2 h resulted in a cloudy solution which was filtered while hot. Slow cooling afforded colorless crystals which were filtered and dried in vacuo. The filtrate was stored at -20 °C overnight to yield a second crop of crystals which were collected by filtration and dried in vacuo. Total yield was 11.1 mmol, 82%. $^1H$ NMR (DMSO-*d6*): δ 3.66 (s,

6 H, -$CH_3$), 6.80 (t, 2 H, *p*-H), 6.87 (s, 2 H, imid H-5), 6.92 (t, 4 H, *m*-H), 7.20 (s, 2 H, imid H-4), 7.29 (d, 4 H, *o*-H), 7.73 (s, 2 H, imid H-2). Anal. Calcd for $C_{20}H_{22}N_4S_2Zn$: C, 53.63; H, 4.95; N, 12.51. Found: C, 54.02; H, 4.91; N, 12.56.

**[$Co(SC_6H_5)_2(MeIm)_2$].** This compound was prepared in a manner similar to that described for [$Zn(SC_6H_5)_2(MeIm)_2$]. Anhydrous cobalt(II) chloride (424 mg, 3.27 mmol) was dissolved in an ethanol (50 ml) solution of thiophenol (724 mg, 6.57 mmol) and lithium metal (51.5 mg, 7.42 mmol). After 2 hours of stirring, 1-methylimidazole (742 mg, 9.04 mmol) was added and stirred for 15 minutes. Ethanol was removed in vacuo to yield a dark green, dry solid. Addition of toluene (50 ml) and refluxing for two h resulted in a dark green, cloudy solution which was filtered while hot. The filtrate was brought to a boil, sealed in the flask and wrapped in cotton for slow cooling. Dark green, tabular crystals (175 mg, 0.396 mmol, 12%) were collected by filtration, washed with pentane and dried in vacuo. Anal. Calcd for $C_{20}H_{22}N_4S_2Co$: C, 54.41; H, 5.02; N, 12.69. Found: C, 54.03; H, 4.89; N, 12.45.

**X-ray Crystallography.** Data collection and reduction were performed as previously described.[5] Briefly, data were collected on an Enraf-Nonius CAD-4F kappa geometry diffractometer with graphite-monochromatized MoKα radiation (λ = 0.71069 Å). An Enraf-Nonius FR558-S liquid nitrogen cryostat was used to maintain crystal temperature at 199 K. SHELXS-86[6] and the TeXsan[7] package of programs were used to solve the structures. Table 2.1 summarizes crystallographic information for the three complexes discussed.

**[$(CH_3)_4N$][$Zn(SC_6H_5)_3(MeIm)$].** A rectangular block measuring ca. 0.22 X 0.23 X 0.37 mm and was mounted on a quartz fiber with vacuum grease. Data were collected by employing the ω-2θ scan technique. No appreciable decay was observed during data collection as evidenced by periodic measurements of three standard reflections. The positions of all non-hydrogen atoms were refined anisotropically. Hydrogen atom positions were calculated.

**$[Zn(SC_6H_5)_2(MeIm)_2]$.** Crystals suitable for X-ray study were grown by pentane diffusion into a chloroform solution of $[Zn(SC_6H_5)_2(MeIm)_2]$. The crystal chosen for analysis, an irregular block measuring ca. 0.25 X 0.28 X 0.32 mm, was mounted on a quartz fiber with vacuum grease. Data were collected by employing the $\omega$-2$\theta$ scan technique. No appreciable decay was observed during data collection as evidenced by periodic measurements of three standard reflections. The positions of all non-hydrogen atoms were refined anisotropically. All hydrogen atoms were found.

**$[Co(SC_6H_5)_2(MeIm)_2]$.** Crystals suitable for X-ray study were grown by pentane diffusion into a chloroform solution of $[Co(SC_6H_5)_2(MeIm)_2]$. The crystal chosen for analysis, an irregular block measuring ca. 0.20 X 0.25 X 0.40 mm, was mounted on a quartz fiber with vacuum grease and paratone oil. Data were collected by employing the $\omega$-2$\theta$ scan technique. No appreciable decay was observed during data collection as evidenced by periodic measurements of three standard reflections. The positions of all non-hydrogen atoms were refined anisotropically. All hydrogen atoms were found.

**Results**

Figure 2.2 displays an ORTEP diagram of the $[Zn(SC_6H_5)_3(MeIm)]^-$ anion. Geometry about the zinc is that of a distorted tetrahedron. The average Zn-S bonds are 2.317(2) Å in length. The single Zn-N bond is 2.072(5) Å. Averaged angles are S-Zn-S at 113.82(7)° and S-Zn-N at 104.8(2)°. Table 2.2 provides the positional parameters with B(eq), and anisotropic thermal parameters are in Table 2.3. All bond lengths are displayed in Table 2.4. Tables 2.5 and 2.6 show bond and torsion angles for this complex.

The structure of $[Zn(SC_6H_5)_2(MeIm)_2]$ also exhibits a distorted tetrahedral structure about the zinc. Figure 2.3 shows an ORTEP diagram of this complex. The averaged Zn-S bond length is 2.2914(7) Å and the averaged Zn-N bond length is

2.039(2) Å. The S-Zn-N angle averaged to 104.49(7)°. The S-Zn-S angle is 128.47(4)° and the N-Zn-N angle is 109.8(1)°. The positional parameters with B(eq) are given in Table 2.7. Table 2.8 shows the anisotropic thermal parameters. Bond lengths are provided in Table 2.9. Bond and torsion angles are provided in Tables 2.10 and 2.11.

The cobalt compound $[Co(SC_6H_5)_2(MeIm)_2]$ is both isomorphous and isostructural with the zinc analog $[Zn(SC_6H_5)_2(MeIm)_2]$. An ORTEP diagram of $[Co(SC_6H_5)_2(MeIm)_2]$ is shown in Figure 2.4. The S-Co-S angle is 126.66(4)° and the N-Co-N angle is 112.9(1)°. The S-Co-N angles average to 104.38(6) Å. Thus, the geometry about the cobalt center is that of a distorted tetrahedron. The average Co-S bond length is 2.2741(6) Å and the average Co-N bond length is 2.019(2) Å. Table 2.12 provides the atomic positional parameters and B(eq). The anisotropic thermal parameters are given in Table 2.13. Tables 2.14 and 2.15 display the bond lengths and angles. Torsional angles are provided in Table 2.16.

**Discussion**

The desired compounds $[(CH_3)_4N][Zn(SC_6H_5)_3(MeIm)]$ and $[Zn(SC_6H_5)_2(MeIm)_2]$ were prepared in high yield and purity in addition to the cobalt analog $[Co(SC_6H_5)_2(MeIm)_2]$. These are the first mononuclear thiolate complexes of these metals not employing bulky or chelating ligands. Previously, sterically bulky thiolates were used to preserve the mononuclear nature of the complexes.[3] Better mimics of $[Zn(S\text{-cys})_3(N\text{-his})]^-$ and $[Zn(S\text{-cys})_2(N\text{-his})_2]$ protein centers will encompass monodentate, aliphatic thiolate ligands such as $^-SC_2H_5$. At the moment, no isolated examples exist.

The new compound $[(CH_3)_4N][Zn(SC_6H_5)_3(MeIm)]$ has bond lengths and angles rather similar to the literature compound $[(C_3H_7)_4N]\{Zn[S\text{-}2,3,5,6\text{-}(CH_3)_4\text{-}C_6H]_3(MeIm)\}$.[2] These bonds and angles are compared in Table 2.17. Such similarities are somewhat surprising in light of the fact that the $^-CH_3$ groups in the 2

and 6 positions of the $^{-}$S-2,3,5,6-$(CH_3)_4$-$C_6H$ ligand are expected to create a degree of steric crowding about the metal center relative to the smaller $^{-}SC_6H_5$ ligands of $[(CH_3)_4N][Zn(SC_6H_5)_3(MeIm)]$.

Bond lengths and angles of $[Zn(SC_6H_5)_2(MeIm)_2]$ are significantly different from those in the compounds $\{Zn[S\text{-}2,3,5,6\text{-}(CH_3)_4\text{-}C_6H]_2(MeIm)_2\}$ and $[Zn\{S\text{-}2,4,6\text{-}[C(CH_3)_3]\text{-}C_6H_2\}_2(MeIm)_2]$, reported previously. Tables 2.17 includes the geometrical parameters about the zinc atoms for these three compounds. Most interesting is the 128.47(4)° S-Zn-S angle of $[Zn(SC_6H_5)_2(MeIm)_2]$ relative to the smaller angles of 109.46(8)° for $\{Zn[S\text{-}2,3,5,6\text{-}(CH_3)_4\text{-}C_6H]_2(MeIm)_2\}$ and 115.5(1)° for $[Zn\{S\text{-}2,4,6\text{-}[C(CH_3)_3]\text{-}C_6H_2\}_2(MeIm)_2]$. Additionally, the 109.9(1)° N-Zn-N angle of $[Zn(SC_6H_5)_2(MeIm)_2]$ is larger than those of $\{Zn[S\text{-}2,3,5,6\text{-}(CH_3)_4\text{-}C_6H]_2(MeIm)_2\}$ and $[Zn\{S\text{-}2,4,6\text{-}[C(CH_3)_3]\text{-}C_6H_2\}_2(MeIm)_2]$ at 101.9(2)° and 101.7(4)°. We have no satisfactory explanation for this trend at the moment.

The cobalt(II) complex $[Co(SC_6H_5)_2(MeIm)_2]$ is isomorphous and isostructural with its zinc analog, $[Zn(SC_6H_5)_2(MeIm)_2]$. Small differences in bond lengths and angles between these two compounds provide a nice comparison of zinc(II) and cobalt(II) binding differences under similar conditions. Table 2.17 details these variations. In general, the bond lengths are 0.02 Å shorter for the cobalt complex. The S-M-S angle is 2° smaller for cobalt and the N-M-N angle is 3° larger for zinc. These structural differences are small and reflect the smaller 0.72 Å covalent radius of four-coordinate cobalt(II) compared to the 0.74 Å radius of four-coordinate zinc(II).[8]

With the compounds $[Zn(SR)_{4-x}(Im)_x]^{(2-x)-}$ in hand, we are now able to examine structural trends in bond lengths and angles. Table 2.17 provides bond length and angle data for $[(CH_3)_4N]_2[Zn(SC_6H_5)_4]$,[9] $[(CH_3)_4N][Zn(SC_6H_5)_3(MeIm)]$, and $[Zn(SC_6H_5)_2(MeIm)_2]$. An approximate 0.03 Å decrease in average Zn-S bond length results from a decreasing number of thiolate ligands. The average Zn-N

bond lengths are also 0.03 Å shorter with fewer thiolates present. We attribute these differences to the effects of charge compensation. The $[Zn(SC_6H_5)_4]^{2-}$ dianion requires less electron density from each ligand relative to the other, less charged species resulting in longer metal-ligand bond lengths. The S-Zn-S angles also display a trend increasing in the order $[(CH_3)_4N]_2[Zn(SC_6H_5)_4]$ < $[(CH_3)_4N][Zn(SC_6H_5)_3(MeIm)]$ < $[Zn(SC_6H_5)_2(MeIm)_2]$ at 109.5°, 113.83(7)°, and 128.47(4)°. These data can be rationalized by shorter bond lengths in the less charged species bringing the ligands closer to one another and forcing them apart, providing the larger S-Zn-S angles.

**Conclusions**

We have prepared and characterized new model complexes representing $[Zn(S\text{-cys})_3(N\text{-his})]^-$ and $[Zn(S\text{-cys})_2(N\text{-his})_2]$ protein centers. These compounds have sterically undemanding ligands and, as such, are likely to have structural characteristics closer to the biological sites than any models reported previously. X-ray crystallographic studies of these compounds revealed structural trends in the $[Zn(SR)_{4-x}(Im)_x]^{(2-x)-}$ series. Shorter bond lengths and increased S-Zn-S angles with decreasing number of thiolate ligands were observed. We ascribed these results to charge differences in the complexes.

**References**

(1) Dance, I. G.; Choy, A.; Scudder, M. L. *J. Am. Chem. Soc.* **1984**, *106*, 6285-6295.

(2) Corwin, D. T.; Gruff, E. S.; Koch, S. A. *Inorg. Chim. Acta* **1988**, *151*, 5-6.

(3) Corwin, D. T.; Koch, S. A. *Inorg. Chem.* **1988**, *27*, 493-496.

(4) Bochman, M.; Bwembya, G. C.; Grinter, R.; Powell, A. K.; Webb, K. J.; Hursthouse, M. B.; Malik, K. M. A.; Mazid, M. A. *Inorg. Chem.* **1994**, *33*, 2290-2296.

(5) Carnahan, E. M.; Rardin, R. L.; Bott, S. G.; Lippard, S. J. *Inorg. Chem.* **1992**, *31*, 5193-5201.

(6) Sheldrick, G. M.; Hruger, C.; Goddard, R. *Crystallographic Computing 3*; Sheldrick, G. M.; Hruger, C.; Goddard, R., Ed.; Oxford University Press: Oxford, 1985, pp 175-189.

(7) *TEXSAN: Single Crystal Structure Analysis Software, Version 1.6*; Molecular Structure Corporation: The Sugarlands, TX, 1992.

(8) Shannon, R. D. *Acta Cryst.* **1976**, *A32*, 751-767.

(9) Ueyama, N.; Sugawara, T.; Sasaki, K.; Nakamura, A.; Yamashita, S.; Wakatsuki, Y.; Yamazaki, H.; Yasuoka, N. *Inorg. Chem.* **1988**, *27*, 741-747.

**Table 2.1.** Crystallographic Information for $[(CH_3)_4N][Zn(SC_6H_5)_3(MeIm)]$, $[Zn(SC_6H_5)_2(MeIm)_2]$, and $[Co(SC_6H_5)_2(MeIm)_2]$

| | $[(CH_3)_4N][Zn(SC_6H_5)_3(MeIm)]$ | $[Zn(SC_6H_5)_2(MeIm)_2]$ | $[Co(SC_6H_5)_2(MeIm)_2]$ |
|---|---|---|---|
| Formula | $C_{26}H_{33}N_3S_3Zn$ | $C_{20}H_{22}N_4S_2Zn$ | $C_{20}H_{22}N_4S_2Co$ |
| Formula weight | 549.16 | 447.95 | 441.49 |
| Crystal system | monoclinic | monoclinic | monoclinic |
| Space group | $P2_1/n$ | C2/c | C2/c |
| *a*, Å | 10.330(5) | 12.372(2) | 12.397(2) |
| *b*, Å | 25.758(2) | 18.703(2) | 18.691(3) |
| *c*, Å | 10.580(1) | 9.329(2) | 9.290(1) |
| β, degrees | 102.00(1) | 100.60(2) | 100.961(8) |
| V, Å$^3$ | 2754(2) | 2121.7(6) | 2113.5(5) |
| Z | 4 | 4 | 4 |
| $d_{calc}$, g cm$^{-3}$ | 1.325 | 1.396 | 1.387 |
| T, K | 199 | 199 | 199 |
| Data collection range deg | $3 \le 2\theta \le 51$ | $3 \le 2\theta \le 55$ | $3 \le 2\theta \le 55$ |
| Data limits | $+h+k\pm l$ | $+h+k\pm l$ | $+h+k\pm l$ |
| Number of data collected | 5753 | 3273 | 3619 |
| p-Factor[a] | 0.031 | 0.030 | 0.030 |
| R(merge)[b] | 0.050 | 0.025 | 0.018 |
| Number of observed unique data[c] | 2574 | 1894 | 1854 |
| Number of parameters | 298 | 123 | 127 |

| | | | |
|---|---|---|---|
| Data/parameter ratio | 8.6 | 15.4 | 14.6 |
| Abs coefficient, $cm^{-1}$ | 11.4 | 13.7 | 10.2 |
| Trans. coefficient, min/max | 0.4758/0.9944 | 0.8898/1.0000 | 0.9215/1.000 |
| $R^d$ | 0.048 | 0.036 | 0.033 |
| $R_w{}^e$ | 0.055 | 0.040 | 0.040 |
| Largest shift/esd, final | 0.000 | 0.000 | 0.000 |
| Largest peak, $e^-/Å^3$ | 0.619 | 0.393 | 0.258 |

[a]Used in the calculation of $\sigma(F^2)$. [b]$R(merge) = \Sigma^n_{i=1}\Sigma^m_{j=1} | \langle F_i^2\rangle - F_{ij}^2 | / \Sigma^n_{i=1} m \times \langle F_i^2\rangle$ where $n$ = number unique reflections observed more than once, $m$ = number of times a given reflection was observed, and $\langle F_i^2\rangle$ is the average value of $F^2$ for reflection $i$. [c]Observation criterion $I > 3\sigma(I)$. [d]$R = [\Sigma | |F_o| - |F_c| | / \Sigma |F_o|]^{1/2}$. [e]$R_w = [\Sigma_w(|F_o| - |F_c|)^2 / \Sigma_w |F_o|^2]^{1/2}$, where $w = 1/\sigma^2(F)$ and $\sigma(F) = [A^2S^2(C + 4B) + (pI)^2]^{1/2}/(2F_oLpTD)$. $A$ is an attenuation factor, $S$ is the scan rate, $C$ is the total number if integrated counts, $B$ is the sum of the left and right backgrounds, $Lp$ is a term to correct for Lorentz and polarization effects, $T$ is the transmission coefficient, and $D$ is a decay correction factor.

**Table 2.2.** Positional parameters and B(eq) for $[(CH_3)_4N][Zn(SC_6H_5)_3(MeIm)]^a$

| atom | x | y | z | B(eq)[b] |
|---|---|---|---|---|
| Zn(1) | 0.02776(7) | 0.85541(3) | 0.20119(7) | 2.45(3) |
| S(1) | -0.1270(2) | 0.79319(7) | 0.1139(2) | 3.14(8) |
| S(2) | 0.2181(2) | 0.83700(7) | 0.1254(2) | 3.25(8) |
| S(3) | 0.0795(2) | 0.87720(7) | 0.4180(2) | 2.84(7) |
| N(1) | -0.0670(5) | 0.9209(2) | 0.1130(5) | 2.6(2) |
| N(2) | -0.1517(5) | 0.9994(2) | 0.0946(5) | 3.3(3) |
| N(3) | -0.0108(5) | 0.2257(2) | 0.2643(5) | 2.9(3) |
| C(1) | -0.0632(6) | 0.7316(3) | 0.1700(6) | 2.5(3) |
| C(2) | 0.0346(6) | 0.7252(3) | 0.2825(6) | 2.7(3) |
| C(3) | 0.0729(7) | 0.6761(3) | 0.3257(6) | 3.4(3) |
| C(4) | 0.0175(7) | 0.6325(3) | 0.2614(7) | 3.5(3) |
| C(5) | -0.0776(7) | 0.6385(3) | 0.1491(7) | 3.7(3) |
| C(6) | -0.1161(6) | 0.6874(3) | 0.1046(6) | 3.2(3) |
| C(7) | 0.3383(6) | 0.8861(3) | 0.1660(6) | 2.9(3) |
| C(8) | 0.4372(7) | 0.8903(3) | 0.0959(7) | 4.0(4) |
| C(9) | 0.5343(8) | 0.9272(4) | 0.1225(9) | 5.6(5) |
| C(10) | 0.5343(8) | 0.9622(4) | 0.221(1) | 6.0(5) |
| C(11) | 0.4385(7) | 0.9583(3) | 0.2937(8) | 4.8(4) |
| C(12) | 0.3413(6) | 0.9210(3) | 0.2661(7) | 3.4(3) |
| C(13) | -0.0664(6) | 0.8961(3) | 0.4641(6) | 2.8(3) |
| C(14) | -0.0638(7) | 0.9379(3) | 0.5494(7) | 3.6(3) |
| C(15) | -0.1741(8) | 0.9526(3) | 0.5943(8) | 4.8(4) |
| C(16) | -0.2882(7) | 0.9258(4) | 0.5577(8) | 4.7(4) |

| | | | | |
|---|---|---|---|---|
| C(17) | -0.2961(7) | 0.8863(3) | 0.4722(9) | 5.0(4) |
| C(18) | -0.1871(7) | 0.8714(3) | 0.4257(7) | 3.7(3) |
| C(19) | -0.1269(7) | 0.9299(3) | -0.0145(6) | 3.7(3) |
| C(20) | -0.1797(7) | 0.9776(3) | -0.0255(6) | 3.8(3) |
| C(21) | -0.0858(6) | 0.9637(3) | 0.1748(6) | 2.9(3) |
| C(22) | -0.190(1) | 1.0507(3) | 0.1293(8) | 5.7(5) |
| C(23) | -0.1181(9) | 0.1871(3) | 0.2335(7) | 5.2(4) |
| C(24) | 0.1181(8) | 0.2017(4) | 0.2574(7) | 5.2(4) |
| C(25) | -0.0355(8) | 0.2700(3) | 0.1730(7) | 4.5(4) |
| C(26) | -0.0037(7) | 0.2448(3) | 0.3988(6) | 3.5(3) |
| H(1) | 0.0745 | 0.7547 | 0.3287 | 3.2 |
| H(2) | 0.1393 | 0.6723 | 0.4020 | 4.1 |
| H(3) | 0.0440 | 0.5989 | 0.2935 | 4.2 |
| H(4) | -0.1164 | 0.6088 | 0.1029 | 4.5 |
| H(5) | -0.1808 | 0.6910 | 0.0268 | 3.8 |
| H(6) | 0.4376 | 0.8668 | 0.0269 | 4.8 |
| H(7) | 0.6014 | 0.9286 | 0.0733 | 6.7 |
| H(8) | 0.5995 | 0.9887 | 0.2378 | 7.2 |
| H(9) | 0.4396 | 0.9816 | 0.3634 | 5.7 |
| H(10) | 0.2753 | 0.9191 | 0.3166 | 4.1 |
| H(11) | 0.0165 | 0.9565 | 0.5772 | 4.4 |
| H(12) | -0.1702 | 0.9816 | 0.6505 | 5.8 |
| H(13) | -0.3631 | 0.9348 | 0.5923 | 5.7 |
| H(14) | -0.3777 | 0.8686 | 0.4441 | 6.0 |
| H(15) | -0.1949 | 0.8436 | 0.3656 | 4.4 |
| H(16) | -0.1301 | 0.9060 | -0.0836 | 4.4 |
| H(17) | -0.2276 | 0.9933 | -0.1024 | 4.5 |

| | | | | |
|---|---|---|---|---|
| H(18) | -0.0562 | 0.9686 | 0.2652 | 3.5 |
| H(19) | -0.1125 | 1.0699 | 0.1668 | 6.8 |
| H(20) | -0.2354 | 1.0681 | 0.0541 | 6.8 |
| H(21) | -0.2455 | 1.0478 | 0.1898 | 6.8 |
| H(22) | -0.2000 | 0.2031 | 0.2368 | 6.2 |
| H(23) | -0.1215 | 0.1736 | 0.1492 | 6.2 |
| H(24) | -0.1017 | 0.1596 | 0.2945 | 6.2 |
| H(25) | 0.1363 | 0.1741 | 0.3179 | 6.2 |
| H(26) | 0.1143 | 0.1886 | 0.1727 | 6.2 |
| H(27) | 0.1861 | 0.2270 | 0.2770 | 6.2 |
| H(28) | 0.0665 | 0.2692 | 0.4205 | 4.2 |
| H(29) | -0.0849 | 0.2610 | 0.4042 | 4.2 |
| H(30) | 0.0119 | 0.2164 | 0.4571 | 4.2 |
| H(31) | -0.0398 | 0.2578 | 0.0875 | 5.4 |
| H(32) | 0.0344 | 0.2945 | 0.1949 | 5.4 |
| H(33) | -0.1169 | 0.2861 | 0.1783 | 5.4 |

[a]Estimated standard deviations in the least significant figure are given in parentheses. See Figure 2.2 for the atom labeling scheme. [b]$B_{eq} = (4/3)[a^2\beta_{11} + b^2\beta_{22} + c^2\beta_{33} + 2ab\cos(\gamma)\beta_{12} + 2ac\cos(\beta)\beta_{13} + 2bc\cos(\alpha)\beta_{23}]$

**Table 2.3.** Anisotropic thermal parameters for $[(CH_3)_4N][Zn(SC_6H_5)_3(MeIm)]^a$

| atom | U11 | U22 | U33 | U12 | U13 | U23 |
|---|---|---|---|---|---|---|
| Zn(1) | 0.0310(4) | 0.0345(5) | 0.0272(4) | 0.0024(4) | 0.0049(3) | 0.0015(4) |
| S(1) | 0.035(1) | 0.044(1) | 0.036(1) | -0.0036(8) | -0.0029(7) | -0.0019(9) |
| S(2) | 0.039(1) | 0.047(1) | 0.040(1) | 0.0034(8) | 0.0140(8) | -0.0068(9) |
| S(3) | 0.0312(9) | 0.050(1) | 0.0249(9) | 0.0019(8) | 0.0021(7) | -0.0000(8) |
| N(1) | 0.034(3) | 0.042(4) | 0.023(3) | 0.008(3) | 0.006(2) | 0.007(3) |
| N(2) | 0.047(4) | 0.039(4) | 0.039(4) | 0.005(3) | 0.004(3) | 0.013(3) |
| N(3) | 0.051(4) | 0.036(4) | 0.026(3) | 0.001(3) | 0.016(3) | -0.001(3) |
| C(1) | 0.029(3) | 0.040(4) | 0.030(4) | -0.009(3) | 0.012(3) | -0.003(3) |
| C(2) | 0.034(4) | 0.041(5) | 0.026(4) | -0.010(3) | 0.007(3) | -0.007(3) |
| C(3) | 0.046(4) | 0.052(6) | 0.031(4) | 0.003(4) | 0.010(3) | 0.005(4) |
| C(4) | 0.051(4) | 0.041(5) | 0.043(4) | -0.002(3) | 0.014(3) | -0.003(4) |
| C(5) | 0.049(4) | 0.045(5) | 0.046(4) | -0.007(4) | 0.005(3) | -0.011(4) |
| C(6) | 0.032(4) | 0.057(5) | 0.030(4) | -0.005(3) | 0.002(3) | -0.011(4) |
| C(7) | 0.033(4) | 0.042(5) | 0.034(4) | 0.009(3) | 0.003(3) | 0.015(3) |
| C(8) | 0.040(4) | 0.068(6) | 0.045(5) | 0.001(4) | 0.014(4) | 0.009(4) |
| C(9) | 0.056(5) | 0.092(8) | 0.073(7) | -0.006(5) | 0.033(5) | 0.007(6) |
| C(10) | 0.052(5) | 0.071(7) | 0.107(9) | -0.018(5) | 0.023(5) | 0.010(6) |
| C(11) | 0.044(5) | 0.065(6) | 0.072(6) | -0.003(4) | 0.011(4) | -0.013(5) |
| C(12) | 0.030(4) | 0.052(5) | 0.046(4) | 0.001(3) | 0.004(3) | 0.002(4) |
| C(13) | 0.038(4) | 0.046(5) | 0.023(3) | -0.003(3) | 0.004(3) | 0.003(3) |
| C(14) | 0.042(4) | 0.061(6) | 0.035(4) | -0.008(4) | 0.009(3) | -0.011(4) |
| C(15) | 0.067(5) | 0.068(6) | 0.053(5) | -0.004(5) | 0.025(4) | -0.019(5) |
| C(16) | 0.054(5) | 0.069(7) | 0.064(6) | 0.000(4) | 0.031(4) | -0.010(5) |

| | | | | | | |
|---|---|---|---|---|---|---|
| C(17) | 0.047(5) | 0.049(6) | 0.098(7) | -0.008(4) | 0.024(5) | -0.022(5) |
| C(18) | 0.040(4) | 0.037(5) | 0.067(5) | -0.005(3) | 0.017(4) | -0.014(4) |
| C(19) | 0.051(4) | 0.063(6) | 0.024(4) | 0.005(4) | 0.005(3) | 0.003(4) |
| C(20) | 0.047(4) | 0.062(6) | 0.031(4) | 0.003(4) | 0.001(3) | 0.020(4) |
| C(21) | 0.050(4) | 0.036(5) | 0.023(4) | 0.003(3) | 0.003(3) | 0.007(3) |
| C(22) | 0.104(7) | 0.046(6) | 0.064(6) | 0.030(5) | 0.017(5) | 0.016(5) |
| C(23) | 0.089(6) | 0.062(6) | 0.043(5) | -0.020(5) | 0.007(4) | 0.002(4) |
| C(24) | 0.073(6) | 0.085(7) | 0.046(5) | 0.032(5) | 0.029(4) | 0.004(5) |
| C(25) | 0.070(5) | 0.053(6) | 0.052(5) | 0.005(4) | 0.021(4) | 0.018(4) |
| C(26) | 0.049(4) | 0.055(5) | 0.032(4) | -0.004(4) | 0.016(3) | -0.007(4) |

[a]The anisotropic temperature factors are of the form $\exp[-2\pi^2(a^{*2}U_{11}h^2 + b^{*2}U_{22}k^2 + c^{*2}U_{33}l^2 + 2a^*b^*U_{12}hk + 2a^*c^*U_{13}hl + 2b^*c^*U_{23}kl)]$. Estimated standard deviations in the least significant figure are given in parentheses. See Figure 2.2 for the atom labeling scheme.

**Table 2.4.** Intramolecular distances (Å) for $[(CH_3)_4N][Zn(SC_6H_5)_3(MeIm)]^a$

| atom | atom | distance | atom | atom | distance |
|---|---|---|---|---|---|
| Zn(1) | S(1) | 2.316(2) | C(10) | H(8) | 0.950 |
| Zn(1) | S(2) | 2.321(2) | C(11) | C(12) | 1.38(1) |
| Zn(1) | S(3) | 2.314(2) | C(11) | H(9) | 0.950 |
| Zn(1) | N(1) | 2.072(5) | C(12) | H(10) | 0.950 |
| S(1) | C(1) | 1.773(7) | C(13) | C(14) | 1.401(9) |
| S(2) | C(7) | 1.761(7) | C(13) | C(18) | 1.384(9) |
| S(3) | C(13) | 1.747(7) | C(14) | C(15) | 1.377(9) |
| N(1) | C(19) | 1.382(8) | C(14) | H(11) | 0.950 |
| N(1) | C(21) | 1.316(8) | C(15) | C(16) | 1.35(1) |
| N(2) | C(20) | 1.364(9) | C(15) | H(12) | 0.951 |
| N(2) | C(21) | 1.337(8) | C(16) | C(17) | 1.35(1) |
| N(2) | C(22) | 1.45(1) | C(16) | H(13) | 0.950 |
| N(3) | C(23) | 1.474(9) | C(17) | C(18) | 1.373(9) |
| N(3) | C(24) | 1.484(8) | C(17) | H(14) | 0.950 |
| N(3) | C(25) | 1.482(9) | C(18) | H(15) | 0.951 |
| N(3) | C(26) | 1.493(8) | C(19) | C(20) | 1.34(1) |
| C(1) | C(2) | 1.401(8) | C(19) | H(16) | 0.950 |
| C(1) | C(6) | 1.384(9) | C(20) | H(17) | 0.950 |
| C(2) | C(3) | 1.374(9) | C(21) | H(18) | 0.950 |
| C(2) | H(1) | 0.950 | C(22) | H(19) | 0.950 |
| C(3) | C(4) | 1.374(9) | C(22) | H(20) | 0.949 |

| | | | | | |
|---|---|---|---|---|---|
| C(3) | H(2) | 0.949 | C(22) | H(21) | 0.951 |
| C(4) | C(5) | 1.38(1) | C(23) | H(22) | 0.949 |
| C(4) | H(3) | 0.950 | C(23) | H(23) | 0.950 |
| C(5) | C(6) | 1.37(1) | C(23) | H(24) | 0.949 |
| C(5) | H(4) | 0.951 | C(24) | H(25) | 0.949 |
| C(6) | H(5) | 0.950 | C(24) | H(26) | 0.950 |
| C(7) | C(8) | 1.386(9) | C(24) | H(27) | 0.951 |
| C(7) | C(12) | 1.385(9) | C(25) | H(31) | 0.949 |
| C(8) | C(9) | 1.37(1) | C(25) | H(32) | 0.951 |
| C(8) | H(6) | 0.950 | C(25) | H(33) | 0.950 |
| C(9) | C(10) | 1.37(1) | C(26) | H(28) | 0.951 |
| C(9) | H(7) | 0.950 | C(26) | H(29) | 0.950 |
| C(10) | C(11) | 1.38(1) | C(26) | H(30) | 0.949 |

[a]Estimated standard deviations in the least significant figure are given in parentheses. See Figure 2.2 for the atom labeling scheme.

**Table 2.5.** Intramolecular bond angles (deg) for $[(CH_3)_4N][Zn(SC_6H_5)_3(MeIm)]^a$

| atom | atom | atom | angle | atom | atom | atom | angle |
|---|---|---|---|---|---|---|---|
| S(1) | Zn(1) | S(2) | 106.56(7) | C(5) | C(6) | H(5) | 119.10 |
| S(1) | Zn(1) | S(3) | 124.14(7) | C(7) | C(8) | H(6) | 118.80 |
| S(1) | Zn(1) | N(1) | 99.3(2) | C(9) | C(8) | H(6) | 118.82 |
| S(2) | Zn(1) | S(3) | 110.75(7) | C(8) | C(9) | H(7) | 120.10 |
| S(2) | Zn(1) | N(1) | 111.4(1) | C(10) | C(9) | H(7) | 120.13 |
| S(3) | Zn(1) | N(1) | 103.8(2) | C(9) | C(10) | H(8) | 120.43 |
| Zn(1) | S(1) | C(1) | 108.0(2) | C(11) | C(10) | H(8) | 120.46 |
| Zn(1) | S(2) | C(7) | 112.0(2) | C(10) | C(11) | H(9) | 119.66 |
| Zn(1) | S(3) | C(13) | 108.0(2) | C(12) | C(11) | H(9) | 119.76 |
| Zn(1) | N(1) | C(19) | 130.5(5) | C(7) | C(12) | H(10) | 119.49 |
| Zn(1) | N(1) | C(21) | 124.3(4) | C(11) | C(12) | H(10) | 119.51 |
| C(19) | N(1) | C(21) | 105.2(6) | C(13) | C(14) | H(11) | 119.08 |
| C(20) | N(2) | C(21) | 106.8(6) | C(15) | C(14) | H(11) | 119.07 |
| C(20) | N(2) | C(22) | 126.5(6) | C(14) | C(15) | H(12) | 120.11 |
| C(21) | N(2) | C(22) | 126.6(6) | C(16) | C(15) | H(12) | 120.15 |
| C(23) | N(3) | C(24) | 110.4(7) | C(15) | C(16) | H(13) | 119.84 |
| C(23) | N(3) | C(25) | 110.8(6) | C(17) | C(16) | H(13) | 119.94 |
| C(23) | N(3) | C(26) | 108.6(5) | C(16) | C(17) | H(14) | 119.73 |
| C(24) | N(3) | C(25) | 108.9(5) | C(18) | C(17) | H(14) | 119.63 |
| C(24) | N(3) | C(26) | 108.5(5) | C(13) | C(18) | H(15) | 119.25 |
| C(25) | N(3) | C(26) | 109.6(6) | C(17) | C(18) | H(15) | 119.25 |

| | | | | | | | |
|---|---|---|---|---|---|---|---|
| S(1) | C(1) | C(2) | 122.8(5) | N(1) | C(19) | H(16) | 125.37 |
| S(1) | C(1) | C(6) | 119.2(5) | C(20) | C(19) | H(16) | 125.34 |
| C(2) | C(1) | C(6) | 117.9(6) | N(2) | C(20) | H(17) | 126.56 |
| C(1) | C(2) | C(3) | 119.8(6) | C(19) | C(20) | H(17) | 126.44 |
| C(2) | C(3) | C(4) | 121.7(6) | N(1) | C(21) | H(18) | 124.20 |
| C(3) | C(4) | C(5) | 118.9(7) | N(2) | C(21) | H(18) | 124.13 |
| C(4) | C(5) | C(6) | 119.9(7) | N(2) | C(22) | H(19) | 109.48 |
| C(1) | C(6) | C(5) | 121.7(6) | N(2) | C(22) | H(20) | 109.38 |
| S(2) | C(7) | C(8) | 119.2(6) | N(2) | C(22) | H(21) | 109.41 |
| S(2) | C(7) | C(12) | 123.7(5) | H(19) | C(22) | H(20) | 109.57 |
| C(8) | C(7) | C(12) | 117.1(7) | H(19) | C(22) | H(21) | 109.49 |
| C(7) | C(8) | C(9) | 122.4(8) | H(20) | C(22) | H(21) | 109.50 |
| C(8) | C(9) | C(10) | 119.8(7) | N(3) | C(23) | H(22) | 109.44 |
| C(9) | C(10) | C(11) | 119.1(8) | N(3) | C(23) | H(23) | 109.41 |
| C(10) | C(11) | C(12) | 120.6(8) | N(3) | C(23) | H(24) | 109.45 |
| C(7) | C(12) | C(11) | 121.0(7) | H(22) | C(23) | H(23) | 109.54 |
| S(3) | C(13) | C(14) | 119.4(5) | H(22) | C(23) | H(24) | 109.49 |
| S(3) | C(13) | C(18) | 124.5(6) | H(23) | C(23) | H(24) | 109.49 |
| C(14) | C(13) | C(18) | 116.0(6) | N(3) | C(24) | H(25) | 109.47 |
| C(13) | C(14) | C(15) | 121.8(7) | N(3) | C(24) | H(26) | 109.48 |
| C(14) | C(15) | C(16) | 119.7(8) | N(3) | C(24) | H(27) | 109.40 |
| C(15) | C(16) | C(17) | 120.2(7) | H(25) | C(24) | H(26) | 109.56 |
| C(16) | C(17) | C(18) | 120.6(7) | H(25) | C(24) | H(27) | 109.48 |

| | | | | | | | |
|---|---|---|---|---|---|---|---|
| C(13) | C(18) | C(17) | 121.5(7) | H(26) | C(24) | H(27) | 109.43 |
| N(1) | C(19) | C(20) | 109.3(6) | N(3) | C(25) | H(31) | 109.54 |
| N(2) | C(20) | C(19) | 107.0(6) | N(3) | C(25) | H(32) | 109.43 |
| N(1) | C(21) | N(2) | 111.7(6) | N(3) | C(25) | H(33) | 109.41 |
| C(1) | C(2) | H(1) | 120.15 | H(31) | C(25) | H(32) | 109.49 |
| C(3) | C(2) | H(1) | 120.02 | H(31) | C(25) | H(33) | 109.56 |
| C(2) | C(3) | H(2) | 119.11 | H(32) | C(25) | H(33) | 109.39 |
| C(4) | C(3) | H(2) | 119.24 | N(3) | C(26) | H(28) | 109.44 |
| C(3) | C(4) | H(3) | 120.54 | N(3) | C(26) | H(29) | 109.47 |
| C(5) | C(4) | H(3) | 120.57 | N(3) | C(26) | H(30) | 109.50 |
| C(4) | C(5) | H(4) | 120.04 | H(28) | C(26) | H(29) | 109.46 |
| C(6) | C(5) | H(4) | 120.02 | H(28) | C(26) | H(30) | 109.49 |
| C(1) | C(6) | H(5) | 119.16 | H(29) | C(26) | H(30) | 109.46 |

[a]Estimated standard deviations in the least significant figure are given in parentheses. See Figure 2.2 for the atom labeling scheme.

**Table 2.6.** Torsion or conformation angles (deg) for $[(CH_3)_4N][Zn(SC_6H_5)_3(MeIm)]^a$

| (1) | (2) | (3) | (4) | angle | (1) | (2) | (3) | (4) | angle |
|---|---|---|---|---|---|---|---|---|---|
| Zn(1) | S(1) | C(1) | C(2) | 22.2(5) | N(1) | Zn(1) | S(1) | C(1) | 177.1(2) |
| Zn(1) | S(1) | C(1) | C(6) | -161.2(4) | N(1) | Zn(1) | S(2) | C(7) | 64.8(3) |
| Zn(1) | S(2) | C(7) | C(8) | -159.3(5) | N(1) | Zn(1) | S(3) | C(13) | 55.0(3) |
| Zn(1) | S(2) | C(7) | C(12) | 21.3(6) | N(1) | C(19) | C(20) | N(2) | 0.9(8) |
| Zn(1) | S(3) | C(13) | C(14) | -140.9(5) | N(1) | C(21) | N(2) | C(20) | 1.6(8) |
| Zn(1) | S(3) | C(13) | C(18) | 41.5(7) | N(1) | C(21) | N(2) | C(22) | 179.9(7) |
| Zn(1) | N(1) | C(19) | C(20) | 177.7(5) | N(2) | C(21) | N(1) | C(19) | -1.0(8) |
| Zn(1) | N(1) | C(21) | N(2) | -178.8(4) | C(1) | C(2) | C(3) | C(4) | 0(1) |
| S(1) | Zn(1) | S(2) | C(7) | 172.1(2) | C(1) | C(6) | C(5) | C(4) | -1(1) |
| S(1) | Zn(1) | S(3) | C(13) | -56.6(3) | C(2) | C(1) | C(6) | C(5) | 1.7(9) |
| S(1) | Zn(1) | N(1) | C(19) | -47.2(6) | C(2) | C(3) | C(4) | C(5) | 1(1) |
| S(1) | Zn(1) | N(1) | C(21) | 130.1(5) | C(3) | C(2) | C(1) | C(6) | -1.3(9) |
| S(1) | C(1) | C(2) | C(3) | 175.3(5) | C(3) | C(4) | C(5) | C(6) | -1(1) |
| S(1) | C(1) | C(6) | C(5) | -175.0(5) | C(7) | C(8) | C(9) | C(10) | -1(1) |
| S(2) | Zn(1) | S(1) | C(1) | 61.3(2) | C(7) | C(12) | C(11) | C(10) | 1(1) |
| S(2) | Zn(1) | S(3) | C(13) | 174.7(2) | C(8) | C(7) | C(12) | C(11) | 0(1) |
| S(2) | Zn(1) | N(1) | C(19) | 64.8(6) | C(8) | C(9) | C(10) | C(11) | 2(1) |
| S(2) | Zn(1) | N(1) | C(21) | -117.9(5) | C(9) | C(8) | C(7) | C(12) | 0(1) |
| S(2) | C(7) | C(8) | C(9) | -179.5(7) | C(9) | C(10) | C(11) | C(12) | -2(1) |
| S(2) | C(7) | C(12) | C(11) | 179.5(6) | C(13) | C(14) | C(15) | C(16) | 1(1) |
| S(3) | Zn(1) | S(1) | C(1) | -69.1(2) | C(13) | C(18) | C(17) | C(16) | 0(1) |

| | | | | | | | | | |
|---|---|---|---|---|---|---|---|---|---|
| S(3) | Zn(1) | S(2) | C(7) | -50.3(2) | C(14) | C(13) | C(18) | C(17) | -2(1) |
| S(3) | Zn(1) | N(1) | C(19) | -175.9(5) | C(14) | C(15) | C(16) | C(17) | -3(1) |
| S(3) | Zn(1) | N(1) | C(21) | 1.3(5) | C(15) | C(14) | C(13) | C(18) | 1(1) |
| S(3) | C(13) | C(14) | C(15) | -176.5(6) | C(15) | C(16) | C(17) | C(18) | 3(1) |
| S(3) | C(13) | C(18) | C(17) | 175.7(6) | C(19) | C(20) | N(2) | C(21) | -1.5(8) |
| C(19) | C(20) | N(2) | C(22) | -179.9(7) | C(20) | C(19) | N(1) | C(21) | 0.0(8) |

[a]The sign is positive if when looking from atom 2 to atom 3 a clockwise motion of atom 1 would superimpose it on atom 4. Estimated standard deviations in the least significant figure are given in parentheses. See Figure 2.2 for the atom labeling scheme.

**Table 2.7.** Positional parameters and B(eq) for $[Zn(SC_6H_5)_2(MeIm)_2]^a$

| atom | x | y | z | B(eq)[b] |
|---|---|---|---|---|
| Zn(1) | 0 | 0.21485(2) | 1/4 | 1.86(2) |
| S(1) | -0.11294(6) | 0.16158(4) | 0.05733(7) | 2.32(3) |
| N(1) | -0.0977(2) | 0.2775(1) | 0.3515(2) | 2.2(1) |
| N(2) | -0.2445(2) | 0.3333(1) | 0.3945(3) | 2.3(1) |
| C(1) | -0.2005(2) | 0.1050(1) | 0.1369(3) | 1.9(1) |
| C(2) | -0.3130(3) | 0.1025(2) | 0.0774(3) | 2.6(1) |
| C(3) | -0.3817(3) | 0.0544(2) | 0.1280(4) | 3.1(1) |
| C(4) | -0.3409(3) | 0.0079(2) | 0.2404(4) | 3.2(1) |
| C(5) | -0.2308(2) | 0.0109(2) | 0.3030(4) | 3.0(1) |
| C(6) | -0.1608(2) | 0.0593(2) | 0.2531(3) | 2.4(1) |
| C(7) | -0.0765(3) | 0.3039(2) | 0.4919(3) | 2.6(1) |
| C(8) | -0.1671(3) | 0.3385(2) | 0.5193(3) | 2.9(1) |
| C(9) | -0.1999(2) | 0.2963(2) | 0.2970(3) | 2.3(1) |
| C(10) | -0.3550(3) | 0.3635(2) | 0.3708(4) | 3.3(1) |
| H(1) | -0.337 | 0.139 | -0.010 | 3.4 |
| H(2) | -0.465 | 0.053 | 0.090 | 3.4 |
| H(3) | -0.400 | -0.020 | 0.289 | 3.4 |
| H(4) | -0.205 | -0.018 | 0.390 | 3.4 |
| H(5) | -0.076 | 0.056 | 0.296 | 3.4 |
| H(6) | -0.005 | 0.288 | 0.559 | 3.4 |
| H(7) | -0.180 | 0.357 | 0.624 | 3.4 |
| H(8) | -0.237 | 0.286 | 0.199 | 3.4 |
| H(9) | -0.405 | 0.351 | 0.285 | 3.4 |

| | | | | |
|---|---|---|---|---|
| H(10) | -0.355 | 0.418 | 0.379 | 3.4 |
| H(11) | -0.402 | 0.344 | 0.437 | 3.4 |

[a]Estimated standard deviations in the least significant figure are given in parentheses. See Figure 2.3 for the atom labeling scheme. [b]$B_{eq} = (4/3)[a^2\beta_{11} + b^2\beta_{22} + c^2\beta_{33} + 2ab\cos(\gamma)\beta_{12} + 2ac\cos(\beta)\beta_{13} + 2bc\cos(\alpha)\beta_{23}]$.

**Table 2.8.** Anisotropic thermal parameters for $[Zn(SC_6H_5)_2(MeIm)_2]^a$

| atom | U11 | U22 | U33 | U12 | U13 | U23 |
|---|---|---|---|---|---|---|
| Zn(1) | 0.0219(2) | 0.0282(3) | 0.0213(2) | 0 | 0.0060(2) | -0.0000 |
| S(1) | 0.0275(4) | 0.0414(4) | 0.0195(3) | -0.0060(3) | 0.0051(3) | -0.0001(3) |
| N(1) | 0.028(1) | 0.032(1) | 0.025(1) | 0.001(1) | 0.009(1) | 0.001(1) |
| N(2) | 0.029(1) | 0.031(1) | 0.032(1) | 0.006(1) | 0.012(1) | 0.003(1) |
| C(1) | 0.028(1) | 0.026(1) | 0.023(1) | -0.001(1) | 0.009(1) | -0.006(1) |
| C(2) | 0.032(2) | 0.040(2) | 0.027(1) | -0.003(1) | 0.005(1) | -0.001(1) |
| C(3) | 0.028(2) | 0.048(2) | 0.042(2) | -0.006(1) | 0.008(2) | -0.007(2) |
| C(4) | 0.044(2) | 0.032(2) | 0.051(2) | -0.007(1) | 0.026(2) | -0.004(2) |
| C(5) | 0.044(2) | 0.034(2) | 0.040(2) | 0.006(1) | 0.018(1) | 0.007(1) |
| C(6) | 0.028(2) | 0.033(2) | 0.033(2) | 0.004(1) | 0.009(1) | 0.001(1) |
| C(7) | 0.035(2) | 0.033(2) | 0.030(2) | -0.000(1) | 0.004(1) | -0.007(1) |
| C(8) | 0.042(2) | 0.036(2) | 0.031(2) | 0.004(1) | 0.009(1) | -0.008(1) |
| C(9) | 0.031(2) | 0.035(2) | 0.023(1) | 0.002(1) | 0.009(1) | 0.002(1) |
| C(10) | 0.032(2) | 0.048(2) | 0.048(2) | 0.011(2) | 0.016(2) | 0.007(2) |

[a]The anisotropic temperature factors are of the form $\exp[-2\pi^2(a^{*2}U_{11}h^2 + b^{*2}U_{22}k^2 + c^{*2}U_{33}l^2 + 2a^*b^*U_{12}hk + 2a^*c^*U_{13}hl + 2b^*c^*U_{23}kl)]$. Estimated standard deviations in the least significant figure are given in parentheses. See Figure 2.3 for the atom labeling scheme.

**Table 2.9.** Intramolecular distances (Å) for $[Zn(SC_6H_5)_2(MeIm)_2]^a$

| atom | atom | distance | ADC(*) | atom | atom | distance | ADC(*) |
|---|---|---|---|---|---|---|---|
| Zn(1) | S(1) | 2.2916(7) | 1 | C(5) | C(6) | 1.390(4) | 1 |
| Zn(1) | S(1) | 2.2912(7) | 2 | C(7) | C(8) | 1.359(4) | 1 |
| Zn(1) | N(1) | 2.038(2) | 1 | C(4) | C(5) | 1.381(5) | 1 |
| Zn(1) | N(1) | 2.039(2) | 2 | C(5) | C(6) | 1.390(4) | 1 |
| S(1) | C(1) | 1.773(3) | 1 | C(7) | C(8) | 1.359(4) | 1 |
| N(1) | C(7) | 1.378(4) | 1 | C(2) | H(1) | 1.059 | 1 |
| N(1) | C(9) | 1.320(4) | 1 | C(3) | H(2) | 1.024 | 1 |
| N(2) | C(8) | 1.368(4) | 1 | C(4) | H(3) | 1.065 | 1 |
| N(2) | C(9) | 1.340(3) | 1 | C(5) | H(4) | 0.981 | 1 |
| N(2) | C(10) | 1.458(4) | 1 | C(6) | H(5) | 1.051 | 1 |
| C(1) | C(2) | 1.401(4) | 1 | C(7) | H(6) | 1.024 | 1 |
| C(1) | C(6) | 1.396(4) | 1 | C(8) | H(7) | 1.078 | 1 |
| C(2) | C(3) | 1.378(4) | 1 | C(9) | H(8) | 0.959 | 1 |
| C(3) | C(4) | 1.385(5) | 1 | C(10) | H(9) | 0.948 | 1 |
| C(4) | C(5) | 1.381(5) | 1 | C(10) | H(10) | 1.015 | 1 |

[a]Estimated standard deviations in the least significant figure are given in parentheses. See Figure 2.3 for the atom labeling scheme.

**Table 2.10.** Intramolecular bond angles (deg) for $[Zn(SC_6H_5)_2(MeIm)_2]^a$

| atom | atom | atom | angle | atom | atom | atom | angle |
|---|---|---|---|---|---|---|---|
| S(1) | Zn(1) | S(1) | 128.47(4) | N(1) | C(9) | N(2) | 111.2(3) |
| S(1) | Zn(1) | N(1) | 106.61(7) | C(1) | C(2) | H(1) | 113.50 |
| S(1) | Zn(1) | N(1) | 102.38(7) | C(3) | C(2) | H(1) | 125.37 |
| S(1) | Zn(1) | N(1) | 102.37(7) | C(2) | C(3) | H(2) | 123.07 |
| S(1) | Zn(1) | N(1) | 106.60(7) | C(4) | C(3) | H(2) | 116.37 |
| N(1) | Zn(1) | N(1) | 109.8(1) | C(3) | C(4) | H(3) | 116.54 |
| Zn(1) | S(1) | C(1) | 105.26(9) | C(5) | C(4) | H(3) | 122.81 |
| Zn(1) | N(1) | C(7) | 128.4(2) | C(4) | C(5) | H(4) | 118.10 |
| Zn(1) | N(1) | C(9) | 125.6(2) | C(6) | C(5) | H(4) | 120.78 |
| C(7) | N(1) | C(9) | 105.8(2) | C(1) | C(6) | H(5) | 121.25 |
| C(8) | N(2) | C(9) | 107.6(2) | C(5) | C(6) | H(5) | 117.89 |
| C(8) | N(2) | C(10) | 126.3(3) | N(1) | C(7) | H(6) | 118.11 |
| C(9) | N(2) | C(10) | 126.1(3) | C(8) | C(7) | H(6) | 131.78 |
| S(1) | C(1) | C(2) | 119.6(2) | N(2) | C(8) | H(7) | 127.00 |
| S(1) | C(1) | C(6) | 122.4(2) | C(7) | C(8) | H(7) | 125.82 |
| C(2) | C(1) | C(6) | 118.0(3) | N(1) | C(9) | H(8) | 124.63 |
| C(1) | C(2) | C(3) | 121.1(3) | N(2) | C(9) | H(8) | 124.18 |
| C(2) | C(3) | C(4) | 120.5(3) | N(2) | C(10) | H(9) | 118.94 |
| C(3) | C(4) | C(5) | 119.2(3) | N(2) | C(10) | H(10) | 112.61 |
| C(4) | C(5) | C(6) | 120.8(3) | N(2) | C(10) | H(11) | 113.73 |
| C(1) | C(6) | C(5) | 120.4(3) | H(9) | C(10) | H(10) | 106.93 |

| | | | | | | | |
|---|---|---|---|---|---|---|---|
| N(1) | C(7) | C(8) | 109.2(3) | H(9) | C(10) | H(11) | 94.09 |
| N(2) | C(8) | C(7) | 106.2(3) | H(10) | C(10) | H(11) | 108.81 |

[a]Estimated standard deviations in the least significant figure are given in parentheses. See Figure 2.3 for the atom labeling scheme.

**Table 2.11.** Torsion or conformation angles (deg) for $[Zn(SC_6H_5)_2(MeIm)_2]^a$

| (1) | (2) | (3) | (4) | angle | (1) | (2) | (3) | (4) | angle |
|---|---|---|---|---|---|---|---|---|---|
| Zn(1) | S(1) | C(1) | C(2) | 137.0(2) | N(1) | Zn(1) | S(1) | C(1) | 179.5(1) |
| Zn(1) | S(1) | C(1) | C(6) | -46.6(2) | N(1) | Zn(1) | N(1) | C(7) | -90.0(2) |
| Zn(1) | S(1) | C(1) | C(2) | 137.0(2) | N(1) | Zn(1) | N(1) | C(9) | 95.9(2) |
| Zn(1) | S(1) | C(1) | C(6) | -46.6(2) | N(1) | C(7) | C(8) | N(2) | 0.0(3) |
| Zn(1) | N(1) | C(7) | C(8) | -175.2(2) | N(1) | C(9) | N(2) | C(8) | -0.3(3) |
| Zn(1) | N(1) | C(9) | N(2) | 175.4(2) | N(1) | C(9) | N(2) | C(10) | 178.9(3) |
| Zn(1) | N(1) | C(7) | C(8) | -175.2(2) | N(2) | C(9) | N(1) | C(7) | 0.2(3) |
| Zn(1) | N(1) | C(9) | N(2) | 175.4(2) | C(1) | C(2) | C(3) | C(4) | 0.8(5) |
| S(1) | Zn(1) | S(1) | C(1) | 56.24(9) | C(1) | C(6) | C(5) | C(4) | -1.0(5) |
| S(1) | Zn(1) | N(1) | C(7) | 159.8(2) | C(2) | C(1) | C(6) | C(5) | 2.7(4) |
| S(1) | Zn(1) | N(1) | C(9) | -14.3(2) | C(2) | C(3) | C(4) | C(5) | 1.0(5) |
| S(1) | Zn(1) | N(1) | C(7) | 23.0(3) | C(3) | C(2) | C(1) | C(6) | -2.6(4) |
| S(1) | Zn(1) | N(1) | C(9) | -151.1(2) | C(3) | C(4) | C(5) | C(6) | -0.9(5) |
| S(1) | C(1) | C(2) | C(3) | 174.0(2) | C(7) | C(8) | N(2) | C(9) | 0.2(3) |
| S(1) | C(1) | C(6) | C(5) | -173.8(2) | C(7) | C(8) | N(2) | C(10) | -179.0(3) |
| N(1) | Zn(1) | S(1) | C(1) | -65.3(1) | C(8) | C(7) | N(1) | C(9) | -0.1(3) |

[a]The sign is positive if when looking from atom 2 to atom 3 a clockwise motion of atom 1 would superimpose it on atom 4. Estimated standard deviations in the least significant figure are given in parentheses. See Figure 2.3 for the atom labeling scheme.

**Table 2.12.** Positional parameters and B(eq) for $[Co(SC_6H_5)_2(MeIm)_2]^a$

| atom | x | y | z | B(eq)[b] |
|---|---|---|---|---|
| Co(1) | 0 | 0.217172(24) | -1/4 | 1.92(2) |
| S(1) | 0.111669(48) | 0.162561(35) | -0.059041(63) | 2.37(2) |
| N(1) | -0.09742(16) | 0.27688(11) | -0.14618(21) | 2.25(8) |
| N(2) | -0.24415(17) | 0.33288(11) | -0.10298(23) | 2.39(8) |
| C(1) | 0.20048(18) | 0.10602(13) | -0.13525(25) | 2.09(9) |
| C(2) | 0.31274(20) | 0.10364(15) | -0.07403(28) | 2.7(1) |
| C(3) | 0.38225(21) | 0.05529(16) | -0.12361(31) | 3.1(1) |
| C(4) | 0.34186(23) | 0.00827(14) | -0.23561(33) | 3.2(1) |
| C(5) | 0.23146(23) | 0.01099(14) | -0.30030(31) | 3.0(1) |
| C(6) | 0.16104(20) | 0.05927(14) | -0.25113(28) | 2.6(1) |
| C(7) | -0.07625(21) | 0.30385(15) | -0.00492(27) | 2.8(1) |
| C(8) | -0.16611(23) | 0.33798(14) | 0.02239(29) | 3.0(1) |
| C(9) | -0.19989(21) | 0.29603(14) | -0.20125(28) | 2.4(1) |
| C(10) | -0.35516(22) | 0.36296(16) | -0.12643(33) | 3.4(1) |
| H(1) | 0.339 | 0.144 | 0.002 | 2.7 |
| H(2) | 0.462 | 0.053 | -0.074 | 1.9 |
| H(3) | 0.397 | -0.033 | -0.264 | 2.7 |
| H(4) | 0.193 | -0.021 | -0.386 | 2.7 |
| H(5) | 0.073 | 0.055 | -0.300 | 2.7 |
| H(6) | -0.001 | 0.289 | 0.060 | 2.7 |
| H(7) | -0.181 | 0.357 | 0.122 | 1.9 |
| H(8) | -0.2418(23) | 0.2828(15) | -0.2923(32) | 3.3(6) |
| H(9) | -0.352 | 0.410 | -0.110 | 1.9 |

| | | | | |
|---|---|---|---|---|
| H(10) | -0.398 | 0.336 | -0.067 | 1.9 |
| H(11) | -0.389 | 0.353 | -0.226 | 1.9 |

[a]Estimated standard deviations in the least significant figure are given in parentheses. See Figure 2.4 for the atom labeling scheme. [b]$B_{eq} = (4/3)[a^2\beta_{11} + b^2\beta_{22} + c^2\beta_{33} + 2ab\cos(\gamma)\beta_{12} + 2ac\cos(\beta)\beta_{13} + 2bc\cos(\alpha)\beta_{23}]$

**Table 2.13.** Anisotropic thermal parameters for $[Co(SC_6H_5)_2(MeIm)_2]^a$

| atom | U11 | U22 | U33 | U12 | U13 | U23 |
|---|---|---|---|---|---|---|
| Co(1) | 0.02068(23) | 0.03221(26) | 0.02073(23) | 0 | 0.00572(16) | 0 |
| S(1) | 0.02683(31) | 0.04328(37) | 0.02024(29) | 0.00552(25) | 0.00524(23) | 0.00046(23) |
| N(1) | 0.0259(10) | 0.0345(11) | 0.0259(10) | 0.00210(83) | 0.00723(80) | -0.00014(85) |
| N(2) | 0.0277(10) | 0.0345(12) | 0.0312(11) | 0.00516(87) | 0.01191(86) | 0.00244(87) |
| C(1) | 0.0241(11) | 0.0317(13) | 0.0250(11) | 0.00215(93) | 0.00825(89) | 0.00559(94) |
| C(2) | 0.0273(12) | 0.0441(15) | 0.0306(13) | 0.0029(11) | 0.0040(10) | 0.0031(11) |
| C(3) | 0.0275(13) | 0.0472(17) | 0.0443(15) | 0.0073(11) | 0.0096(11) | 0.0086(13) |
| C(4) | 0.0402(15) | 0.0334(14) | 0.0524(17) | 0.0073(11) | 0.0198(13) | 0.0057(12) |
| C(5) | 0.0417(15) | 0.0344(14) | 0.0427(15) | -0.0059(11) | 0.0168(12) | -0.0076(11) |
| C(6) | 0.0291(12) | 0.0365(14) | 0.0334(13) | -0.0054(10) | 0.0100(10) | -0.0021(11) |
| C(7) | 0.0338(13) | 0.0420(15) | 0.0293(13) | 0.0005(11) | 0.0035(10) | -0.0072(11) |
| C(8) | 0.0412(15) | 0.0413(15) | 0.0320(14) | 0.0018(12) | 0.0111(12) | -0.0068(11) |
| C(9) | 0.0282(12) | 0.0382(14) | 0.0272(12) | 0.0023(10) | 0.00866(98) | 0.0008(10) |
| C(10) | 0.0370(14) | 0.0479(16) | 0.0471(16) | 0.0137(13) | 0.0186(12) | 0.0070(13) |

[a]The anisotropic temperature factors are of the form $\exp[-2\pi^2(a^{*2}U_{11}h^2 + b^{*2}U_{22}k^2 + c^{*2}U_{33}l^2 + 2a^*b^*U_{12}hk + 2a^*c^*U_{13}hl + 2b^*c^*U_{23}kl)]$. Estimated standard deviations in the least significant figure are given in parentheses. See Figure 2.4 for the atom labeling scheme.

**Table 2.14.** Intramolecular distances (Å) for $[Co(SC_6H_5)_2(MeIm)_2]^a$

| atom | atom | distance | ADC(*) | atom | atom | distance | ADC(*) |
|---|---|---|---|---|---|---|---|
| Co(1) | S(1) | 2.2741(6) | 1 | C(4) | C(5) | 1.387(4) | 1 |
| Co(1) | S(1) | 2.2741(6) | 55402 | C(5) | C(6) | 1.392(4) | 1 |
| Co(1) | N(1) | 2.019(2) | 1 | C(7) | C(8) | 1.349(4) | 1 |
| Co(1) | N(1) | 2.019(2) | 55402 | C(2) | H(1) | 1.041 | 1 |
| S(1) | C(1) | 1.768(2) | 1 | C(3) | H(2) | 1.015 | 1 |
| N(1) | C(7) | 1.384(3) | 1 | C(4) | H(3) | 1.103 | 1 |
| N(1) | C(9) | 1.325(3) | 1 | C(5) | H(4) | 1.041 | 1 |
| N(2) | C(8) | 1.369(3) | 1 | C(6) | H(5) | 1.102 | 1 |
| N(2) | C(9) | 1.342(3) | 1 | C(7) | H(6) | 1.045 | 1 |
| N(2) | C(10) | 1.464(3) | 1 | C(8) | H(7) | 1.043 | 1 |
| C(1) | C(2) | 1.400(3) | 1 | C(9) | H(8) | 0.94(3) | 1 |
| C(1) | C(6) | 1.400(3) | 1 | C(10) | H(9) | 0.892 | 1 |
| C(2) | C(3) | 1.387(4) | 1 | C(10) | H(10) | 0.973 | 1 |
| C(3) | C(4) | 1.381(4) | 1 | C(10) | H(11) | 0.956 | 1 |

[a]Estimated standard deviations in the least significant figure are given in parentheses. See Figure 2.4 for the atom labeling scheme.

**Table 2.15.** Intramolecular bond angles (deg) for $[Co(SC_6H_5)_2(MeIm)_2]^a$

| atom | atom | atom | angle | atom | atom | atom | angle |
|---|---|---|---|---|---|---|---|
| S(1) | Co(1) | S(1) | 126.66(4) | N(1) | C(9) | N(2) | 111.2(2) |
| S(1) | Co(1) | N(1) | 101.90(6) | C(1) | C(2) | H(1) | 114.03 |
| S(1) | Co(1) | N(1) | 106.86(6) | C(3) | C(2) | H(1) | 124.49 |
| S(1) | Co(1) | N(1) | 106.86(6) | C(2) | C(3) | H(2) | 119.74 |
| S(1) | Co(1) | N(1) | 101.90(6) | C(4) | C(3) | H(2) | 119.79 |
| N(1) | Co(1) | N(1) | 112.9(1) | C(3) | C(4) | H(3) | 118.56 |
| Co(1) | S(1) | C(1) | 106.79(8) | C(5) | C(4) | H(3) | 121.90 |
| Co(1) | N(1) | C(7) | 129.2(2) | C(4) | C(5) | H(4) | 125.83 |
| Co(1) | N(1) | C(9) | 125.5(2) | C(6) | C(5) | H(4) | 113.48 |
| C(7) | N(1) | C(9) | 105.2(2) | C(1) | C(6) | H(5) | 122.00 |
| C(8) | N(2) | C(9) | 107.5(2) | C(5) | C(6) | H(5) | 117.22 |
| C(8) | N(2) | C(10) | 126.3(2) | N(1) | C(7) | H(6) | 116.22 |
| C(9) | N(2) | C(10) | 126.2(2) | C(8) | C(7) | H(6) | 133.63 |
| S(1) | C(1) | C(2) | 120.2(2) | N(2) | C(8) | H(7) | 124.25 |
| S(1) | C(1) | C(6) | 121.9(2) | C(7) | C(8) | H(7) | 128.53 |
| C(2) | C(1) | C(6) | 117.8(2) | N(1) | C(9) | H(8) | 127(2) |
| C(1) | C(2) | C(3) | 121.2(2) | N(2) | C(9) | H(8) | 121(2) |
| C(2) | C(3) | C(4) | 120.4(2) | N(2) | C(10) | H(9) | 109.86 |
| C(3) | C(4) | C(5) | 119.3(2) | N(2) | C(10) | H(10) | 108.35 |
| C(4) | C(5) | C(6) | 120.7(3) | N(2) | C(10) | H(11) | 107.34 |
| C(1) | C(6) | C(5) | 120.5(2) | H(9) | C(10) | H(10) | 115.33 |

| | | | | | | | |
|---|---|---|---|---|---|---|---|
| N(1) | C(7) | C(8) | 109.6(2) | H(9) | C(10) | H(11) | 110.35 |
| N(2) | C(8) | C(7) | 106.4(2) | H(10) | C(10) | H(11) | 105.25 |

[a]Estimated standard deviations in the least significant figure are given in parentheses. See Figure 2.4 for the atom labeling scheme.

**Table 2.16.** Torsion or conformation angles (deg) for $[Co(SC_6H_5)_2(MeIm)_2]^a$

| (1) | (2) | (3) | (4) | angle | (1) | (2) | (3) | (4) | angle |
|---|---|---|---|---|---|---|---|---|---|
| Co(1) | S(1) | C(1) | C(2) | 136.1(2) | N(1) | Co(1) | S(1) | C(1) | -62.8(1) |
| Co(1) | S(1) | C(1) | C(6) | -48.0(2) | N(1) | Co(1) | N(1) | C(7) | -88.6(2) |
| Co(1) | S(1) | C(1) | C(2) | 136.1(2) | N(1) | Co(1) | N(1) | C(9) | 94.3(2) |
| Co(1) | S(1) | C(1) | C(6) | -48.0(2) | N(1) | C(7) | C(8) | N(2) | -0.4(3) |
| Co(1) | N(1) | C(7) | C(8) | -177.0(2) | N(1) | C(9) | N(2) | C(8) | 0.1(3) |
| Co(1) | N(1) | C(9) | N(2) | 177.3(2) | N(1) | C(9) | N(2) | C(10) | 179.3(2) |
| Co(1) | N(1) | C(7) | C(8) | -177.0(2) | N(2) | C(9) | N(1) | C(7) | -0.3(3) |
| Co(1) | N(1) | C(9) | N(2) | 177.3(2) | C(1) | C(2) | C(3) | C(4) | 0.2(4) |
| S(1) | Co(1) | S(1) | C(1) | 56.84(8) | C(1) | C(6) | C(5) | C(4) | 0.0(4) |
| S(1) | Co(1) | N(1) | C(7) | 25.6(2) | C(2) | C(1) | C(6) | C(5) | 1.6(4) |
| S(1) | Co(1) | N(1) | C(9) | -151.4(2) | C(2) | C(3) | C(4) | C(5) | 1.5(4) |
| S(1) | Co(1) | N(1) | C(7) | 160.1(2) | C(3) | C(2) | C(1) | C(6) | -1.7(4) |
| S(1) | Co(1) | N(1) | C(9) | -16.9(2) | C(3) | C(4) | C(5) | C(6) | -1.5(4) |
| S(1) | C(1) | C(2) | C(3) | 174.3(2) | C(7) | C(8) | N(2) | C(9) | 0.2(3) |
| S(1) | C(1) | C(6) | C(5) | -174.3(2) | C(7) | C(8) | N(2) | C(10) | -179.0(2) |
| N(1) | Co(1) | S(1) | C(1) | 178.6(1) | C(8) | C(7) | N(1) | C(9) | 0.5(3) |

[a]The sign is positive if when looking from atom 2 to atom 3 a clockwise motion of atom 1 would superimpose it on atom 4. Estimated standard deviations in the least significant figure are given in parentheses. See Figure 2.4 for the atom labeling scheme.

**Table 2.17.** Selected bond lengths and angles for thiolate complexes.

| compound | M-S (Å) | M-N (Å) | S-M-S (°) | S-M-N (°) | N-M-N (°) |
|---|---|---|---|---|---|
| $[(CH_3)_4N][Zn(SC_6H_5)_3$-(MeIm)] | 2.317(2) | 2.072(5) | 113.82(7) | 104.8(2) | - |
| $[(C_3H_7)_4N]$-{Zn[S-2,3,5,6-$(CH_3)_4$-$C_6H]_3$(MeIm)}[a] | 2.325(4) | 2.06(1) | 113.6(1) | 104.9(4) | - |
| $[Zn(SC_6H_5)_2(MeIm)_2]$ | 2.2914(7) | 2.039(2) | 128.47(4) | 104.49(7) | 109.8(1) |
| {Zn[S-2,3,5,6-$(CH_3)_4$-$C_6H]_2(MeIm)_2$}[b] | 2.300(2) | 2.047(6) | 109.46(8) | 113.2(2) | 101.9(2) |
| [Zn{S-2,4,6-[$C(CH_3)_3$]-$C_6H_2$}$_2(MeIm)_2$][c] | 2.315(3) | 2.047(12) | 115.5(1) | 109.7(3) | 101.7(4) |
| $[Co(SC_6H_5)_2(MeIm)_2]$ | 2.2741(6) | 2.019(2) | 126.66(4) | 104.38(6) | 2.019(2) |
| $[(CH_3)N_4]_2[Zn$-$(SC_6H_5)_4]$[d] | 2.357(3) | - | 109.5 | - | - |

[a]From reference 2. [b]From reference 3. [c]From reference 4. [d]From reference 9.

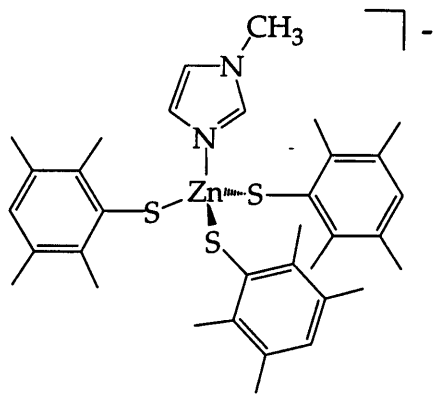

$[(C_3H_7)_4N]\{Zn[S\text{-}2,3,5,6\text{-}(CH_3)_4\text{-}C_6H]_3(MeIm)\}^2$

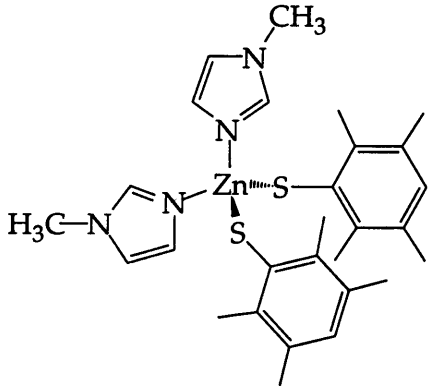

$\{Zn[S\text{-}2,3,5,6\text{-}(CH_3)_4\text{-}C_6H]_2(MeIm)_2\}^3$

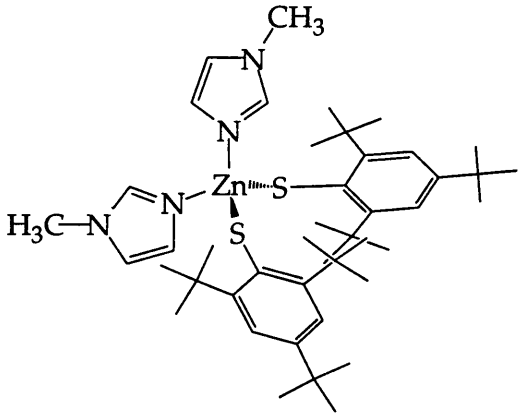

$[Zn\{S\text{-}2,4,6\text{-}[C(CH_3)_3]\text{-}C_6H_2\}_2(MeIm)_2]^4$

**Figure 2.1.** $[Zn(SR)_3(Im)]^-$ and $[Zn(SR)_2(Im)_2]$ complexes known prior to the work reported here.

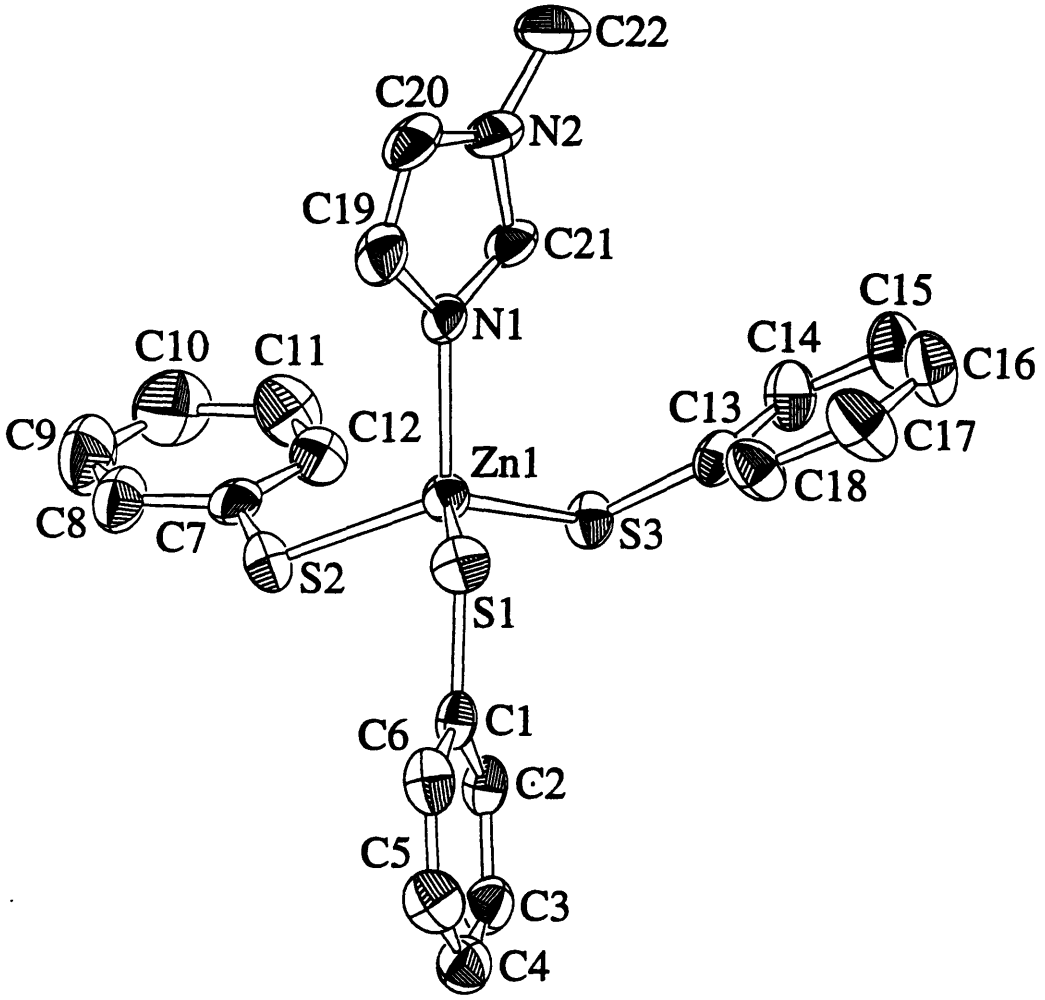


**Figure 2.2.** ORTEP diagram of the $[Zn(SC_6H_5)_3(MeIm)]^-$ anion showing the 50% probability thermal ellipsoids for all non-hydrogen atoms.

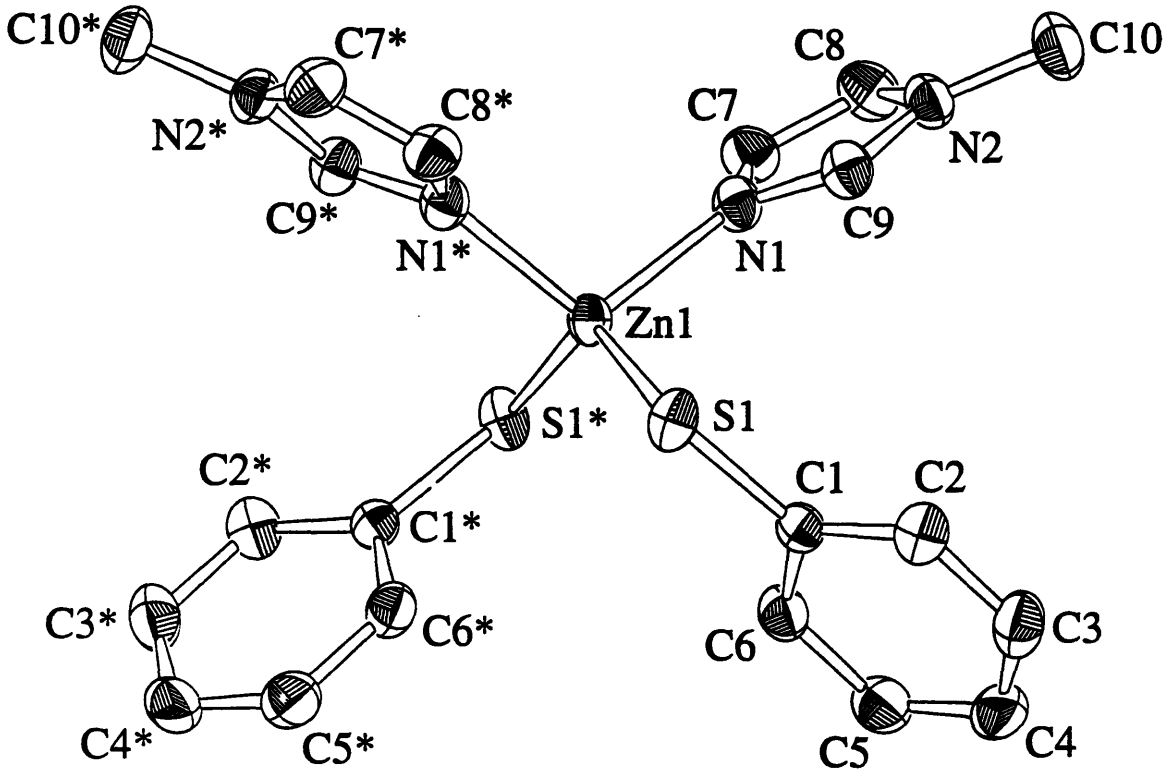


**Figure 2.3.** ORTEP diagram of $[Zn(SC_6H_5)_2(MeIm)_2]$ showing the 50% probability thermal ellipsoids for all non-hydrogen atoms.

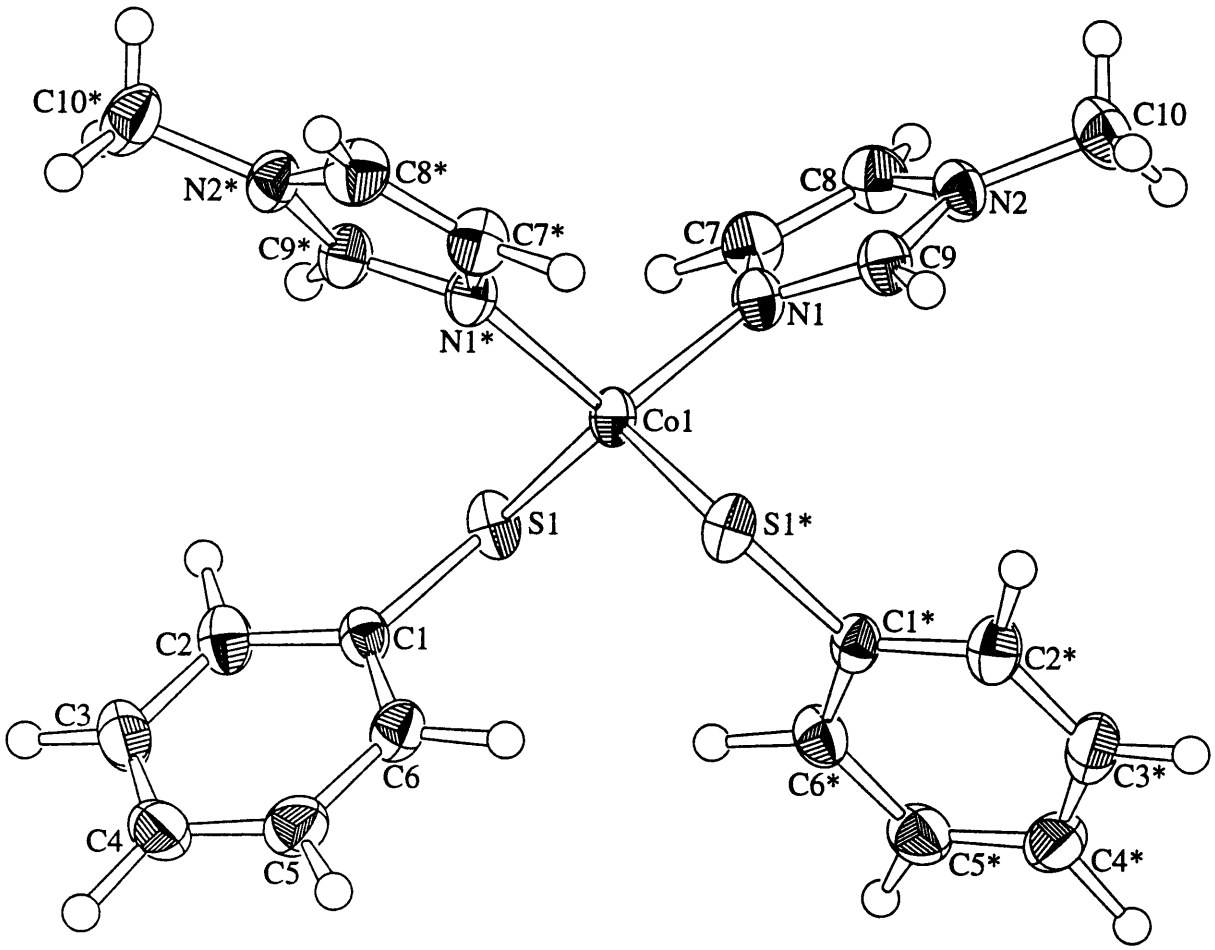


**Figure 2.4.** ORTEP diagram of $[Co(SC_6H_5)_2(MeIm)_2]$ showing the 50% probability thermal ellipsoids for all non-hydrogen atoms.

*Chapter Three*

# Methyl Transfer to Mercury Thiolates: Effects of Coordination Number and Ligand Dissociation

## Abstract

**Abstract:** The complexes $[(CH_3)_4N]_2[Hg(SC_6H_5)_4]$ and $[(C_4H_9)_4N][Hg(SC_6H_5)_3]$ demethylate $(CH_3O)_3PO$ as revealed by $^1H$, $^{31}P\{^1H\}$, and $^{199}Hg\{^1H\}$ NMR spectroscopy in DMSO-*d6* solution. The products of the $[Hg(SC_6H_5)_4]^{2-}$ reaction are $CH_3SC_6H_5$, $(CH_3O)_2PO_2^-$, and $[Hg(SC_6H_5)_3]^-$, whereas $[Hg(SC_6H_5)_3]^-$ demethylates $(CH_3O)_3PO$ to yield $CH_3SC_6H_5$ and $\{Hg(SC_6H_5)_2[(CH_3O)_2PO_2]\}^-$. Kinetic and solution equilibria studies reveal complete dissociation of a thiolate from $[Hg(SC_6H_5)_4]^{2-}$. This dissociated thiolate is the nucleophile active toward $(CH_3O)_3PO$. These results imply that the metal center of the inactive mercury derivative of the *Escherichia coli* Ada DNA alkylation repair protein comprises a three-coordinate $[Hg(S\text{-cysteine})_3]^-$ moiety and an unbound, protonated cysteine (HS-Cys69).

## Introduction

DNA is exposed environmentally to nonenzymatic alkylating agents.[1-5] Resulting lesions such as $O^6$-methylguanine and $O^4$-methylthymine disrupt traditional Watson-Crick base pairing and provide duplex DNA with mismatched base pairs.[6-12] These mutations are responsible, ultimately, for the deleterious effects of alkylating chemicals. To combat these processes, most organisms have protein systems responsible for repairing alkylated and mismatched DNA.[2,6,13]

One widely studied example is the Ada protein of *Escherichia coli*. By direct transfer of the offending alkyl groups to cysteine residues within the protein,[14-21] Ada repairs $O^6$-alkylguanine, $O^4$-alkylthymine, and the $S_p$ diastereomer of alkylphosphotriesters.[20-22] Two different active sites confer these repair capabilities upon the protein.[17,18,20] The alkylated base lesions are repaired by Cys321 in the C-terminal domain of the protein,[14,18,19] which is part of an Asn-$X_6$-Pro-Cys-His-Arg-Val-$X_9$-Tyr-$X_{13/14}$-Glu consensus sequence common to all known $O^6$-methylguanine transferases.[23] Alkylphosphotriesters are repaired by Cys69 in the N-terminal domain of the protein,[17,18] one of four cysteine residues which are bound to a zinc ion.[15,24-26] In addition to reversing phosphate damage, alkylation of Cys69 affects a structural change in the protein that enhances genome affinity.[15,16,18,27-29] Binding of the Cys69-alkylated Ada to DNA is then responsible for inducing production of gene products that are part of the cellular response to alkylation damage.[29-33] These resulting proteins include both Ada and other alkylation repair proteins.[20,22,30-38]

Both direct biochemical[15,16,24-27,39,40] and inorganic modeling studies[41,42] of the Ada $[Zn(S\text{-cys})_4]^{2-}$ site have elucidated the role of the metal center in DNA repair and cellular regulation. We developed a functional

small molecule mimic in which $[(CH_3)_4N]_2[Zn(SC_6H_5)_4]$ represents the $[Zn(S\text{-}cys)_4]^{2-}$ protein site and $(CH_3O)_3PO$ represents a methylphosphotriester lesion.[41,42] Our results showed that both $[Zn(SR)_4]^{2-}$ and $RS^-$ are active in methyl transfer, whereas RSH is not. Equilibria studies showed ready dissociation of a benzenethiolate ligand from $[(CH_3)_4N]_2[Zn(SC_6H_5)_4]$ in dimethyl sulfoxide (DMSO) solution. The nucleophile active in methyl transfer was determined to be the dissociated thiolate.

Our studies coupled with protein work distinguishing the nature of Cys69 from the three other zinc ligands[15,16,24,39] formed the basis for a proposed mechanism of alkylphosphotriester repair by Ada. In this mechanism, zinc coordination of Cys69 prevents protonation by accessible solvent to preserve thiolate nucleophilicity. Transient dissociation of Cys69 from zinc enables a thiolate nucleophile to react with the alkylphosphotriester lesion. Cys69 is in equilibrium between zinc-bound and free states.

To understand further the chemistry of the $[Zn(S\text{-}cys)_4]^{2-}$ center in Ada, many metal substitution studies have been carried out.[15,16,24,27,40] The cadmium form of N-terminal Ada fragments exhibited both a structure similar to the zinc form and methylphosphotriester repair capability.[15,16,24,27] The second-order rate constant of methylphosphotriester repair by Cd-N-Ada10 was one-quarter that of Zn-N-Ada10.[27] A preliminary report of a cobalt-substituted Ada fragment (Co-N-Ada16) exists, although details are not currently available.[16] Most recently, a mercury form of N-Ada17 was prepared to examine the potential effects of mercury exposure on cellular ability to repair alkylated nucleic acids.[40] Although the structure of Hg-N-Ada17 appears similar to that of Zn-N-Ada17, no methylphosphotriester repair activity was observed.

We envision three possible explanations for the native structure and inactivity of Hg-N-Ada17. First, the mercury cysteine thiolate center could be three-coordinate, with Cys38, 42, and 72 acting as ligands. In such a situation, Cys69 might be protonated and deactivated for methyl transfer. Second, Cys69 could be coordinated to mercury in a three-coordinate center, resulting in diminished nucleophilicity and the observed lack of reactivity. Third, all four cysteine residues (38, 42, 69, and 72) could bind mercury; which would also decrease the nucleophilicity of Cys69.

In the present investigation, we have extended our functional model system for methylphosphotriester repair by Ada to mercury thiolates. The solution behavior and reactivity of the mercury thiolate complexes $[(CH_3)_4N]_2[Hg(SC_6H_5)_4]$ and $[(C_4H_9)_4N][Hg(SC_6H_5)_3]$ with $(CH_3O)_3PO$ were investigated. The results afford insight into the nature of the mercury cysteine site of Hg-N-Ada17.

## Experimental

**General.** Owing to the photosensitivity of mercury compounds, all procedures were performed in a reduced light environment. Solutions were manipulated in a darkened hood and reaction flasks were covered with aluminum foil. All manipulations were carried out under argon by using standard Schlenk techniques. Solvents were degassed with argon. DMSO-*d6* was dried, degassed, and distilled according to standard procedures.[43] Analytical NMR spectra were recorded at 25 ± 1 °C on Varian Unity 300, Unity Plus 300, and VXR-500 instruments. All $^{31}P\{^1H\}$ and $^{199}Hg\{^1H\}$ (at 53.707 MHz) NMR spectra were recorded on samples of 211 mM concentration. The compound $[(C_4H_9)_4N][Hg(SC_6H_5)_3]$ was synthesized according to a literature

procedure[44] and characterized by elemental analysis and $^1$H NMR spectroscopy.

**Kinetic Studies.** Kinetic runs were performed under pseudo-first-order conditions with 5.0 mM metal thiolate and 1.0 mM $(CH_3O)_3PO$. Reactions were monitored by $^1$H NMR spectroscopy in DMSO-*d6* at 26.9 (± 0.7) °C. Typical $^1$H NMR parameters for kinetic studies were 4 scans per spectrum, 40 second relaxation delay between scans, 60 spectra per experiment, and a data collection time of 8 h. Concentrations of reactants and products were determined by referencing peak integrals to the resonances of $(CH_3)_4N^+$ and $(C_4H_9)_4N^+$ counterions, the concentrations of which were determined from known starting material quantities and known solution volumes. Rate constants were determined by curve fitting $(CH_3O)_3PO$ concentration versus time plots with a standard, integrated expression for first-order decay.[45] The pseudo-first-order rate constant for the $[(CH_3)_4N]_2[Hg(SC_6H_5)_4]$ reaction was determined in triplicate. The rate constant provided is an average of the three kinetic runs with the error reflecting one standard deviation. The slow reaction of $[(C_4H_9)_4N][Hg(SC_6H_5)_3]$ permitted only an upper limit of the pseudo-first-order rate constant to be determined. The initial rate method was used in this case.[45]

**$[(CH_3)_4N]_2[Hg(SC_6H_5)_4]$.** Benzenethiol (16.6 g, 151 mmol), $(C_2H_5)_3N$ (15.3 g, 151 mmol), and $(CH_3)_4NCl$ (5.94 g, 54.2 mmol) were combined in methanol (140 mL). To this solution was added $Hg(NO_3)_2{\cdot}H_2O$ (6.91 g, 20.2 mmol) in methanol (60 mL) over 30 min. During addition of the mercury solution, a white precipitate formed which dissolved upon further stirring. *n*-Propanol (140 mL) was added over a 10 min period and the reaction mixture was stored at -20 °C overnight. The resulting, off-white crystals were collected, washed with *n*-propanol, and dried in vacuo. Yield: 10.9 g, 69 %. $^1$H NMR (DMSO-

*d6*): δ 3.06 (s, 24 H, $(CH_3)N^+$), 6.71 (t, 4 H, *p*-H), 6.86 (t, 8 H, *m*-H), 7.28 (d, 8 H, *o*-H). Anal. Calcd for $C_{32}H_{44}N_2S_4Hg$: C, 48.93; H, 5.65; N, 3.57. Found: C, 49.14; H, 5.75; N, 3.57.

**Results**

**Reaction of $[(CH_3)_4N]_2[Hg(SC_6H_5)_4]$ with $(CH_3O)_3PO$.** An equimolar DMSO-*d6* solution of $[(CH_3)_4N]_2[Hg(SC_6H_5)_4]$ and $(CH_3O)_3PO$ reacted quantitatively to form $[Hg(SC_6H_5)_3]^-$, $CH_3SC_6H_5$, and $(CH_3O)_2PO_2^-$ products as revealed by $^1H$ NMR spectroscopy (Figure 3.1). The methylated thiolate $CH_3SC_6H_5$ was not coordinated to the mercury ion since its $^1H$ NMR resonances were identical to those of a genuine sample. The $^{31}P\{^1H\}$ NMR spectrum of the reaction mixture exhibited one peak of δ = 2.54 ppm, $\Delta\nu_{1/2}$ = 3.1 Hz, the sharpness of which peak contrasts with the broad ($\Delta\nu_{1/2}$ = 60 Hz) peak at δ = 1.70 ppm in the analogous zinc reaction. This peak in the zinc reaction was assigned to $(CH_3O)_2PO_2^-$ in equilibrium between free and zinc-bound states.[41,42] The sharp $^{31}P\{^1H\}$ NMR resonance in the mercury reaction indicated the absence of any such equilibrium process. Following the reaction, the $^1H$ NMR resonances of the product $[Hg(SC_6H_5)_3]^-$ (*ortho* = 7.27 ppm, *meta* = 7.01 ppm and *para* = 6.88 ppm) were slightly shifted from those of the starting $[Hg(SC_6H_5)_4]^{2-}$ complex (*ortho* = 7.28 ppm, *meta* = 6.86 ppm, and *para* = 6.71 ppm), but were similar to those of $[(C_4H_9)_4N][Hg(SC_6H_5)_3]$ (*ortho* = 7.24 ppm, *meta* = 6.99 ppm and *para* = 6.87 ppm), reflecting the lower charge. The $^{199}Hg\{^1H\}$ NMR spectrum of the reaction product displayed one peak at -407 ppm ($\Delta\nu_{1/2}$ = 57.4 Hz; Figure 3.2). This chemical shift value is very similar to that of the starting $[(CH_3)_4N]_2[Hg(SC_6H_5)_4]$, -421 ppm and close to that of $[(C_4H_9)_4N][Hg(SC_6H_5)_3]$, -359 ppm (Figure 3.2). Previous $^{199}Hg$ NMR studies have established the viability of three-coordinate $[Hg(SR)_3]^-$ (SR =

-$SC(CH_3)_3$,[46] -$SC_6H_5$[47]) species in acetonitrile and DMSO solutions, and most mononuclear, homoleptic mercury thiolate complexes characterized crystallographically are three-coordinate.[48,49]

**Reaction of $[(C_4H_9)_4N][Hg(SC_6H_5)_3]$ with $(CH_3O)_3PO$.** Methyl transfer from $(CH_3O)_3PO$ to $[(C_4H_9)_4N][Hg(SC_6H_5)_3]$ occurred quite slowly, forming products similar to those found for $[(CH_3)_4N]_2[Hg(SC_6H_5)_4]$. As indicated by $^1H$ NMR spectroscopy, $(CH_3O)_2PO_2^-$, $\{Hg(SC_6H_5)_2\}$, and free $CH_3SC_6H_5$ were formed. The $^{31}P\{^1H\}$ NMR spectrum displayed one sharp peak ($\delta$ = 2.50 ppm, $\Delta\nu_{1/2}$ = 3.8 Hz) attributable to $(CH_3O)_2PO_2^-$. The $^{199}Hg\{^1H\}$ NMR spectrum (Figure 3.2) of a stoichiometric reaction mixture of $[(C_4H_9)_4N][Hg(SC_6H_5)_3]$ and $(CH_3O)_3PO$ displayed a single peak at -613 ppm when the reaction was 23 % complete as determined by $^1H$ NMR spectroscopy. By comparison, the starting material $[(C_4H_9)_4N][Hg(SC_6H_5)_3]$ had a resonance at -359 ppm ($\Delta\nu_{1/2}$ = 35.5 Hz) (Figure 3.2). Oxygen donors shift $^{199}Hg$ NMR resonances upfield.[50] Thus, we attribute these spectral results to tight binding of the demethylated phosphate to the $\{Hg(SC_6H_5)_2\}$ moiety. The appearance of only one resonance in the $^{199}Hg\{^1H\}$ NMR spectrum of this reaction solution indicated that the $\{Hg(SC_6H_5)_2[(CH_3O)_2PO_2]\}^-$ product is in equilibrium with the remaining $[Hg(SC_6H_5)_3]^-$ starting material. The $^{199}Hg\{^1H\}$ NMR chemical shift of $\{Hg(SC_6H_5)_2[(CH_3O)_2PO_2]\}^-$ can be calculated from eq 3.1, in which the

$$\delta_{obs} = (\delta_{HgS3})(\chi_{HgS3}) + (\delta_{HgS2OP})(\chi_{HgS2OP}) \qquad (3.1)$$

observed chemical shift ($\delta_{obs}$) is a function of the chemical shifts of $[Hg(SC_6H_5)_3]^-$ ($\delta_{HgS3}$) and $\{Hg(SC_6H_5)_2[(CH_3O)_2PO_2]\}^-$ ($\delta_{HgS2OP}$) and their respective mole fractions ($\chi_{HgS3}$ and $\chi_{HgS2OP}$). From the reaction solution at

23 % completion and the data presented above, we calculate a $^{199}Hg\{^1H\}$ NMR shift for $\{Hg(SC_6H_5)_2[(CH_3O)_2PO_2]\}^-$ of -1465 ppm.

**Kinetic Studies.** In order to compare the mercury complex reactions with those of its zinc, cobalt, and cadmium analogs, kinetic data were obtained. The tetrathiolate $[(CH_3)_4N]_2[Hg(SC_6H_5)_4]$ reacted with $(CH_3O)_3PO$ with a pseudo-first-order rate constant of $(1.1 \pm 0.1) \times 10^{-4}$ $s^{-1}$, essentially the same rate constant as the free benzene thiolate itself (Table 3.1). In contrast, the trithiolate $[(C_4H_9)_4N][Hg(SC_6H_5)_3]$ reacted significantly more slowly than any of the tetrathiolate metal complexes (Table 3.1). An upper limit of $3 \times 10^{-7}$ $s^{-1}$ was estimated for the reaction of $[(C_4H_9)_4N][Hg(SC_6H_5)_3]$ with $(CH_3O)_3PO$.

**Solution Behavior.** In order to address the question of whether the active nucleophiles of $[(CH_3)_4N]_2[Hg(SC_6H_5)_4]$ and $[(C_4H_9)_4N][Hg(SC_6H_5)_3]$ are dissociated or metal-bound thiolates, a series of DMSO-*d6* solutions were prepared containing mercury complexes alone and with added benzenethiolate, each species being present at 50 mM. Figure 3.3 displays the $^1H$ NMR spectra of these solutions in the aromatic region. In all cases, distinct ortho (most downfield), meta, and para (most upfield) resonances are visible. The solution containing $[(CH_3)_4N]_2[Hg(SC_6H_5)_4]$ and $(CH_3)_4N(SC_6H_5)$ displayed only one set of benzenethiolate resonances, indicating rapid exchange between bound and free states. The chemical shifts of the resonances for the solution containing $[(CH_3)_4N]_2[Hg(SC_6H_5)_4]$ and those for the solution containing $[(C_4H_9)_4N][Hg(SC_6H_5)_3]$ + $(CH_3)_4N(SC_6H_5)$ were almost identical. The peaks of $[(CH_3)_4N]_2[Hg(SC_6H_5)_4]$ were broader and displayed diminished splitting relative to those of each $[(C_4H_9)_4N][Hg(SC_6H_5)_3]$ and $(CH_3)_4N(SC_6H_5)$, indicating slower exchange between bound and free benzenethiolate. The sharper peaks of $[(C_4H_9)_4N][Hg(SC_6H_5)_3]$, by contrast, suggested little or no ligand dissociation.

**Reaction of $[(CH_3)_4N]_2[Hg(SC_6H_5)_4]$ and $(CH_3O)_3PO$ with a Protic Acid.** To prove experimentally that protonation of a thiolate can inactivate its methyl transfer capability, we added $HBF_4$ etherate to a mercury thiolate methyl transfer reaction. Addition of $(CH_3O)_3PO$ to a DMSO-*d6* solution containing $[(CH_3)_4N]_2[Hg(SC_6H_5)_4]$ and $HBF_4{\cdot}O(C_2H_5)_2$, each at 211 mM concentration, blocked methyl transfer. No $CH_3SC_6H_5$ formed even after one month, as monitored by $^1H$ NMR spectroscopy. For comparison, a reaction of $[(CH_3)_4N]_2[Hg(SC_6H_5)_4]$ and $(CH_3O)_3PO$ without added acid at similar concentrations formed products quantitatively after one month.

## Discussion

**Solution Behavior and Reactivity.** The pseudo-first-order rate constant for methyl transfer from $(CH_3O)_3PO$ to $[Hg(SC_6H_5)_4]^{2-}$ is identical to that of benzenethiolate (Table 3.1). Rate constants for the complexes $[M(SC_6H_5)_4]^{2-}$ (M = Zn(II), Co(II), and Cd(II)) are below or close to that of $C_6H_5S^-$ (Table 3.1). Since metal thiolates generally have decreased nucleophilicity relative to free thiolates,[42] these results indicate that $[Hg(SC_6H_5)_4]^{2-}$ reacts exclusively via dissociated thiolate. The very similar $^{199}Hg\{^1H\}$ NMR chemical shifts of $[Hg(SC_6H_5)_4]^{2-}$ before and after reaction with $(CH_3O)_3PO$, along with the $^1H$ NMR data showing rapid equilibrium between bound and free $C_6H_5S^-$ for the $[Hg(SC_6H_5)_4]^{2-}$ complex, support this conclusion.

The aromatic $^1H$ NMR peaks of $[Hg(SC_6H_5)_4]^{2-}$ are broader and exhibited diminished splitting relative to those of $C_6H_5S^-$ and $[Hg(SC_6H_5)_3]^-$, indicating the presence of an equilibrium between mercury-bound and free benzenethiolate. The $^1H$ NMR spectrum of an equimolar mixture of $[Hg(SC_6H_5)_4]^{2-}$ and $C_6H_5S^-$ displayed one set of benzenethiolate peaks, as expected for rapid exchange of bound and free thiolates. Previous work also

revealed ligand loss from $[Hg(S\text{-}p\text{-}C_6H_4Cl)_4]^{2-}$ in DMSO, as evidenced by a change in $^{199}Hg$ NMR chemical shift values upon titration with added ligand.[47] Taken together, these results reveal that $[Hg(SC_6H_5)_4]^{2-}$ completely dissociates a thiolate in DMSO solution, which then reacts with $(CH_3O)_3PO$ to yield the products observed (Scheme 3.1). Such a scheme is similar to that previously determined for $[Zn(SC_6H_5)_4]^{2-}$, in which dissociated benzenethiolate reacts with $(CH_3O)_3PO$.[42]

The slow reaction of $[Hg(SC_6H_5)_3]^-$ may be a function of diminished ligand dissociation relative to $[Hg(SC_6H_5)_4]^{2-}$. Dissociation of an anionic ligand from a monoanionic complex such as $[Hg(SC_6H_5)_3]^-$ is expected to be less facile than that from a dianion such as $[Hg(SC_6H_5)_4]^{2-}$. Sharp, well defined $^1H$ NMR resonances of $[Hg(SC_6H_5)_3]^-$ and the predominance of $[Hg(SR)_3]^-$ units in the solution[46,47] and solid states[44,46,51-54] are consistent with $[Hg(SC_6H_5)_3]^-$ remaining largely intact in DMSO solution. At this time, we cannot ascribe the reactivity of $[Hg(SC_6H_5)_3]^-$ exclusively to a dissociated or a metal-bound thiolate nucleophile.

**Relevance to Hg-N-Ada17.** The facile reaction of $[Hg(SC_6H_5)_4]^{2-}$ with $(CH_3O)_3PO$ suggests that the mercury derivative of N-Ada17 should be capable of methylphosphotriester repair. Such is not the case, however.[40] The inactivity of Hg-N-Ada17 can be explained by the present results in the context of previous studies on Ada protein fragments. Cadmium substitution for zinc in active N-terminal fragments of Ada indicated Cys69 to be different from the three other ligating cysteine residues (Cys38, Cys42, and Cys72).[15,16,24] Although $^1H$-$^{113}Cd$ scalar coupling was observed for Cys38, Cys42, and Cys72, none appeared for Cys69. Reaction of the zinc form of a 10 kDa N-terminal fragment (Zn-N-Ada10) with $CH_3I$ demonstrated enhanced nucleophilicity of Cys69 relative to the remaining three ligand residues.[39]

The ready dissociation of benzenethiolate from $[Hg(SC_6H_5)_4]^{2-}$, and the predominance of three-coordinate mercury thiolates disfavor a four-coordinate $[Hg(S\text{-cys})_4]^{2-}$ environment in Hg-N-Ada17. Tight zinc binding of Cys38, Cys42, and Cys72 in Zn-N-Ada10 implies that a three-coordinate mercury center of Hg-N-Ada17 would most likely include these residues. Protonation of Cys69 by accessible water would greatly diminish its nucleophilicity and, consequently, its alkylphosphotriester repair activity. We have shown experimentally that protonation of a dissociated thiolate inactivates the nucleophile with respect to methyl transfer ability. Thus, we attribute the inability of Hg-N-Ada17 to repair alkylphosphotriesters to a three-coordinate mercury center involving Cys38, 42, and 72 and a protonated, deactivated Cys69 residue.

**Acknowledgment**

This research was supported by grant CA34992 from the National Cancer Institute (S.J.L.) and by grant ES07373 from the National Institute of Environmental Health Sciences (K.E.W.). J.J.W. is predoctoral trainee under N.C.I. training grant CA09112. We thank Wayne Casey for his assistance with the $^{199}Hg$ NMR measurements which were performed at the Dartmouth NMR/EPR Facility.

**References**

(1) Counts, J. L.; Goodman, J. I. *Cell* **1995**, *83*, 13-15.

(2) Lindahl, T. *Nature* **1993**, *362*, 709-715.

(3) Mathews, C. K.; van Holde, K. E. *Biochemistry*; Benjamin/Cummings Pub. Co. Inc.: Reading, MA, 1990.

(4) Singer, B.; Grunberger, D. *Molecular Biology of Mutagens and Carcinogens*; Plenum Press: New York, 1983.

(5) Singer, B. *Prog. Nucl. Acid Res. Mol. Biol.* **1975**, *15*, 219-284.

(6) Friedberg, E. C.; Walker, G. C.; Siede, W. *DNA Repair and Mutagenesis*; ASM Press: Washington D. C., 1995.

(7) Laird, P. W.; Jackson-Grusby, L.; Fazeli, A.; Dickinson, S. L.; Jung, W. E.; Li, E.; Weinberg, R. A.; Jaenisch, R. *Cell* **1995**, *81*, 197-205.

(8) Guttenplan, J. B. *Mutat. Res.* **1990**, *233*, 177-187.

(9) Swann, P. F. *Mutat. Res.* **1990**, *233*, 81-94.

(10) Loechler, E. L.; Green, C. L.; Essigmann, J. M. *Proc. Natl. Acad. Sci. U. S. A.* **1984**, *81*, 6271-6275.

(11) Hall, J. A.; Saffhill, R. *Nucl. Acid Res.* **1983**, *11*, 4185-4193.

(12) Schendel, P. F.; Robins, P. E. *Proc. Natl. Acad. Sci. U. S. A.* **1978**, *74*, 6017-6020.

(13) Friedberg, E. C. *BioEssays* **1994**, *16*, 645-649.

(14) Moore, M. H.; Gulbis, J. M.; Dodson, E. J.; Demple, B.; Moody, P. C. E. *EMBO J.* **1994**, *13*, 1495-1501.

(15) Myers, L. C.; Cushing, T. D.; Wagner, G.; Verdine, G. L. *Chem. and Biol.* **1994**, *1*, 91-97.

(16) Ohkubo, T.; Sakashita, H.; Sakuma, T.; Kainosho, M.; Sekiguchi, M.; Morikawa, K. *J. Am. Chem. Soc.* **1994**, *116*, 6035-6036.

(17) Sedgwick, B.; Robins, P.; Totty, N.; Lindahl, T. *J. Biol. Chem.* **1988**, *263*, 4430-4433.

(18) Takano, K.; Nakabeppu, Y.; Sekiguchi, M. *J. Mol. Biol.* **1988**, *201*, 261-271.

(19) Demple, B.; Sedgwick, B.; Robins, P.; Totty, N.; Waterfield, M. D.; Lindahl, T. *Proc. Natl. Acad. Sci. U. S. A.* **1985**, *82*, 2688-2692.

(20) McCarthy, T. V.; Lindahl, T. *Nucl. Acid Res.* **1985**, *13*, 2683-2698.

(21) Demple, B.; Jacobsson, A.; Olsson, M.; Robins, P.; Lindahl, T. *J. Biol. Chem.* **1982**, *257*, 13776-13780.

(22) Teo, I.; Sedgwick, B.; Demple, B.; Li, B.; Lindahl, T. *EMBO J.* **1984**, *3*, 2151-2157.

(23) Wibley, J. E. A.; McKie, J. H.; Embrey, K.; Marks, D. S.; Douglas, K. T.; Moore, M. H.; Moody, P. C. E. *Anti-Cancer Drug Design* **1995**, *10*, 75-95.

(24) Myers, L. C.; Terranova, M. P.; Ferentz, A. E.; Wagner, G.; Verdine, G. L. *Science* **1993**, *261*, 1164-1167.

(25) Myers, L. C.; Verdine, G. L.; Wagner, G. *Biochemistry* **1993**, *32*, 14089-14094.

(26) Myers, L. C.; Terranova, M. P.; Nash, H. M.; Markis, M. A.; Verdine, G. L. *Biochemistry* **1992**, *31*, 4541-4547.

(27) Myers, L. C.; Jackow, F.; Verdine, G. L. *J. Biol. Chem.* **1995**, *270*, 6664-70.

(28) Saget, B. M.; Walker, G. C. *Proc. Natl. Acad. Sci. U. S. A.* **1994**, *91*, 9730-9734.

(29) Teo, I.; Sedgwick, B.; Kilpatrick, M. W.; McCarthy, T. V.; Lindahl, T. *Cell* **1986**, *45*, 315-324.

(30) Shevell, D. E.; Friedman, B. M.; Walker, G. C. *Mutat. Res.* **1990**, *233*, 53-72.

(31) Lindahl, T.; Sedgewick, B.; Sekiguchi, M.; Nakabeppu, Y. *Ann. Rev. Biochem.* **1988**, *57*, 133-157.

(32) Nakabeppu, Y.; Sekiguchi, M. *Proc. Natl. Acad. Sci. U. S. A.* **1986**, *83*, 6297-6301.

(33) Volkert, M. R.; Nguyen, D. C. *Proc. Natl. Acad. Sci. U. S. A.* **1984**, *81*, 4110-4114.

(34) Nakabeppu, Y.; Kondo, H.; Kawabata, S.-I.; Iwanaga, S.; Sekiguchi, M. *J. Biol. Chem.* **1985**, *260*, 7281-7288.

(35) McCarthy, T. V.; Karran, P.; Lindahl, T. *EMBO J.* **1984**, *3*, 545-550.

(36) Nakabeppu, Y.; Miyata, T.; Kondo, H.; Iwanaga, S.; Sekiguchi, M. *J. Biol. Chem.* **1984**, *259*, 13730-13736.

(37) Evensen, G.; Seeberg, E. *Nature* **1982**, *296*, 773-775.

(38) Karran, P.; Hjelmgren, T.; Lindahl, T. *Nature* **1982**, *296*, 770-773.

(39) Myers, L. C.; Wagner, G.; Verdine, G. L. *J. Am. Chem. Soc.* **1995**, *117*, 10749-10750.

(40) Wetterhahn, K. E.; Verdine, G. L., unpublished results.

(41) Wilker, J. J.; Lippard, S. J. *J. Am. Chem. Soc.* **1995**, *117*, 8682-8683.

(42) Wilker, J. J.; Lippard, S. J., submitted for publication.

(43) Gordon, A. J.; Ford, R. A. *The Chemist's Companion. A Handbook of Practical Data, Techniques, and References*; John Wiley and Sons: New York, 1972.

(44) Christou, G.; Folting, K.; Huffman, J. C. *Polyhedron* **1984**, *3*, 1247-1253.

(45) Wilkins, R. G. *Kinetics and Mechanism of Reactions of Transition Metal Complexes*; Second ed.; VCH Publishers Inc.: New York, 1991.

(46) Watton, S. P.; Wright, J. G.; MacDonnell, F. M.; Bryson, J. W.; Sabat, M.; O'Halloran, T. V. *J. Am. Chem. Soc.* **1990**, *112*, 2824-2826.

(47) Natan, M. J.; Millikan, C. F.; Wright, J. G.; O'Halloran, T. V. *J. Am. Chem. Soc.* **1990**, *112*, 3255-3257.

(48) Cambridge Structural Database, April 1996 Release.

(49) Allen, F. H.; Kennard, O.; Taylor, R. *Acc. Chem. Res.* **1983**, *16*, 146-153.

(50) Kidd, R. G.; Goodfellow, R. J. In *NMR and the Periodic Table*; Harris, R. K. and Mann, B. E., Ed.; Academic Press: New York, 1978, pp 195-278.

(51) Alsina, T.; Clegg, W.; Fraser, K. A.; Sola, J. *J. Chem. Soc. Dalton Trans.* **1992**, 1393-1399.

(52) Santos, R. A.; Gruff, E. S.; Koch, S. A.; Harbison, G. S. *J. Am. Chem. Soc.* **1991**, *113*, 469.

(53) Gruff, E. S.; Koch, S. A. *J. Am. Chem. Soc.* **1990**, *112*, 1245.

(54) Behrens, U.; Hoffmann, K.; Klar, G. *Chem. Ber.* **1977**, *110*, 3672-3677.

**Table 3.1.** Pseudo-First-Order Rate Constants for Reactions of Benzenethiolate and its Metal Complexes with $(CH_3O)_3PO$.[a]

| compound | $k$ ($s^{-1}$) |
|---|---|
| $[(CH_3)_4N]_2[Hg(SC_6H_5)_4]$ | $(1.1 \pm 0.1) \times 10^{-4}$ |
| $[(C_4H_9)_4N][Hg(SC_6H_5)_3]$ | $\leq 3 \times 10^{-7}$ |
| $[(CH_3)_4N]_2[Cd(SC_6H_5)_4]$ [b] | $(3 \pm 1) \times 10^{-5}$ |
| $[(CH_3)_4N]_2[Co(SC_6H_5)_4]$ [b] | $(4 \pm 1) \times 10^{-5}$ |
| $[(CH_3)_4N]_2[Zn(SC_6H_5)_4]$ [b] | $(8.2 \pm 0.6) \times 10^{-5}$ |
| $(CH_3)_4N(SC_6H_5)$ [b] | $(1.1 \pm 0.3) \times 10^{-4}$ |

[a]Reactions were carried out with 5.0 mM thiolate or metal complex and 1.0 mM $(CH_3O)_3PO$ in DMSO-*d6*. Error estimates reflect one standard deviation from the average of three runs. [b]From Wilker, J. J. and Lippard, S. J., submitted for publication.

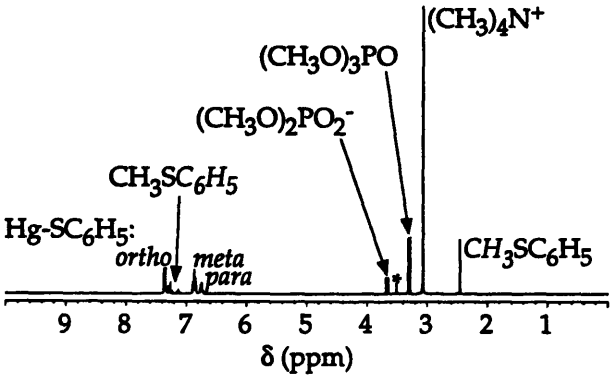


**Figure 3.1.** The $^1H$ NMR spectrum in DMSO-*d6* of an equimolar reaction of $[(CH_3)_4N]_2[Hg(SC_6H_5)_4]$ and $(CH_3O)_3PO$ in progress. The asterisk denotes $H_2O$. Starting reagent concentrations were 211 mM each. This spectrum was taken two days after mixing of the reagents.

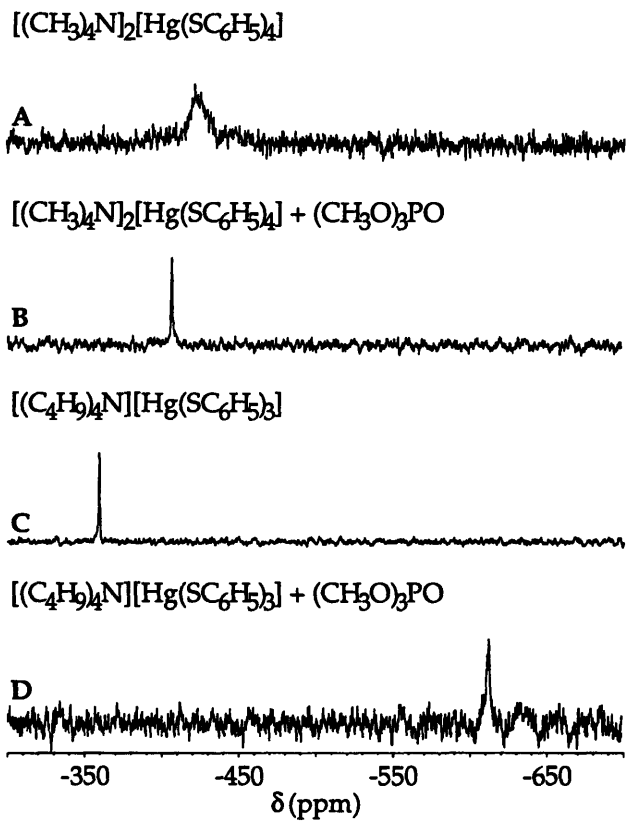


**Figure 3.2.** $^{199}Hg\{^{1}H\}$ NMR spectra in DMSO-*d6* of $[(CH_3)_4N]_2[Hg(SC_6H_5)_4]$ (A), the reaction product of $[(CH_3)_4N]_2[Hg(SC_6H_5)_4]$ and $(CH_3O)_3PO$ (B), $[(C_4H_9)_4N][Hg(SC_6H_5)_3]$ (C), and the reaction of $[(C_4H_9)_4N][Hg(SC_6H_5)_3]$ with $(CH_3O)_3PO$ at 23 % completion (D). Starting concentrations were 211 mM in all cases.

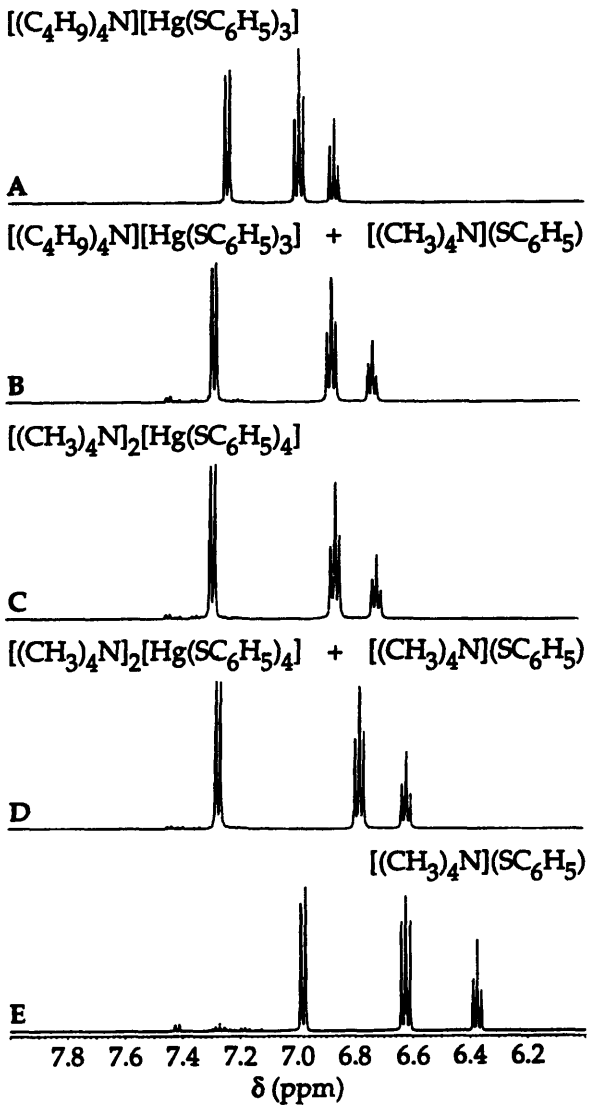


**Figure 3.3.** Aromatic region $^1H$ NMR spectra in DMSO-*d6* of $[(C_4H_9)_4N][Hg(SC_6H_5)_3]$ (A), $[(C_4H_9)_4N][Hg(SC_6H_5)_3]$ and $(CH_3)_4N(SC_6H_5)$ (B), $[(CH_3)_4N]_2[Hg(SC_6H_5)_4]$ (C), $[(CH_3)_4N]_2[Hg(SC_6H_5)_4]$ and $(CH_3)_4N(SC_6H_5)$ (D), and $(CH_3)_4N(SC_6H_5)$ (E). The concentration of each species is 50 mM.

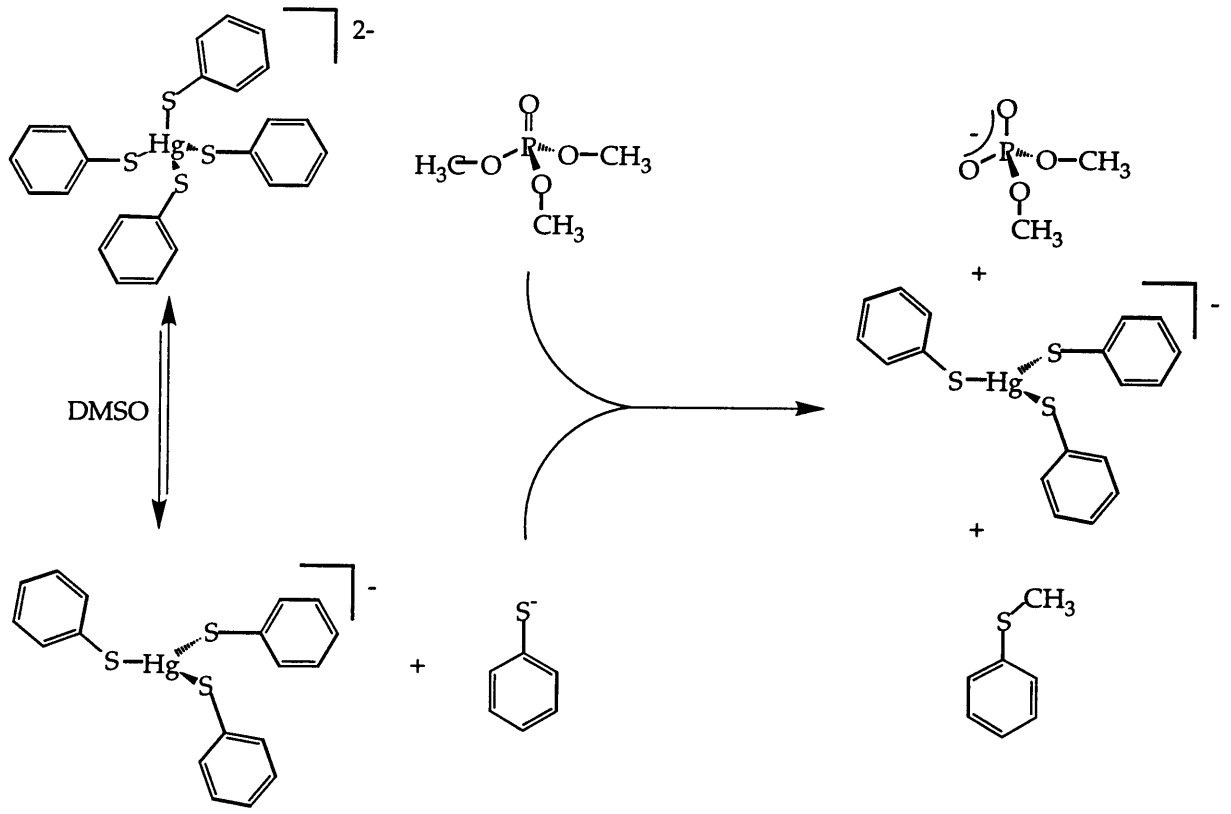


**Scheme 3.1**

*Chapter Four*

# Kinetic Studies of the Methylation of Iron-Sulfur Complexes by Trimethylphosphate

**Abstract**

Reaction of $[(C_4H_9)_4N]_2[Fe_4S_4(SC_6H_5)_4]$ with $(CH_3O)_3PO$ in DMSO-*d6* afforded $[(C_4H_9)N]_2\{Fe_4S_4(SC_6H_5)_3[(CH_3O)_2PO_2]\}$ and $CH_3SC_6H_5$ as revealed by $^1H$ and $^{31}P\{^1H\}$ NMR spectroscopy. The ethanethiolate analog $[(C_4H_9)_4N]_2[Fe_4S_4(SC_2H_5)_4]$ reacted with $(CH_3O)_3PO$ to yield $[(C_4H_9)_4N]_2$-$[Fe_4S_4(SC_2H_5)_3(DMSO)]$, $(CH_3O)_2PO_2^-$, and $CH_3SC_2H_5$. The more reduced species $[(C_2H_5)_4N]_3[Fe_4S_4(SC_2H_5)_4]$ also gave $(CH_3O)_2PO_2^-$ and $CH_3SC_2H_5$ in addition to an unidentified iron thiolate species. Stoichiometric methylation of mononuclear $[(C_2H_5)_4N]_2[Fe(SC_2H_5)_4]$ by $(CH_3O)_3PO$ afforded an uncharacterized iron-containing species as well as $(CH_3O)_2PO_2^-$ and $CH_3SC_2H_5$. Kinetic studies revealed a rate constant for methylation of $[(C_2H_5)_4N]_3[Fe_4S_4(SC_2H_5)_4]$ to be more than 200-fold higher than that of the more oxidized analogs $[(C_4H_9)_4N]_2[Fe_4S_4(SR)_4]$ (R = $C_6H_5$, $C_2H_5$). The compound $[(C_2H_5)_4N]_2[Fe(SC_2H_5)_4]$ had the highest rate constant, $\geq 5 \times 10^{-3}$ $s^{-1}$ with 5.0 mM complex and 1.0 mM $(CH_3O)_3PO$ concentration Attempts to prepare site-differentiated tetranuclear iron-sulfur complexes by removing one thiolate via methylation and addition of second, capping ligands are described. We discuss these results in the context of metal thiolate moieties affecting repair of DNA alkylation damage.

**Introduction**

Tetranuclear iron-sulfur clusters having cuboidal structures are well known in bioinorganic chemistry. They occur in three distinct oxidation states, mediating electron transfer reactions in a variety of protein environments which afford a wide range of oxidation potentials.[1-4] The $\{Fe_4S_4\}^{2+}$ cluster of aconitase, by contrast, catalyzes the interconversions of citrate, *cis*-aconitate, and isocitrate without changing oxidation state.[5,6] This hydratase/dehydratase activity depends upon the ability of an iron atom at a cube corner to alternate between four- and six-coordinate geometries, differentiating this iron-sulfur-cluster-dependent transformation from similar reactions catalyzed by zinc enzymes.

More recently, three examples of iron-sulfur clusters have been found in DNA repair proteins. Endonuclease III (endo III)[7-9] and MutY[10-12] from *Escherichia coli* and ultraviolet endonuclease (UV endonuclease)[13] of *Micrococcus luteus* all have glycolysis activity and $\{Fe_4S_4\}^{2+}$ units which seemingly do not participate directly in their catalytic activity. Endo III removes the products of purine reduction, cleavage, and hydration.[14,15] MutY initiates repair of spontaneous guanine-adenine (G-A) and 7,8-dihydro-8-oxoguanine-adenine (8-oxoG-A) mismatches by eliminating the offending base (i.e. A) and creating an apurinic site.[14,16-18] UV endonuclease removes light-induced thymine dimers.[13] The postulated structural role of the $\{Fe_4S_4\}^{2+}$ cluster in these repair enzymes is similar to that of the prototypical zinc finger motif [Zn(*S*-cysteine)$_2$(*N*-histidine)$_2$], in which a metal center is employed to stabilize protein secondary structure.[19-22]

Previously, we investigated the reactions of zinc(II) and related metal thiolate complexes with $(CH_3O)_3PO$ as models for the zinc-containing *E. coli* Ada protein.[23-25] In Ada, a $[Zn(S\text{-cys})_4]^{2-}$ unit repairs DNA alkylation damage

by stoichiometric transfer of the alkyl group to a thiolate ligand.[26-29] Reaction of $[(CH_3)_4N]_2[Zn(SC_6H_5)_4]$ with $(CH_3O)_3PO$ afforded chemistry which paralleled DNA methylphosphotriester repair.[23,24]

The present study was undertaken to explore the possibility that iron-sulfur clusters might similarly accept a methyl group from $(CH_3O)_3PO$ and, if so, to determine whether alkylation would occur at the sulfide or the terminal thiolate group. An earlier report described briefly the reaction of $[(C_2H_5)_4N]_2[Fe_4S_4(SC_6H_5)_4]$ with one equivalent of $CF_3SO_3CH_3$ in *N*-methyl-2-pyrrolidinone (NMP) to yield $CH_3SC_6H_5$ and an uncharacterized iron-containing species, presumably $[Fe_4S_4(SC_6H_5)_3(CF_3SO_3)]^{2-}$.[30] In our investigations, several specific questions were posed. How will the rate constants for demethylation of $(CH_3O)_3PO$ by the clusters compare with those of the zinc thiolates; will the reaction rate depend on the cluster charge; will the methylated thiolate remain coordinated; if a thiolate were released from an $[Fe_4S_4(SR)_4]^{2-}$ complex by methylation, could another ligand be added to capture a site-differentiated cluster; could dealkylation be used as a general probe for the nucleophilicity of iron-sulfur complexes; and is there potential for iron-sulfur centers to have such a functional role in DNA repair?

To address these questions, we investigated the alkylation of tetranuclear iron-sulfur clusters having two oxidation states and two different terminal thiolate ligand types. The mononuclear complex $[(C_2H_5)_4N]_2[Fe(SC_2H_5)_4]$ was also examined. To permit comparisons with zinc complexes investigated previously, $(CH_3O)_3PO$ was used as the alkylating agent and dimethyl sulfoxide (DMSO) as solvent.[23-25] Reaction products were characterized in solution by $^1H$ and $^{31}P\{^1H\}$ nuclear magnetic resonance (NMR) spectroscopy. The kinetics of the methylation reactions were examined, and attempts were made to prepare site-differentiated $[Fe_4S_4(SC_6H_5)_3(L)]^{2+}$ clusters.

## Experimental

**General.** All procedures were carried out under an argon or nitrogen atmosphere by using standard Schlenk and glove box techniques. Solvents were dried, degassed, and distilled according to standard methods.[31,32] NMR spectra were collected in DMSO-*d6* at 25 ± 1 °C on a Varian Unity 300 instrument. All analytical NMR spectra were recorded on samples with complex concentrations of 50 mM with the exception of $[(C_4H_9)_4N]_2[Fe_4S_4(SC_2H_5)_4]$, which was at 10 mM owing to solubility limitations. The compounds $[(C_4H_9)_4N]_2[Fe_4S_4(SC_6H_5)_4]$,[33] $[(C_4H_9)_4N]_2[Fe_4S_4(SC_2H_5)_4]$,[33] $[(C_2H_5)_4N]_3[Fe_4S_4(SC_2H_5)_4]$,[34] and $[(C_2H_5)_4N]_2[Fe(SC_2H_5)_4]$[35] were prepared according to literature methods and characterized by $^1H$ NMR spectroscopy and elemental analysis.

**Kinetics.** Kinetic experiments were performed under pseudo-first-order conditions with the metal complex concentration of 5.0 mM and $(CH_3O)_3PO$ at 1.0 mM. This relatively low iron complex concentration was chosen to minimize the effects of ion pairing.[24] Reactions were monitored by $^1H$ NMR spectroscopy in DMSO-*d6* at 26 (± 1) °C. Typical $^1H$ NMR parameters for kinetic studies included 4 scans per spectrum, 40 second relaxation delays between scans, and 60 spectra per experiment. The total time of data collection was 10 h. Solution volumes were standardized by using calibrated 1 mL volumetric flasks. Concentrations of reactants and products were determined by referencing peak integrals to the resonances of $R_4N^+$ counterions, the concentrations of which were determined from starting material quantities and known solution volumes. For the reactions of $[(C_2H_5)_4N]_3[Fe_4S_4(SC_2H_5)_4]$ and $[(C_2H_5)_4N]_2[Fe(SC_2H_5)_4]$, rate constants were determined by curve fitting $(CH_3O)_3PO$ concentration-versus-time plots with a standard, integrated expression for first-order decay.[36] Pseudo-first-order

rate constants for $[(C_2H_5)_4N]_3[Fe_4S_4(SC_2H_5)_4]$ were determined in triplicate. The rate constant provided is an average of the three kinetic runs and the error shown reflects one standard deviation. The slow reactions of $[(C_4H_9)_4N]_2[Fe_4S_4(SR)_4]$ (R = $C_6H_5$ and $C_2H_5$) permitted only an upper limit of the pseudo-first-order rate constants to be determined. The initial rate method was used in these cases.[36]

**Results**

**Reaction of $[(C_4H_9)_4N]_2[Fe_4S_4(SC_6H_5)_4]$ with $(CH_3O)_3PO$.** This reaction in DMSO-*d6* yielded $CH_3SC_6H_5$ and could be readily monitored by $^1H$ NMR spectroscopy (Figure 4.1). The thioether product was uncoordinated since its $^1H$ NMR resonances are identical to those of a genuine sample. The resonances of the benzenethiolate cluster ligands remained unchanged after the reaction, indicating an intact $\{Fe_4S_4\}^{2+}$ core structure. No resonances were observed for the expected phosphate product, $(CH_3O)_2PO_2^-$, in either the $^1H$ or $^{31}P\{^1H\}$ NMR spectra. We interpret the absence of these signals as evidence that the $(CH_3O)_2PO_2^-$ anion is coordinated to the paramagnetic cluster, resulting in broad, unobservable resonances. The reaction products are therefore tentatively assigned as depicted in Scheme 4.1.

**Reaction of $[(C_4H_9)_4N]_2[Fe_4S_4(SC_2H_5)_4]$ with $(CH_3O)_3PO$.** This compound reacted similarly to transfer a methyl group. The $^1H$ NMR spectrum revealed peaks of the methylated thiolate $CH_3SC_2H_5$ and the persistence of resonances attributed to $^-SC_2H_5$ ligation of the $\{Fe_4S_4\}^{2+}$ core. The $CH_3SC_2H_5$ chemical shifts were identical to those of a genuine sample, indicating that it was not coordinated to the cluster. In this case, however, the phosphate product $(CH_3O)_2PO_2^-$ was observed in both the $^1H$ and $^{31}P\{^1H\}$ NMR spectra. As the reaction proceeded, a doublet grew in at 3.22 ppm, similar in shift to the 3.33

ppm methyl resonance in $(NH_4)[(CH_3O)_2PO_2]$. The $^{31}P\{^1H\}$ NMR spectrum of $(CH_3O)_2PO_2^-$ generated in the reaction showed one sharp ($\Delta\nu_{1/2}$ = 3.8 Hz) peak also similar in linewidth ($\Delta\nu_{1/2}$ = 5.1 Hz) to that in a sample of $(NH_4)[(CH_3O)_2PO_2]$. From these results, we conclude that $(CH_3O)_2PO_2^-$ is uncoordinated. Presumably, solvent fills the empty coordination site of the intact cluster and the reaction proceeds as indicated in Scheme 4.2.

**Reaction of $[(C_2H_5)_4N]_3[Fe_4S_4(SC_2H_5)_4]$ with $(CH_3O)_3PO$.** These reactants also undergo methyl transfer. In the $^1H$ NMR spectrum of the products, both $CH_3SC_2H_5$ and $(CH_3O)_2PO_2^-$ appeared at shift values similar to those of genuine samples (Figure 4.2). In addition, there was one sharp ($\Delta\nu_{1/2}$ = 3.9 Hz) peak in the $^{31}P\{^1H\}$ NMR spectrum attributable to uncoordinated $(CH_3O)_2PO_2^-$. The remaining $^-SC_2H_5$ ligands remained coordinated to iron, as indicated by their paramagnetically shifted $^1H$ NMR resonances at 2.59 ppm ($\Delta\nu_{1/2}$ = 75.8 Hz) and 14.6 ppm ($\Delta\nu_{1/2}$ = 168 Hz). These shift values, however, differ greatly from those of the starting material, 4.88 ppm ($\Delta\nu_{1/2}$ = 81.5 Hz) and 33.0 ppm ($\Delta\nu_{1/2}$ = 483 Hz), which disappeared after the reaction.

**Reaction of $[(C_2H_5)_4N]_2[Fe(SC_2H_5)_4]$ with $(CH_3O)_3PO$.** This mononuclear complex also reacted to form $CH_3SC_2H_5$ and $(CH_3O)_2PO_2^-$, both of which were uncoordinated judging by their $^1H$ NMR resonances. The observed $^{31}P\{^1H\}$ resonance of $(CH_3O)_2PO_2^-$ is sharp ($\Delta\nu_{1/2}$ = 6.0 Hz), confirming the conclusion that this product is not coordinated to iron. The remaining three thiolates continued to bind to the iron center, with paramagnetically shifted $^-SC_2H_5$ resonances at 6.32 ppm ($\Delta\nu_{1/2}$ = 61.5 Hz) and 70.5 ppm ($\Delta\nu_{1/2}$ = 152 Hz). These values differ greatly from those of the starting $[(C_2H_5)_4N]_2[Fe(SC_2H_5)_4]$ complex, 9.97 ppm ($\Delta\nu_{1/2}$ = 156 Hz) and 196 ppm ($\Delta\nu_{1/2}$ = 483 Hz), no resonances of which were observed following the reaction.

**Kinetics Studies.** Reactions of $[(C_4H_9)_4N]_2[Fe_4S_4(SR)_4]$ (R = $C_6H_5$ and $C_2H_5$) were slow and provided similar rate constants. Upper limits of $\leq 1 \times 10^{-7}$ $s^{-1}$ and $\leq 4 \times 10^{-7}$ $s^{-1}$ were obtained. The more reduced complex $[(C_2H_5)_4N]_3[Fe_4S_4(SC_2H_5)_4]$ reacted with a higher rate constant of $(7.8 \pm 0.7) \times 10^{-5}$ $s^{-1}$. The mononuclear tetrathiolate $[(C_2H_5)_4N]_2[Fe(SC_2H_5)_4]$ exhibited the highest pseudo-first-order rate constant, the value of which could only be estimated as $\geq 5 \times 10^{-3}$ $s^{-1}$ under the conditions employed here. Table 4.1 summarizes these results.

**Attempts to Prepare a Site-Differentiated $\{Fe_4S_4\}^{2+}$ Cluster.** In an attempt to isolate a site-specifically modified tetranuclear iron-sulfur cluster,[37-39] a thiolate ligand was removed by methylation and a second, capping ligand was added. In these trials, $[(C_4H_9)_4N]_2[Fe_4S_4(SC_6H_5)_4]$ was first allowed to react with one equivalent of $CH_3I$ in DMSO-*d6*. Subsequently, an equimolar quantity of $Na[HB(pz)_3]$ (pz = pyrazolyl), $(CH_3)_4N(OOCCH_3)$, or $NaSC_2H_5$ was added. The $^1H$ NMR spectra of these reaction solutions all displayed the resonances of uncoordinated $CH_3SC_6H_5$. The $^-SC_6H_5$ resonances indicated persistence of the $\{Fe_4S_4\}^{2+}$ core. In none of the reactions, however, were distinct resonances of $Na[HB(pz)_3]$, $(CH_3)_4N(OOCCH_3)$, or $NaSC_2H_5$ observed. Paramagnetic broadening of these ligands had occurred, rendering them unobservable and suggesting formation of the desired complexes. Efforts were made to isolate the desired site-differentiated tetranuclear complexes with bound capping ligands. In $CH_3CN$, solutions of $[(C_4H_9)_4N]_2$-$[Fe_4S_4(SC_6H_5)_4]$ and $CH_3I$ were treated with one of the ligands $Na[HB(pz)_3]$, $(CH_3)_4N(OOCCH_3)$, and $NaSC_2H_5$. Vapor diffusion of diethyl ether into the resulting reaction mixture yielded black, needle-like crystals in each case. An X-ray crystallographic unit cell determination at 188 K indicated the presence

of the starting material $[(C_4H_9)_4N]_2[Fe_4S_4(SC_6H_5)_4]$ (orthorhombic unit cell with $a$ = 11.888(5) Å, $b$ = 23.21(1) Å, and $c$ = 22.22(1) Å).[40]

**Discussion**

**Reaction Stoichiometry.** Tetranuclear iron-sulfur complexes readily react with $(CH_3O)_3PO$ transferring the methyl group to a terminal thiolate ligand. Although free sulfide ion may be a superior nucleophile, coordination of this moiety to three iron atoms in the cuboidal structure substantially diminishes its nucleophilicity. The thiolate ion, in contrast, binds only one metal ion, leaving two lone pairs available for electrophilic attack by trimethylphosphate. These results and the persistence of intact $\{Fe_4S_4\}^{2+}$ core units after the reaction are in agreement with an earlier account describing reactions of $[Fe_4S_4(SR)_4]^{2-}$ (R = $C_6H_5$, $CH_2C_6H_5$, $C(CH_3)_3$) complexes with the electrophiles $CH_3COCl$, $(CH_3CO)_2O$, and $HOCOCH_3$.[30] The products of the more reduced compounds $[(C_2H_5)_4N]_3[Fe_4S_4(SC_2H_5)_4]$ and $[(C_2H_5)_4N]_2[Fe(SC_2H_5)_4]$, however, had ethanethiolate resonances which indicated that the $\{Fe_4S_4\}^{+}$ core and $\{Fe(SC_2H_5)_3\}^{-}$ moiety were no longer intact following methylation. The $^1H$ NMR chemical shifts of the products did not match those of any known iron-sulfur complexes so we were unable to identify them.

The products of the ethanethiolate cluster reaction, $[Fe_4S_4(SC_2H_5)_3(DMSO)]^{-}$, $CH_3SC_2H_5$, and $(CH_3O)_2PO_2^{-}$, differed from those found for the analogous benzenethiolate complex, $\{Fe_4S_4(SC_6H_5)_3[(CH_3O)_2PO_2]\}^{2-}$ and $CH_3SC_2H_5$. This difference reflects the greater electron-releasing character of the $^{-}SC_2H_5$ ligands which may provide sufficient electron density to the $\{Fe_4S_4\}^{2+}$ core such that a neutral DMSO solvent molecule is adequate to fill the vacant coordination site created by thiolate methylation.

Benzenethiolate, by contrast, is less basic[41] and the $(CH_3O)_2PO_2^-$ anion binds to this complex.

**Kinetics and Mechanism.** Rate constants for the reactions of $[(C_4H_9)_4N]_2[Fe_4S_4(SC_2H_5)_4]$ and $[(C_2H_5)_4N]_3[Fe_4S_4(SC_2H_5)_4]$ with $(CH_3O)_3PO$ nicely illustrate the effect of charge on methyl transfer capability. The $[Fe_4S_4(SC_2H_5)_4]^{3-}$ cluster reacted at least 200 times faster than the more oxidized complex $[Fe_4S_4(SC_2H_5)_4]^{2-}$. The fact that a more negatively charged cluster reacts with an electrophile with a higher rate constant was not unexpected, but the magnitude of difference is surprising. Under identical conditions, the $[Zn(SC_6H_5)_4]^{2-}$ dianion reacted only 15 times faster with $(CH_3O)_3PO$ than $[Zn(SC_6H_5)_3(MeIm)]^-$ (MeIm = 1-methylimidazole) (Table 4.1). The difference in reactivity by a factor of at least 200 between $[Zn(SC_6H_5)_3(MeIm)]^-$ and $[Zn(SC_6H_5)_2(MeIm)_2]$, however, was more pronounced (Table 4.1). In the reactions of these zinc complexes, the active nucleophile is thiolate dissociated from the metal complexes, rather than a zinc-bound thiolate.[24] The different rate constants reflected varied degrees of ligand dissociation. Perhaps, this explanation also holds true for the iron complexes examined here (*vide infra*).

The dianionic clusters $[Fe_4S_4(SR)_4]^{2-}$ (R = $C_6H_5$ and $C_2H_5$) exhibited rate constants for methyl transfer approximately 100-fold lower than those of $[M(SC_6H_5)_4]^{2-}$ (M = Zn, Co, Cd, Hg; Table 4.1). The latter four complexes are dianions, each having four thiolates. We attribute the pronounced kinetic differences to the delocalized electronic state of the $\{Fe_4S_4\}^{2+}$ core.[42] The negative charge of $[Fe_4S_4(SR)_4]^{2-}$ is distributed over the entire unit, resulting in lower charge density at any one {Fe(SR)} corner relative to the that in mononuclear $[M(SR)_4]^{2-}$ anions. Thus, the $[Fe_4S_4(SR)_4]^{2-}$ clusters have overall decreased nucleophilicity and a lesser tendency for ligand dissociation,

either property of which would decrease the rate constant for dealkylating $(CH_3O)_3PO$ relative to that of the mononuclear complexes. The $[Fe(SC_2H_5)_4]^{2-}$ dianion thus exhibited a rate constant not only higher than that of the dianions $[Fe_4S_4(SR)_4]^{2-}$ (R = $C_6H_5$ and $C_2H_5$), but also the trianion $[Fe_4S_4(SC_2H_5)_4]^{3-}$ (Table 4.1).

The $pK_a$ of $HSC_2H_5$ is approximately 4 units higher than that of $HSC_6H_5$, which may provide an explanation for the 200-fold difference in rate constants for $[Fe(SC_2H_5)_4]^{2-}$ and $[M(SC_6H_5)_4]^{2-}$ (M = Zn, Co, Cd, Hg).[41] The greater basicity of the $^-SC_2H_5$ ligand will enhance its reactivity relative to $^-SC_6H_5$ and is likely to result in higher rate constants for all $[M(SC_2H_5)_4]^{2-}$ complexes. The reactivity of both $[(C_4H_9)_4N]_2[Fe_4S_4(SR)_4]$ (R = $C_6H_5$ and $C_2H_5$) were examined in order to measure the effect of thiolate ligand type on reactivity. Unfortunately, the rate constants for these two compounds were low, making a quantitative comparison difficult.

We turn now to the question of whether the active thiolate nucleophile in these studies is bound to iron or dissociated. The low rate constants for methyl transfer from $(CH_3O)_3PO$ to $[(C_4H_9)_4N]_2[Fe_4S_4(SR)_4]$ (R = $C_6H_5$ and $C_2H_5$) suggest that, if the observed reactivity were due entirely to dissociated thiolate, the degree of dissociation must be low relative to that of $[(CH_3)_4N]_2[Zn(SC_6H_5)_4]$ (≥ 75 % dissociation of one ligand)[24] and $[(CH_3)_4N]_2[Hg(SC_6H_5)_4]$ (approximately 100 % dissociation).[25] Previous experiments revealed that the cuboidal structures of $[(C_2H_5)_4N]_3$-$[Fe_4S_4(SC_6H_5)_4]$ and $[(C_2H_5)_4N]_3[Fe_4S_4(SCH_2C_6H_5)_4]$ are preserved in $CH_3CN$ solution.[43] An examination of thiolate ligand exchange in $[(C_6H_5)_4As]_2[Fe_4S_4\{SC(CH_3)_3\}_4]$ indicated the rate-determining step to be protonation of a coordinated thiolate by the added thiol.[44] We cannot rule

out, however, that transiently dissociated thiolate serves as the nucleophile toward $(CH_3O)_3PO$.

The formal oxidation states of the metal ions may be important in determining both the thiolate dissociation constants and overall cluster nucleophilicity. In the case of $[M(SR)_4]^{2-}$ (M = Zn, Co, Cd, Hg, or Fe) anions, the metals are all in the 2+ state. The $[Fe_4S_4(SR)_4]^{2-}$ (R = $C_6H_5$ and $C_2H_5$) and $[Fe_4S_4(SC_6H_5)_4]^{3-}$ clusters all have Fe(III) character, which should cause them to bind thiolate ligands with higher affinity and to have lower equilibria constants for dissociation. If the thiolate nucleophile for alkyl transfer is dissociated, the greater Fe(III) character of $[Fe_4S_4(SR)_4]^{2-}$ (R = $C_6H_5$ and $C_2H_5$) may enhance ligand binding and explain the lower observed kinetic results.

**Biological Implications.** The present results suggest that tetranuclear iron-sulfur centers in proteins could repair DNA alkylation damage. The kinetic data, however, indicate that all clusters would not perform this task equally well. Presumably, the $[Zn(S\text{-cys})_4]^{2-}$ center of Ada is optimal for DNA repair and was selected through evolution. Here, we find that the $[Fe_4S_4(SC_6H_5)_4]^{2-}$ complex reacts with $(CH_3O)_3PO$ with a rate constant about 200 times less than that of the analogous mononuclear zinc species, $[Zn(SC_6H_5)_4]^{2-}$. Although iron-sulfur centers appear to be capable of alkylphosphotriester repair, use of these moieties may not be compatible with a biological time scale. Repair involves formation of a transient protein-DNA complex and alkyl transfer must occur rapidly.[45] The more reduced complex $[Fe_4S_4(SC_2H_5)_4]^{3-}$, however, has a more suitable rate constant for methyl transfer (Table 4.1) and could be an appropriate center for repairing DNA alkylation damage. Its potential instability with respect to oxidation, however, may select against such a role for this cluster.

Previously, we concluded that the low nucleophilicity of $[Zn(SC_6H_5)_2(MeIm)_2]$ and, by analogy, $[Zn(S\text{-cys})_2(N\text{-his})_2]$ sites, contributed to their suitability for folding protein secondary structure.[23,24] Although $[Fe_4S_4(S\text{-cys})_4]^{2-}$ centers are charged, the present experiments similarly demonstrate a low reactivity for these moieties. Neutral $[Zn(SC_6H_5)_2(MeIm)_2]$ is less reactive toward $(CH_3O)_3PO$ than $[Fe_4S_4(SR)_4]^{2-}$ (R = $C_6H_5$ and $C_2H_5$), but all react rather slowly. We conclude that $[Fe_4S_4(S\text{-cys})_4]^{2-}$ clusters are suitable for folding protein structures, but less so than the $[Zn(S\text{-cys})_2(N\text{-his})_2]$ center.

**Site-Specifically Modified Clusters.** By using the tridentate ligand 1,3,5-tris((4,6-dimethyl-3-mercaptophenyl)thio)-2,4,6-tris(*p*-tolylthio)benzene ($L\cdot(SH)_3$), a series of $\{Fe_4S_4\}^{2+}$ complexes was prepared in which three iron atoms are bound by $L\cdot(S^-)_3$ and the fourth iron is ligated by various mono-, di-, and tridentate ligands.[37-39] These studies have provided the only means so far of directing ligand substitution chemistry to one corner of the iron-sulfur cube and isolating the site-differentiated cluster. The present methyl transfer reactions similarly remove one thiolate ligand and afford the $\{Fe_4S_4(SR)_3\}^-$ cluster. Thus, methylation with $(CH_3O)_3PO$ may provide a facile route to the site-specifically modified clusters $\{Fe_4S_4(SC_6H_5)_3[(CH_3O)_2PO_2]\}^{2-}$ and $[Fe_4S_4(SC_2H_5)_3(DMSO)]^{2-}$. Previous studies have shown, however, that electrophilic and ligand substitution reactions of $[Fe_4S_4(XAr)_4]^{2-}$ (X = O, S, Ar = $C_6H_5$, $C_6H_4$-*p*-$CH_3$) clusters afford statistical distributions among $[Fe_4S_4(XAr)_{4-n}(L)_n]^{2-}$ products.[30,46,47] Such species were observable by $^1H$ NMR spectroscopy. Either different *p*-$CH_3$ resonances for each species present or contact shifted resonances for both XAr and L ligands were observed. In our studies, only the $^-SC_6H_5$ and $^-SC_2H_5$ ligands displayed $^1H$ NMR resonances attributed to $\{Fe_4S_4\}^{2+}$ core binding. The peaks were broad, however, and did

not permit us to gain insight about the statistical nature of the products. Thus, $\{Fe_4S_4(SC_6H_5)_3[(CH_3O)_2PO_2]\}^{2-}$ and $[Fe_4S_4(SC_2H_5)_3\text{-}(DMSO)]^-$ could exist as the series of $\{Fe_4S_4(SC_6H_5)_{4-n}[(CH_3O)_2PO_2]_n\}^{2-}$ and $[Fe_4S_4(SC_2H_5)_{4-n}(DMSO)_n]^{(2-n)-}$ complexes. Attempts to isolate site-differentiated complexes in the solid state afforded only $[(C_4H_9)_4N]_2[Fe_4S_4(SC_6H_5)_4]$. As before,[24] this result may only attest to the stability of tetrathiolate species in the solid state and not exclude the existence of the desired reaction products in solution.

## Conclusions

We have provided a detailed study of the alkylation reactions of iron-sulfur complexes. The kinetic results of thiolate methylation permitted a comparison of the general nucleophilic character of each complex. Although tetranuclear iron-sulfur species may be capable of repairing DNA alkylation damage, mononuclear tetrathiolate metal centers appear more adept at such reactions. Models for $\{Fe_4S_4\}^{2+}$ protein sites were fairly unreactive and, as such, may be better suited to structural role. Our studies show a continued parallel between the development of zinc and iron thiolate protein chemistry. Thiolate moieties of both metals appear proficient at accepting alkyl groups and stabilizing protein secondary structure.

## Acknowledgment

This research was supported by grant CA34992 from the National Cancer Institute. J. J. W. is predoctoral trainee under N.C.I. training grant CA09112.

**References**

(1) Lippard, S. J.; Berg, J. M. *Principles of Bioinorganic Chemistry*; University Science Books: Mill Valley, CA, 1994.

(2) Beinert, H. *FASEB J.* **1990**, *4*, 2483-2491.

(3) Spiro, T. G. *Iron-Sulfur Proteins*; Spiro, T. G., Ed.; John Wiley and Sons: New York, 1982.

(4) Lovenberg, W. *Iron-Sulfur Proteins*; Lovenberg, W., Ed.; Academic Press: New York, 1973; Vol. 1-3.

(5) Lauble, H.; Kennedy, M. C.; Beinert, H.; Stout, C. D. *Biochem.* **1992**, *31*, 2735-2748.

(6) Zheng, L.; Kennedy, M. C.; Beinert, H.; Zalkin, H. *J. Biol. Chem.* **1992**, *267*, 7895-7903.

(7) Thayer, M. M.; Ahern, H.; Xing, D.; Cunningham, R. P.; Tainer, J. A. *EMBO J.* **1995**, *14*, 4108-4120.

(8) Kuo, C.-F.; McRee, D. E.; Fisher, C. L.; O'Handley, S. F.; Cunningham, R. P.; Tainer, J. A. *Science* **1992**, *258*, 434-440.

(9) Bailly, V.; Verly, W. G. *Biochem J.* **1987**, *242*, 565-572.

(10) Manuel, R. C.; Czerwinski, E. W.; Lloyd, R. S. *J. Biol. Chem.* **1996**, *271*, 16218-16226.

(11) Tsai-Wu, J.-J.; Liu, H.-F.; Lu, A.-L. *Proc. Natl. Acad. Sci. USA* **1992**, *89*, 8779-8783.

(12) Michaels, M. L.; Pham, L.; Nghiem, Y.; Cruz, C.; Miller, J. H. *Nucl. Acids. Res.* **1990**, *18*, 3841-3845.

(13) Piersen, C. E.; Prince, M. A.; Augustine, M. L.; Dodson, M. L.; Lloyd, R. S. *J. Biol. Chem.* **1995**, *270*, 23475-23484.

(14) Sun, B.; Latham, K. A.; Dodson, M. L.; Lloyd, R. S. *J. Biol. Chem.* **1995**, *270*, 19501-19508.

(15) Kow, Y. W.; Wallace, S. S. *Biochem.* **1987**, *26*, 8200-8206.

(16) Lu, A.-L.; Tsai-Wu, J.-J.; Cillo, J. *J. Biol. Chem.* **1995**, *270*, 23582-23588.

(17) Michaels, M. L.; Cruz, C.; Grollman, A. P.; Miller, J. H. *Proc. Natl. Acad. Sci. USA* **1992**, *89*, 7022-7025.

(18) Michaels, M. L.; Tchou, J.; Grollman, A. P.; Miller, J. H. *Biochem.* **1992**, *31*, 10964-10968.

(19) Berg, J. M.; Shi, Y. *Science* **1996**, *271*, 1081-1085.

(20) Klug, A.; Schwabe, J. W. R. *FASEB J.* **1995**, *9*, 597-604.

(21) Rhodes, D.; Klug, A. *Sci. Am.* **1993**, *268*, 56-65.

(22) Vallee, B. L.; Auld, D. S. *Acc. Chem. Res.* **1993**, *26*, 543-551.

(23) Wilker, J. J.; Lippard, S. J. *J. Am. Chem. Soc.* **1995**, *117*, 8682-8683.

(24) Wilker, J. J.; Lippard, S. J., Submitted for publication.

(25) Wilker, J. J.; Wetterhahn, K. E.; Lippard, S. J., Submitted for publication.

(26) Myers, L. C.; Cushing, T. D.; Wagner, G.; Verdine, G. L. *Chem. and Biol.* **1994**, *1*, 91-97.

(27) Myers, L. C.; Terranova, M. P.; Ferentz, A. E.; Wagner, G.; Verdine, G. L. *Science* **1993**, *261*, 1164-1167.

(28) Myers, L. C.; Verdine, G. L.; Wagner, G. *Biochem.* **1993**, *32*, 14089-14094.

(29) Myers, L. C.; Terranova, M. P.; Nash, H. M.; Markis, M. A.; Verdine, G. L. *Biochem.* **1992**, *31*, 4541-4547.

(30) Johnson, R. W.; Holm, R. H. *J. Am. Chem. Soc.* **1978**, *100*, 5338-5344.

(31) Perrin, D. D.; Armarego, W. L. F. *Purification of Laboratory Chemicals*; Third ed.; Butterworth-Heinemann Ltd.: Boston, 1988.

(32) Gordon, A. J.; Ford, R. A. *The Chemist's Companion. A Handbook of Practical Data, Techniques, and References*; John Wiley and Sons: New York, 1972.

(33) Christou, G.; Garner, C. D.; Balasubramaniam, A.; Ridge, B.; Rydon, H. N. In *Inorganic Syntheses*; Fackler, J. P., Ed.; John Wiley and Sons: New York, 1982; Vol. 21, pp 33-37.

(34) Hagen, K. S.; Watson, A. D.; Holm, R. H. *Inorg. Chem.* **1984**, *23*, 2984-2990.

(35) Hagen, K. S.; Watson, A. D.; Holm, R. H. *J. Am. Chem. Soc.* **1983**, *105*, 3905-3913.

(36) Wilkins, R. G. *Kinetics and Mechanism of Reactions of Transition Metal Complexes*; Second ed.; VCH Publishers Inc.: New York, 1991.

(37) Weigel, J. A.; Holm, R. H. *J. Am. Chem. Soc.* **1991**, *113*, 4184-4191.

(38) Ciurli, S.; Carrie, M.; Weigel, J. A.; Carney, M. J.; Stack, T. D. P.; Papaefthymiou, G. C.; Holm, R. H. *J. Am. Chem. Soc.* **1990**, *112*, 2654-2664.

(39) Stack, T. D. P.; Holm, R. H. *J. Am. Chem. Soc.* **1988**, *110*, 2484-2494.

(40) Excoffon, P.; Laugier, J.; Lamotte, B. *Inorg. Chem.* **1991**, *30*, 3075-3081.

(41) Crampton, M. R. In *The Chemistry of the Thiol Group*; Patai, S., Ed.; John Wiley and Sons: New York, 1974, pp 379-415.

(42) Holm, R. H.; Averill, B. A.; Herskovitz, T.; Frankel, R. B.; Gray, H. B.; Siiman, O.; Grunthaner, F. J. *J. Am. Chem. Soc.* **1974**, *96*, 2644-2646.

(43) Laskowski, E. J.; Frankel, R. B.; Gillum, W. O.; Papaefthymiou, G. C.; Renaud, J.; Ibers, J. A.; Holm, R. H. *J. Am. Chem. Soc.* **1978**, *100*, 5322-5337.

(44) Dukes, G. R.; Holm, R. H. *J. Am. Chem. Soc.* **1975**, *97*, 528-533.

(45) Friedberg, E. C.; Walker, G. C.; Siede, W. *DNA Repair and Mutagenesis*; ASM Press: Washington D. C., 1995.

(46) Kanatzidis, M. G.; Baenziger, N. C.; Coucouvanis, D.; Simopoulos, A.; Kostikas, A. *J. Am. Chem. Soc.* **1984**, *106*, 4500-4511.

(47) Cleland, W. E.; Holtman, D. A.; Sabat, M.; Ibers, J. A.; DeFotis, G. C.; Averill, B. A. *J. Am. Chem. Soc.* **1983**, *105*, 6021-6031.

**Table 4.1.** Pseudo-First-Order Rate Constants for Reactions of Thiolate Complexes with $(CH_3O)_3PO$.[a]

| compound | $k$ ($s^{-1}$) |
|---|---|
| $[(C_2H_5)_4N]_3[Fe_4S_4(SC_2H_5)_4]$ | $(7.8 \pm 0.7) \times 10^{-5}$ |
| $[(C_4H_9)_4N]_2[Fe_4S_4(SC_2H_5)_4]$ | $\leq 4 \times 10^{-7}$ |
| $[(C_4H_9)_4N]_2[Fe_4S_4(SC_6H_5)_4]$ | $\leq 1 \times 10^{-7}$ |
| $[(C_2H_5)_4N]_2[Fe(SC_2H_5)_4]$ | $\geq 5 \times 10^{-3}$ |
| $[(CH_3)_4N]_2[Zn(SC_6H_5)_4]$[b] | $(8.2 \pm 0.6) \times 10^{-5}$ |
| $[(CH_3)_4N]_2[Co(SC_6H_5)_4]$[c] | $(4 \pm 1) \times 10^{-5}$ |
| $[(CH_3)_4N]_2[Cd(SC_6H_5)_4]$[c] | $(3 \pm 1) \times 10^{-5}$ |
| $[(CH_3)_4N]_2[Hg(SC_6H_5)_4]$[d] | $(1.1 \pm 0.1) \times 10^{-4}$ |
| $[(CH_3)_4N][Zn(SC_6H_5)_3(MeIm)]$[b] | $(6 \pm 1) \times 10^{-6}$ |
| $[Zn(SC_6H_5)_2(MeIm)_2]$[b] | $\leq 3 \times 10^{-8}$ |
| $(CH_3)_4N(SC_6H_5)$[b] | $(1.1 \pm 0.3) \times 10^{-4}$ |

[a]Reactions were carried out with 5.0 mM thiolate complex and 1.0 mM $(CH_3O)_3PO$ in DMSO-*d6*. [b]From reference 23. [c]From reference 24. [d]From reference 25.

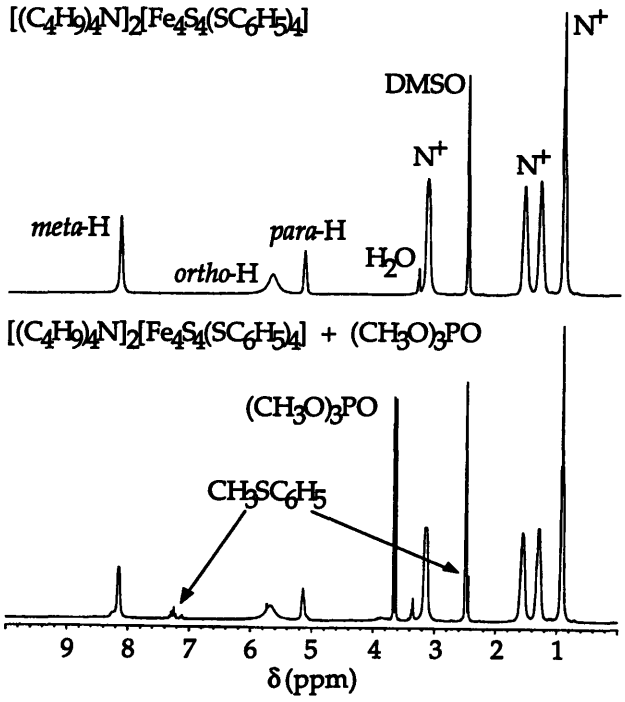


**Figure 4.1.** $^1H$ NMR spectra in DMSO-*d6* of $[(C_4H_9)_4N]_2[Fe_4S_4(SC_6H_5)_4]$ (top) and $[(C_4H_9)_4N]_2[Fe_4S_4(SC_6H_5)_4]$ after reaction with $(CH_3O)_3PO$ for 33 days at room temperature (bottom). Peaks labeled $N^+$ indicate $(C_4H_9)_4N^+$ counterion resonances. The starting concentration of each species was 50 mM.

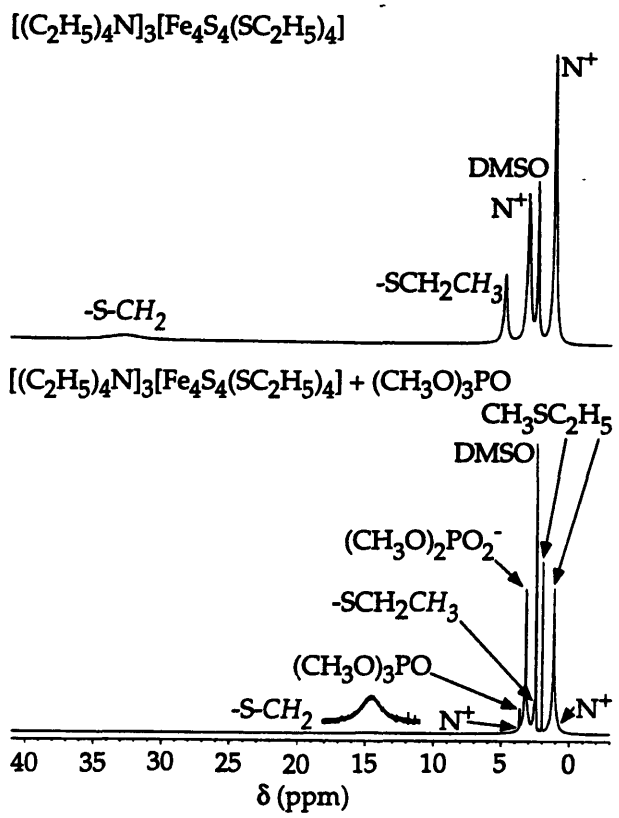


**Figure 4.2.** $^1$H NMR spectra in DMSO-*d6* of $[(C_2H_5)_4N]_3[Fe_4S_4(SC_2H_5)_4]$ (top) and $[(C_2H_5)_4N]_3[Fe_4S_4(SC_2H_5)_4]$ after reaction with $(CH_3O)_3PO$ for 22 hours at room temperature (bottom). Peaks labeled $N^+$ indicate $(C_2H_5)_4N^+$ counterion resonances. The starting concentration of each species was 50 mM. The inset is the same spectrum plotted on a higher vertical scale.

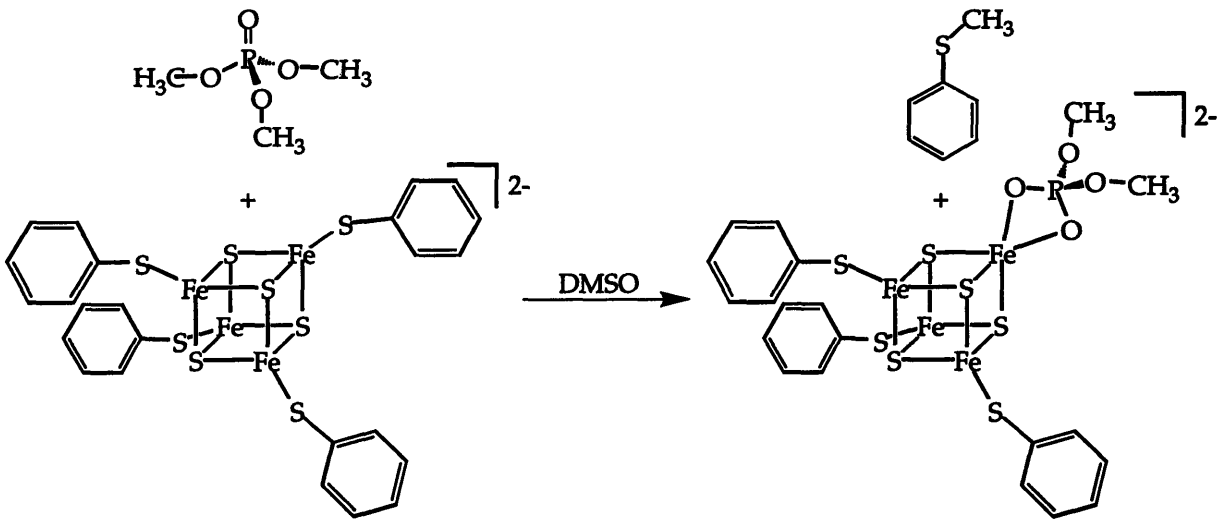


**Scheme 4.1**

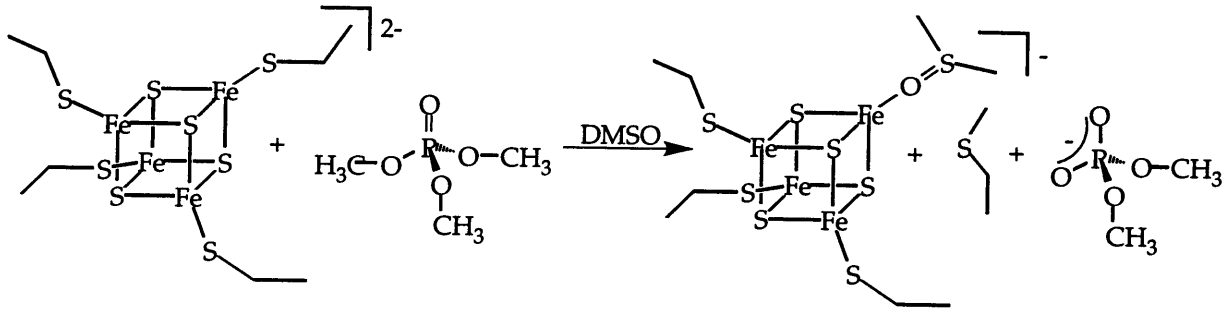


**Scheme 4.2**